CRANFIELD UNIVERSITY

CENTRE FOR PHOTONICS AND OPTICAL ENGINEERING
SCHOOL OF ENGINEERING

Ph.D. THESIS
Academic year 2002-2003

Simon Philip Reilly

TUNEABLE AND SWITCHABLE DUAL WAVELENGTH LASER DIODES USING FIBRE BRAGG GRATING EXTERNAL CAVITIES

Supervisors: Stephen W. James & Ralph P. Tatam

2003

This thesis is submitted in partial fulfilment of the requirements for the degree of Doctor of Philosophy

Abstract

This thesis describes two external cavity laser diode designs. The first utilises a Bragg grating fabricated in highly birefringent optical fibre and offers, through the use of a waveplate, the ability to switch between modes that are separated in both polarisation and wavelength, due to the differing refractive index in either eigenmode. The laser offers three stabilised states of operation, single mode operation for either axis of the fibre, or a third state in which both modes lase simultaneously with a wavelength separation of 0.3 nm. The application of transverse strain on the fibre Bragg grating was also demonstrated as a method of tuning the wavelength separation between these modes.

The second external cavity laser design utilises two spatially and spectrally separate Bragg gratings fabricated in mono-mode fibre. This allows two longitudinal modes corresponding to the Bragg wavelengths to oscillate simultaneously. The application of longitudinal strain allowed either fibre Bragg grating to be tuned, thus generating a stabilised tuneable beat frequency, which was demonstrated between 130 GHz – 2.28 THz. A three fibre Bragg grating laser is also presented which allowed three modes to oscillate simultaneously.

Both the laser based on a Bragg grating fabricated in highly birefringent fibre and the laser based on multiple Bragg gratings fabricated in single mode fibre demonstrated reduced injection current threshold and mode hop free operation over the full injection current range.

A practical application for the two fibre Bragg grating lasers is presented where the properties of independently tuneable dual wavelength operation are used to interrogate a miniature fibre Fabry-Perot sensor. The wavelength separation of the two oscillating modes can be tuned to reach a point of quadrature for the sensor cavity. A sensing system demonstrating this technique is presented which detected vibrations up to 500 Hz in cavities of 16-34 μm.

Acknowledgements

Thanks are due to the following people for their direct or indirect help during the course of this research. Thanks must go to Steve Staines for excellent practical help with almost every stage of the project. Thanks also for the advice and expertise of Dr. Helen Ford, Dr. Roger Groves and Dr. Chen Chun Ye in many stages of the work. Special thanks to Chen for his help fabricating the fibre Bragg gratings

Thanks must go to Prof. Ralph Tatam as an invaluable source of ideas and insight in many areas of the project and for giving me the opportunity to study for the Ph.D.

Special thanks must go to my supervisor Dr. Steve James for excellent supervision from start to finish, being endless source of technical wisdom and much patience especially during the writing of the thesis.

Thank you to Richard Hamilton, Robert Stokes and Sammy Cheung especially during my final months at Cranfield, and the late Alison Maxwell.

Also thanks must be given to the staff of the National Physical Laboratory during the writing of the thesis.

Finally many thanks to my parents Sharon and Philip Reilly for much help and support throughout many years. After clouds comes sunshine....

Contents

List of figures and tables

1. Introduction.

Semiconductor lasers are the most widely used types of laser; they are incorporated into consumer items such as CD players and laser printers and they are widely used in the telecommunications industry. Mass production enables them to be low cost, they are small and do not require water-cooling. They are capable of operating on multi or single longitudinal modes and they have dimensions that make them ideal for incorporation in optoelectronics systems.

The performance of the semiconductor laser is limited though, specifically in terms instabilities in the spectrum of the output. These traits can be overcome, but at a large cost relative to a mass produced laser diode. Cavity structures such as distributed feedback lasers and distributed Bragg reflectors[1.1] are capable of achieving some of the performance refinements such as single mode operation, which is discussed further in chapter 3. Many applications require narrow linewidth, tuneability, multiple wavelengths and a smooth linear injection current to output power curve.

Optical sensing systems often require a narrow linewidth to improve resolution and dynamic range, for example a Doppler velocimetry system would benefit from a laser output which had minimum frequency fluctuations thus reducing uncertainty in the measurand[1.2]. Most interferometry systems also require a source with a stable spectral output and narrow linewidth (long coherence length) to prevent ambiguities in experimental readings. The telecommunications industry require narrow linewidth sources as modern technologies like the internet place increasing demand on the capacity of communications networks, with communications channels being increasingly packed. Narrower laser linewidths allow more communication channels to be effectively multiplexed and they also give a better signal to noise ratio when combined with another wavelength to generate a carrier frequency.

Multiple wavelength lasers are capable of synthetic wavelength generation for optical signal processing in metrology systems, carrier frequency generation and multiple wavelength fibre Bragg sensor interrogation[1.3] all can benefit from the use of lasers capable of simultaneous operation at a number of wavelengths.

Laser diodes are incapable of this in their simplest structure, which consists of a Fabry-Perot cavity formed by the cleaved end faces of the semiconductor chip. In general they operate on multi-longitudinal modes, where the mode spacing is governed by the laser cavity and may not be controlled. The devices are also sensitive to optical feedback, which can cause instability in the spectral output.

There are alternative ways of achieving the performance required from a laser diode. For example, the use of complex cavity structures to force the laser to operate at the desired wavelengths, e.g. distributed feedback (DFB), distributed Bragg reflector lasers (DBR) and bulk optic external cavity systems featuring diffraction gratings[1.4]. The external cavity fibre Bragg grating feedback technique that has been the subject of a number of publications, and is being investigated in this thesis, has a number of advantages over the other techniques. A Bragg grating can be written into the core of an optical fibre using UV irradiation[1.5], it then acts as a wavelength selective reflector. Light at the Bragg wavelength is coupled backwards while all other wavelengths are allowed to pass through the grating. Fibre Bragg gratings (FBG) are easily manufactured at well defined wavelengths. They may be used as a wavelength selective feedback element, forcing the laser to oscillate at the wavelength defined by the Bragg reflection. Thus low cost, Fabry-Perot laser diode structures may be forced to oscillate under conditions defined by the user, potentially increasing the yield of laser devices from a semiconductor wafer. This is a big advantage over DFB and DBR lasers, which have to be tested individually before packaging and are only available at certain wavelengths. These advantages will be discussed in more detail later chapters of the thesis. The fibre Bragg grating external cavity lasers reported in this thesis have a number of novel properties which allow independent multiple wavelength tuneability and switchability.

1.1 Aims and Objectives of Thesis

The aim of this project was to build a tuneable, multiple wavelength external cavity semiconductor laser with specification suitable for optical sensing applications. The design principle is illustrated in Fig 1.1

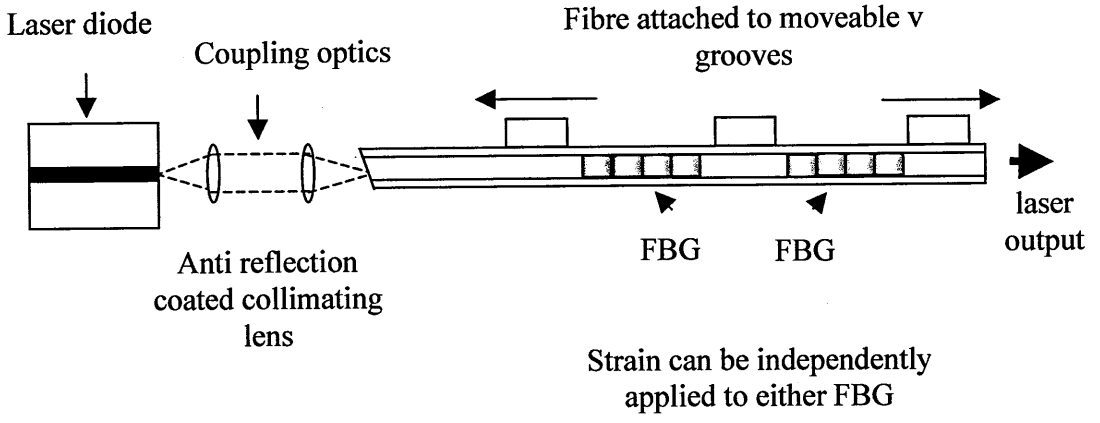

Fig 1.1 Configuration for dual FBG external cavity laser.

The properties of these lasers were fully tested including parameters such as linewidth, tuneability and stability. The laser systems were also incorporated into an optical sensor system which benefited from the unique properties of these novel lasers. Potential applications include interrogation of multiplexed fibre Bragg sensors, generation of synthetic wavelengths in optical signal processing for interferometric sensors, shearography systems and in the generation of carrier signals for heterodyne processing schemes.

1.2 Thesis Outline

Chapter 2 features an explanation of the fundamentals of fibre optics, single mode and high birefringence fibres. A section is also included on fibre Bragg gratings which discusses their characteristics, their fabrication and their response under the application of

strain, as a foundation for the experimental work contained in later chapters. Chapter 3 is a background discussion on laser diodes and their dynamics, which relate to this proposed work. Alternative techniques are introduced and evaluated before an overview of the fibre Bragg external cavity laser is presented which reviews the significant work in the field, focussing on designs and phenomena that have an influence on the direction of this project. Some of the most up to date work in the area is also shown to demonstrate the current state of the research interest. A section is presented on dual wavelength laser's, a review of their applications, specifically in microwave generation and beat signal applications. Chapter 4 features experimental work demonstrating the benefit of application of an external cavity to a standard laser diode. This includes linewidth reduction, threshold reduction and mode hop reduction. The high birefringent switchable laser is presented in chapter 5, as well as its switchability properties the use of transverse strain on the Bragg grating to tune the wave separation is presented. A dual Bragg grating laser is experimentally evaluated in chapter 6 and initial results from a three Bragg grating laser to illustrate the laser's potential. Chapter 7 covers the application of a dual fibre Bragg grating laser to an optical sensing system. The interrogation of a miniature Fabry-Perot cavity is demonstrated and the use of the dual Bragg grating laser's ability to independently tune wavelength is shown as the laser is tuned to quadrature and a number of different frequency vibrations applied to the sensor. Finally, there is a chapter concluding the work presented and discussing potential future work.

References

(1.1) J.M. Senior 'Optical fibre communications: principles and practice', 2nd edn. Prentice Hall, 1992.

(1.2) F. Durst, A. Melling and J. Whitelaw, 'Principle and practice of laser Doppler anemometry' Academic Press, London, 1976.

(1.3) A. Wilson, S.W. James and R.P.Tatam, 'Time-division-multiplexing of In-fibre Bragg gratings using a pulsed laser diode source', Presented at 12th Optical Fibre sensors conference, OFS-12, Williamsburg VA, USA, Nov. 1997

(1.4) J. Wittmann and G. Gaukel, 'Narrow linewidth laser with a prism grating: GRINrod lens combination serving an external cavity', Electronics Lett., 1987, Vol. 23, pp. 524-525.

(1.5) M.L. Dockney, S.W. James and R.P. Tatam, 'Fibre Bragg gratings fabricated using a wavelength tuneable laser source and a phase mask based interferometer' Measurement Science and Technology. 1996, Vol. 7, pp. 445-448.

2: Fibre optics and Fibre Bragg gratings

The use of a glass fibre waveguide to carry an optical signal was first proposed in the late 1960's[2.1] and has a number of attractive features. These include a very large potential bandwidth compared with conventional co-axial cable or millimetre wave radio, particularly when the optical signal can be wavelength division multiplexed (WDM). Optical fibres are electrical insulators as they are fabricated from glass or occasionally a plastic polymer, so they do not suffer interference problems making them ideal for use in electrically hazardous environments. Optical fibres can also be isolated from each other easily and so do not suffer from cross-talk. The base material cost of fibre is very low as fibres are made from silica which is derived from sand. They are very low loss relative to co-axial cable and as they do not radiate significantly they offer excellent signal security. Fibres are also small and lightweight, 125 μm diameter, no thicker than a human hair, allowing their insertion to cause a minimum of disturbance, particularly useful for embedded sensing applications and in particular strain measurement. As well as the use of fibres for delivery in sensor systems they can also be used as sensors themselves due to their sensitivity to strain and temperature.

2.1 Optical fibres

Optical fibres are dielectric waveguides, comprising a circular core along which light propagates. The fibres use total internal reflection to retain the light in the fibre core. To achieve such confinement, the refractive index of the core must be higher than that of the surrounding cladding. In theory air could be used to form the cladding of the fibre, but the exposed fibre core, typically as narrow as ~ 5 μm in diameter, could then be easily damaged, snapped or bent excessively and the cladding refractive index could not be as easily controlled which could in turn affect the total internal reflection properties of the

fibre. The maximum angle a ray of light is allowed to propagate in the fibre is given by the critical angle, as illustrated by ϕ_c in Fig 2.1. Using Snells law[2.2]:

$$\sin\phi_c = \frac{n_2}{n_1} \qquad (2.1)$$

The refractive index of the core is denoted by n_1, the cladding refractive index is denoted by n_2 and ϕ_c is the critical angle. The critical angle is the angle of acceptance to the core at which light will be refracted rather than reflected. Therefore as such light of incidence less than the critical angle within the fibre is allowed to propagate down the fibre by a process of reflection with relatively low loss. As shown in Fig. 2.1

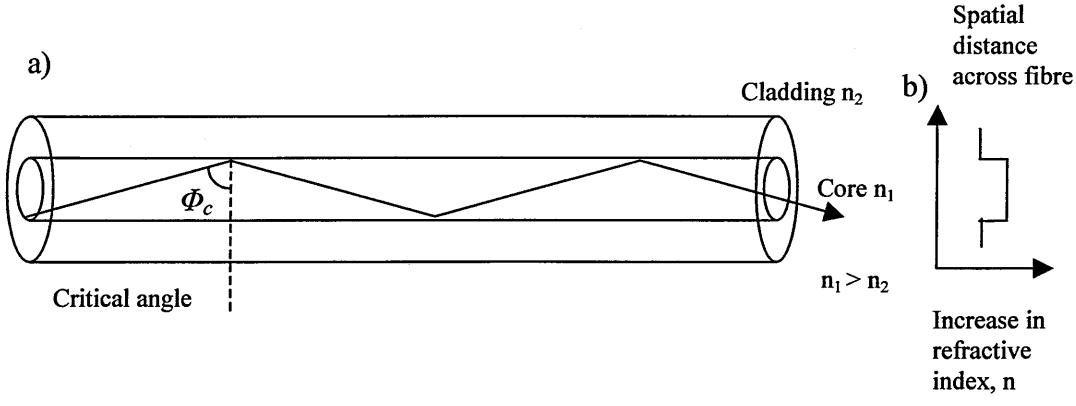

Fig. 2.1 a) Transmission of light in an optical fibre using the total internal reflection mechanism. b) Profile of relative refractive indices of the core and cladding.

For a more in depth analysis of the behaviour of optical fibres, electromagnetic wave theory must be used. A condition of waveguide mode propagation requires that the phase of a wave must be the same after two reflections, modulo 2π, as the wave which has propagated without reflection. As shown in Fig 2.2

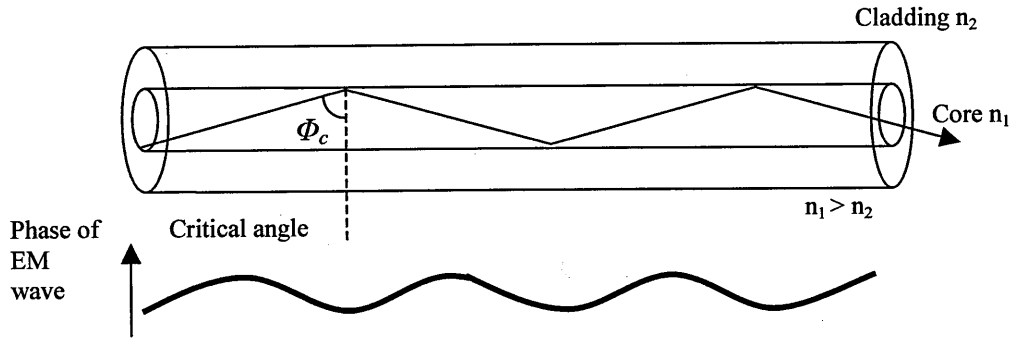

Fig 2.2 Illustration of the phase of an allowed mode within a waveguide.

This can be viewed as a boundary condition, for a given wavelength, core diameter and difference in refractive index between core and cladding of the fibre. Therefore only a number of discrete modes are allowed to propagate. If a fibre is bent then the angle of incidence on the core cladding interface increases. This change in incident angle depends on a ratio between core radius and bend radius[2.3]. As a result fibres that have a relatively large core diameter can allow the angle of incidence to easily exceed the critical angle leading to large power losses in the fibre, thus making smaller core fibres less suseptible to bend induced losses. The number of modes supported by the fibre is reduced as the core size is reduced.

2.1.1 Single mode fibres

When more than one mode, or path of light, is allowed to propagate along a fibre, signal dispersion can occur due to the differing path lengths. This limits bandwidth in

communication systems and interferometric fibre sensing techniques therefore require single mode fibre, as multiple path length differences will introduce uncertainty to the interferometric signal created by the measurand. To create single mode (SM) fibre the core diameter of the fibre must be reduced to allow only the fundamental mode to propagate above a given wavelength, the cut-off wavelength[2.4].

$$a = \frac{V\lambda_{cut}}{2\pi n_1 (2\Delta)^{\frac{1}{2}}} \tag{2.2}$$

Where is a the core radius, λ_{cut} is the cut-off wavelength above which single mode operation can exist, n_1 is the core refractive index and Δ is the difference in refractive, $(n_1\text{-}n_2/n_1)$ index between core and cladding. V is the normalised cut-off frequency when it lies between $(0 \leq V < 2.405)$[2.4] single mode operation will occur in the fibre. Therefore a smaller core diameter decreases the cut-off wavelength, however the small core size can be problematic, potentially reducing coupling efficiency of the light to other fibres or components when the fibre has to be interfaced, due to a decrease in alignment tolerance.

2.1.2 Polarisation maintaining fibre

The state of polarisation at the output of the fibre is important in applications such as coherent communications networks or interferometric sensing[2.4]. The polarisation state of light is not generally maintained over more than a few metres in standard single mode cylindrically symmetric optical fibres. Fibres that can maintain the polarisation state are known as highly birefringent fibres (Hi-Bi). These fibres work on the principle of modal birefringence; they exhibit a different effective refractive index in either orthogonal principal mode and light polarised along one of the principal axes will retain its polarisation for the length of the fibre, with minimal coupling to the orthogonal mode. There are two methods of introducing birefringence into the fibre, and they result in

differing levels of birefringence. One is geometric shape birefringence, for example by making the core elliptical[2.4]. The other is stress induced birefringence, which uses stress rods in the cladding. The circularly asymmetrical inserts, often glass doped with Boron, have a different coefficient of thermal expansion compared with that of the cladding. As the fibre cools the rods introduce stresses into the core of the fibre resulting in the birefringence[2.4]. Standard SM fibres generally have a small amount of birefringence resulting from imperfections introduced during manufacture, or arising from bending or lateral pressure, leading to an unpredictable polarisation state at the fibre output. Fig 2.3 shows three typical types of Hi-Bi fibre. Fig 2.3a) shows an elliptical core fibre, in which the refractive index difference between core and cladding is higher than in the stress induced Hi-Bi fibres but the birefringence is normally smaller[2.4]. Fig 2.3b) and 2.3c) show PANDA and bow tie fibre respectively. The complications involved in the techniques used to manufacture Hi-Bi fibre however mean they are more expensive than standard SM fibre.

2.3a)

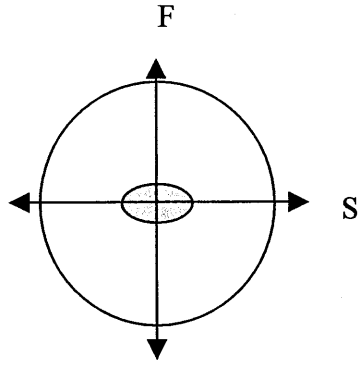

2.3b)

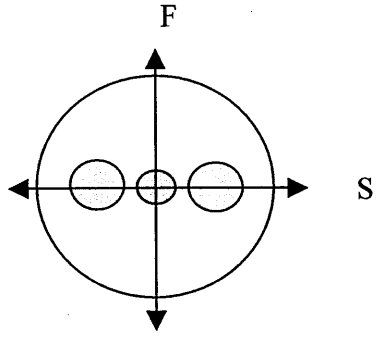

2.3c)

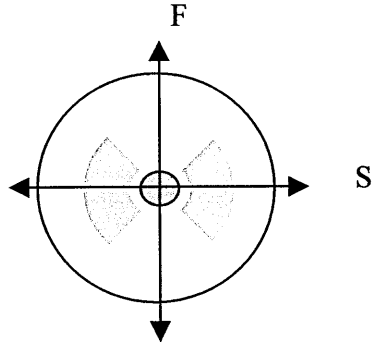

Fig 2.3 Cross section of Hi-Bi fibre indicating the orientation of the fast axis (f) and slow axis (s), 2.3a) is elliptical core fibre, 2.3b) PANDA type stress rod Hi-Bi fibre, 2.3c) bow-tie type Hi-Bi fibre stress inducing rods. S is the slow axis and F is the fast axis.

2.2 Fibre Bragg gratings

A fibre Bragg grating (FBG)[2.5, 2.6] is a periodic variation of the refractive index of the core of an optical fibre. The refractive index variation can be induced by exposure of the fibre to a spatially modulated ultra-violet (UV) wavelength intensity pattern, arising from the fibres photosensitivity at that wavelength. The FBG couples optical power from a forward propagating mode to a backward propagating mode at a wavelength corresponding to the periodicity of refractive index modulation, while all other wavelengths are allowed to pass through. Therefore, the grating acts as a wavelength selective coupler, the selected wavelength is known as the Bragg wavelength (λ_{FBG}). In the transmission spectrum a narrow band will be missing. Conversely, when looking at the reflective spectrum, a narrow band will be seen at the wavelength that was missing from the transmission spectrum. Fig. 2.4 Illustrates the spectrum observed of a FBG being illuminated by a broadband source in the transmission spectrum and the band stop effect at the Bragg wavelength is clearly visible. The spectrum was taken during the experimental work undertaken for this project

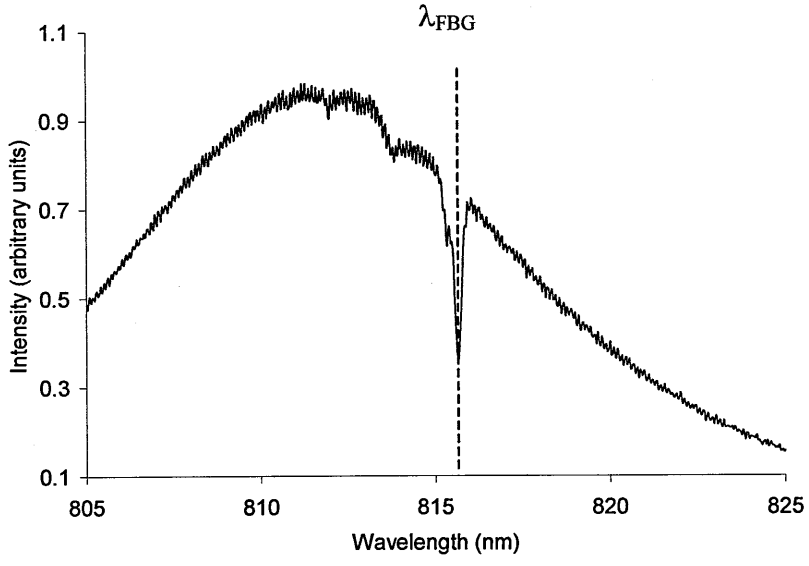

Fig 2.4 Spectrum of a Bragg grating when illuminated by a broadband optical source. The dotted line shows the band stop Bragg wavelength in the spectrum.

2.2.1 Bragg grating principles

Fibre Bragg gratings are a periodic change in refractive index within the core of the fibre, phase matched optical power from each modulation of refractive index is coupled into a reverse propagating fibre guided mode. This produces a reflection of the wavelength satisfying the Bragg condition below:

$$\lambda_{FBG} = 2n_{eff}\,\Lambda \qquad (2.3)$$

λ_{FBG} is the wavelength of the peak reflectivity of the grating, n_{eff} is the effective refractive index of the mode propagating in the fibre and Λ is the periodicity of the grating. Its output is near Gaussian in spectral profile[2.6]. Fig 2.5, demonstrates its principle of operation.

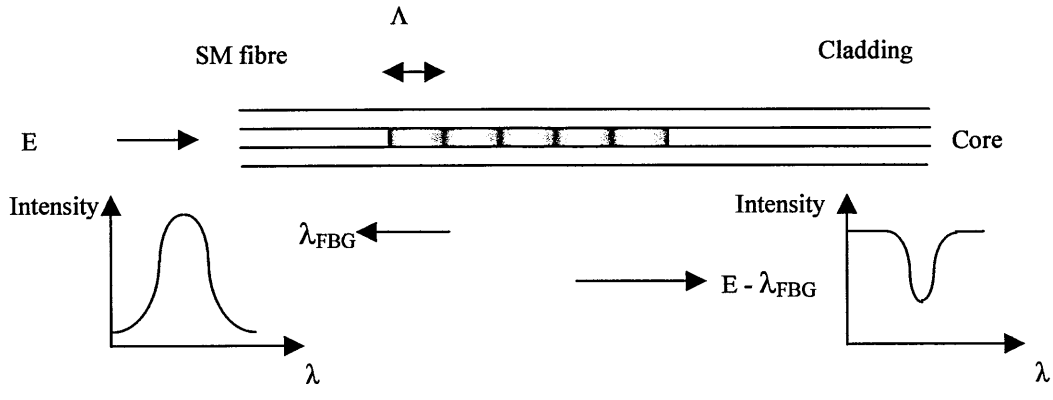

Fig 2.5 Schematic of the operating principle of a Bragg grating. E is the spectrum of the illuminating light.

The amplitude of the periodic variation of refractive index and the length of the FBG govern the reflectivity and bandwidth of the grating at the Bragg wavelength. For a FBG

with constant period and modulation amplitude, the peak reflectivity of the grating, R_{FBG}, is given by the following equation[2.5]:

$$R_{FBG} = \tanh^2(\Omega l) \tag{2.4}$$

Where l is the physical length of the grating and Ω is the backwards coupling coefficient corresponding to a sinusoidal periodic variation in refractive index for a given amplitude variation in refractive index Δn, which is typically 10^{-5} to 10^{-6} [2.6], Ω is given by[2.6]:

$$\Omega = \frac{\pi \Delta n}{\lambda_{FBG}} M_p \tag{2.5}$$

Where M_p is the fraction of the fundamental mode intensity within the fibre core, which can be approximated as $1-V^{-2}$, V is the normalized frequency of the fibre as shown in Eq (2.2). Therefore, the reflectivity is related to the amplitude of the variation of the refractive index and to the length of the grating. The higher Δn and the longer the FBG, the higher the reflectivity. Reflectivities of between 0.1% and 100% have been obtained experimentally at a range of Bragg wavelengths[2.7]. The bandwidth of the Bragg wavelength spectrum is also controlled by the length of the grating and by the amplitude of refractive index modulation along the core of the fibre. An equation for the FBGs approximate full-width-half-maximum (FWHM) is given in (2.6)[2.8]:

$$\Delta\lambda = \lambda_B \zeta \sqrt{\left(\frac{\Delta n}{2n_0}\right)^2 + \left(\frac{1}{N}\right)} \tag{2.6}$$

Where N is the number of grating planes, the change in refractive index, Δn, of the grating is taken into account in the equation by ζ, which is given a value of ~ 1 for FBGs near 100% reflectivity and ~ 0.5 for weak reflective gratings. As shown in equation (2.5),

the longer the grating the narrower the bandwidth, however, the greater the amplitude of refractive index modulation the broader the FWHM of the FBG. Typically FWHMs of FBGs are within the range 0.1-0.5 nm. Side bands to the Bragg wavelength can often be seen in the reflected spectrum of FBGs. These side bands are due to multiple reflections to and from opposite ends of the length of the grating. This effect can be suppressed by using apodized FBGs, which are fabricated with the amplitude of the refractive index modulation varying over the length of the grating thus reducing reflections between opposite ends of the FBG[2.9]. Other variations on the standard FBG are available including the chirped grating in which the period of the FBG is varied along the length of the grating. Chirped gratings are of particular use in telecommunications for dispersion compensation[2.10]. Blazed Bragg gratings feature the periodic modulation of refractive index at an angle to the fibre axis thus coupling light out of the fibre core into cladding modes, which can be used for filtering out unwanted frequencies[2.11]

2.2.2 Strain and temperature sensitivity of FBGs

The central wavelength of FBGs is sensitive to external environmental parameters such as strain and temperature. The Bragg wavelength depends on the periodicity of the grating and on the effective refractive index of the core; both of these parameters can be altered by changes in strain and temperature and this relationship is linear. Equation (2.7) relates the change in wavelength to the applied strain and temperature[2.6].

$$\lambda_{FBG} = 2\left(\Lambda\frac{\delta n_{eff}}{\delta l} + n_{eff}\frac{\delta\Lambda}{\delta l}\right)\Delta l + 2\left(\Lambda\frac{\delta n_{eff}}{\delta T} + n_{eff}\frac{\delta\Lambda}{\delta T}\right)\Delta T \qquad (2.7)$$

λ_{FBG} is the Bragg wavelength, n_{eff} is the effective refractive index, Δl is the change in length of the grating, Λ is the periodicity of the grating, and ΔT is temperature. The first term shows the influence of axial strain, applied longitudinally with fibre, on the wavelength reflected from the FBG. This corresponds to a change in the grating period and the strain-optic induced refractive index change. The 2nd term of the equation

illustrates the effect of temperature change on an optical fibre. The change in the Bragg wavelength is due to thermal expansion changing the grating period and the refractive index. Considering only the strain effect, the Bragg wavelength can be expressed by the following equation[2.12]:

$$\Delta\lambda_B = \lambda_B(1-p_e)\varepsilon_z \tag{2.8}$$

Where ε_z is the magnitude of strain applied, p_e is the effective strain-optic constant, defined as[2.6]

$$p_e = \frac{n_{eff}^2}{2}[p_{12} - \nu(p_{11}+p_{12})] \tag{2.9}$$

ν is Poisson's ratio, and p_{11} and p_{12} are components of the strain-optic tensor. Typical values for these in a germanosilicate fibre are $p_{11} = 0.113$, $p_{12} = 0.252$, $\nu = 0.16$ and $n_{eff} = 1.482$[2.6].

Thermal expansion also alters the grating period of the fibre. The change in wavelength of the Bragg grating is represented by (2.10).

$$\Delta\lambda_B = \lambda_{FBG}(\alpha_\Lambda + \alpha_n)\Delta \tag{2.10}$$

α_Λ is the thermal expansion coefficient of silica fibre, (approximately $0.55*10^{-6}$ for silica)[2.6]. α_n represents the thermo-optic coefficient (approximately $8.6*10^{-6}$ for silica-core germania-doped fibre, at room temperature)[2.6].

$$\alpha_\Lambda = \left(\frac{1}{\Lambda}\right)\left(\frac{\delta\Lambda}{\delta T}\right) \tag{2.11}$$

$$\alpha_n = \left(\frac{1}{n_{eff}}\right)\left(\frac{\delta n_{eff}}{\delta T}\right) \tag{2.12}$$

The diagram below illustrates the responsivity of FBGs to both strain and temperature as well as their linear response to these two parameters.

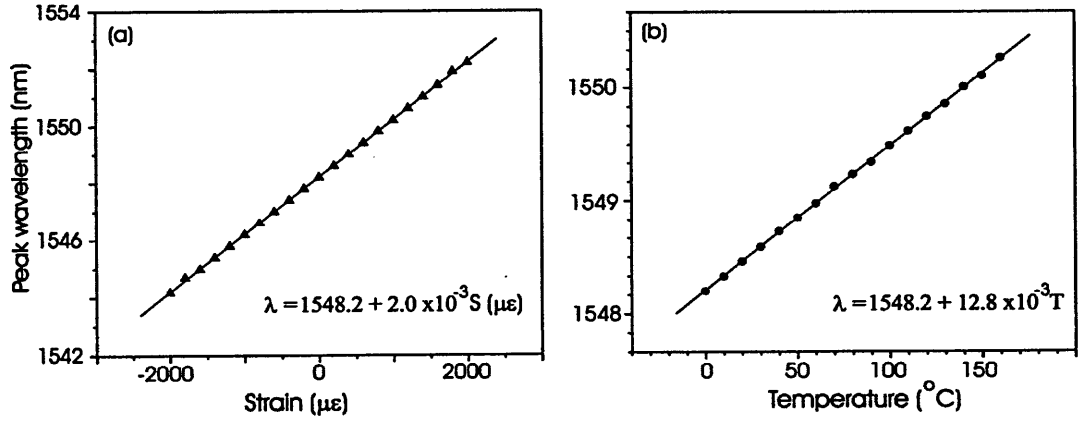

Fig. 2.6 Spectral response of the Bragg grating[2.6] a) under application of stress, b) under varying temperature conditions for an FBG fabricated at 1550 nm.

2.2.3 Transverse strain of FBGs

When a FBG is fabricated in polarisation maintaining fibre, two Bragg wavelengths are formed due to the different refractive index of each of the eigenaxes. This is illustrated in Fig. 2.6. The separation of the two Bragg wavelengths is a function of the birefringence, the higher the birefringence, the larger the separation between the Bragg wavelengths. When transverse strain is applied orthogonally to the direction of the fibre core, it has the effect of increasing the birefringence. In Hi-Bi fibre however the strain and the direction in which it is applied can be measured by monitoring the Bragg wavelength separation, $\Delta\lambda_{FBG,}$ and as such has been proposed as a multi-axis strain sensor[2.13]. Transverse strain applied to Hi-Bi fibre will alter the birefringence of the fibre by an amount directly

proportional to the amount of strain applied transversely and the relative angle the load is applied to the birefringence axes, thus changing the λ_{FBG} separation.

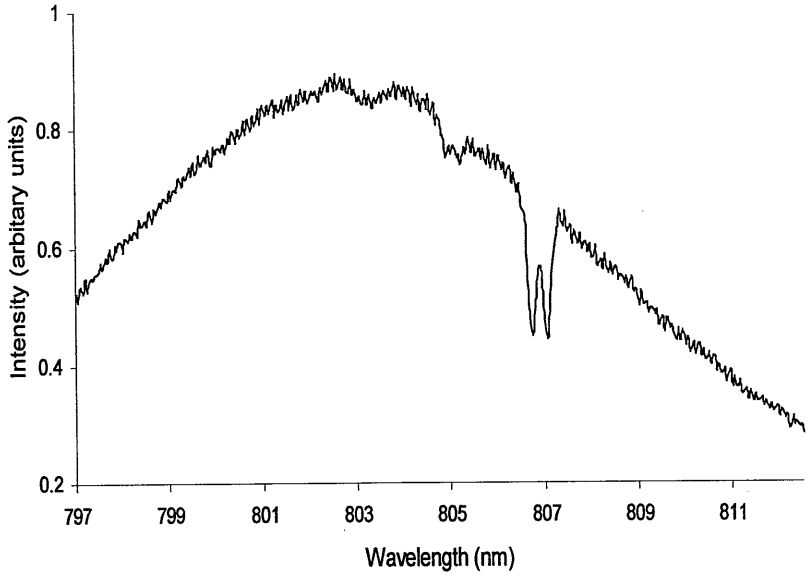

Fig. 2.7 Transmission Spectrum of an FBG fabricated in Hi-Bi fibre, viewed in transmission when illuminated with a broadband source. The FBG shown was fabricated in Fibrecore bow-tie HB750. The λ_{FBg} separation is approximately 0.3nm.

Axial strain applied to a Hi-Bi grating will shift both the Bragg wavelengths in the same way as shown in Fig. 2.6, but the difference between the Bragg wavelengths of either eigenmode will not change, as both modes are being subjected to the same strain. Transverse strain has the effect of altering $\Delta\lambda_{FBg}$ as the refractive index will increase in the eigenmode which lies in the plane of applied strain due to the strain-optic effect. Conversely, in the eigenmode perpendicular to the direction of applied strain a decrease in refractive index will occur, due to an opposing effect, less sensitive than compressive strain. The two orthogonally polarised Bragg wavelengths shift under transverse strain is given by the equations below[2.14]

$$\frac{\Delta\lambda_2}{\lambda_{2,i}} = -\frac{n_0^2}{2}\left[p_{11}\varepsilon_2 + p_{12}\varepsilon_3\right] \tag{2.13}$$

$$\frac{\Delta\lambda_3}{\lambda_{3,i}} = -\frac{n_0^2}{2}\left[p_{11}\varepsilon_3 + p_{12}\varepsilon_2\right] \tag{2.14}$$

where ε_2 and ε_3 are the average transverse strains in the core of the fibre, p_{11} and p_{12} are the strain-optic coefficients for the core, n_0 is the nominal index of refraction of the core and $\lambda_{2,i}$ and $\lambda_{3,i}$ are the initial, unstrained wavelengths of the peaks. The two graphs, Fig 2.8 (a) & (b) show the Bragg wavelengths as the FBG is subjected to transverse strain. Hi-Bi fibre which has a shorter beat length will have a larger separation of the Bragg wavelengths, a fibre with a beat length of 1.6 mm will produce a Bragg separation of 0.3 nm and $\Delta n \approx 0.5*10^3$. The shift in either λ_{FBG} is linear, although for a given direction of strain application the sensitivities are different. This can be expected as the transverse strain will produce compressive strain in the direction of applied strain and an opposing tensile strain perpendicular to the direction of applied strain[2.14] in the same way as boron doped rods induce the permanent birefringence in the fibre during manufacture.

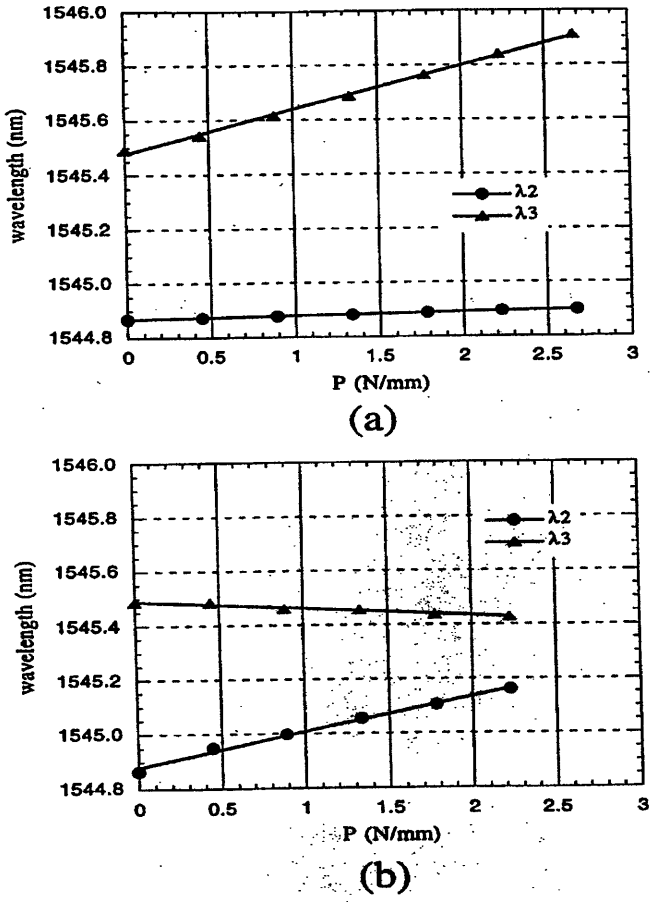

Fig 2.8 The response of a FBG fabricated in Hi-Bi fibre to transverse strain applied from (a) $\theta = 0°$, slow axis and (b) $\theta = 90°$, fast axis. Uncoated 3M-PS-6621 fibre was used, results reproduced from (2.13)

2.2.4 Fibre Bragg grating fabrication

Photosensitivity of optical fibres was first discovered during experiments on germania-doped silica fibre[2.5]. During these experiments studying non-linear effects using a high intensity beam, it was noticed that attenuation increased in the fibre and a reflection from the fibre developed over time. Under analysis, it was deduced that a standing wave was forming in the fibre, produced by the interference between the 488 nm laser light

launched into the fibre and the Fresnel reflection from the cleaved distal end of the fibre. The maxima intensity points of this standing wave changed the refractive index within the fibre permanently. The induced periodic variation in refractive index along the fibre had the same spatial periodicity as the standing wave formed between the laser beam and its Fresnel reflection from the end of the fibre, therefore an FBG was being formed at the wavelength of the illuminating laser beam, 488 nm. The amplitude of the reflection grew with time while the fibre was irradiated with the high intensity beam, until a saturation point was reached. FBGs of this kind were known as self organising or self induced, due to their spontaneous formation. Estimates of the amplitude of modulation of the refractive index across the FBG periodicity (Δn) were 10^{-5} to 10^{-6} and the FBG had a bandwidth of >200 MHz, which equates to a length of ~ 1 m. Initially FBGs could only be fabricated at limited wavelengths[2.6]. However, subsequent experimental work by Stone[2.7] demonstrated that any germania-doped silica fibre was photosensitive in the ultra violet (UV) range. The holographic writing technique[2.16] shown in Fig 2.9, in which a two beam interferometer is used to form an interference pattern on the fibre provided the freedom to fabricate the FBG across a wide range of wavelengths[2.12].

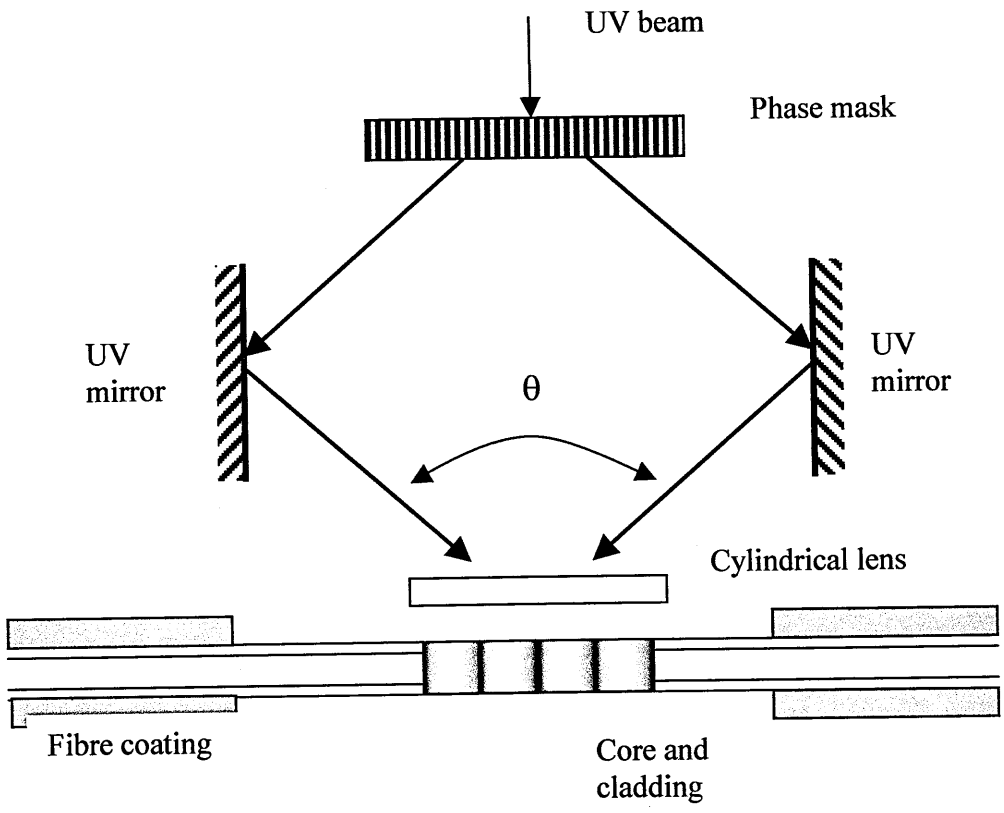

Fig. 2.9 Interference pattern on the fibre of the amplitude splitting holographic FBG fabrication technique[2.6] .

Phase masks, which are diffractive optical elements used to spatially modulate the UV writing beam, are now commonplace to produce gratings at wavelengths set by the pre-made mask[2.15] as the mask lets light through it only in a spatial periodicity determined at the phase masks manufacture. Therefore if the fibre is placed just behind mask for fabrication an interference pattern closely related to the phase masks periodicity is irradiated on the fibre.

Hydrogen loading is also often used in the manufacturing FBGs, it is carried out prior to the UV exposure of the fibre by diffusing H_2 molecules into the fibre at low temperature and high pressure. Exposure to UV irradiation or intense heat will cause the H_2 to react in the glass, typically at Ge sites. This results in a large permanent refraction

index change[2.16]. This technique has been proven with any GeO_2 doped fibre and does not require any special processing techniques.

The FBGs that have been used in this project have been fabricated using the holographic side writing technique first demonstrated by Meltz et al[2.15]. This method allows the Bragg wavelength of the grating to be chosen independently of the wavelength of the irradiating UV light. The equation (2.15)[2.6] relates the Bragg wavelength of the FBG to the UV writing wavelength and the angle of the intersecting beams.

$$\lambda_{fBg} = \frac{n_{eff}\lambda_{uv}}{\sin\left(\frac{\theta}{2}\right)} \tag{2.15}$$

θ is the symmetrical angle at which the light from the UV mirrors is incident on the fibre, λ_{FBG} is the Bragg reflection wavelength, n_{eff} is the effective refractive index of propagating fibre mode and λ_{uv} is the wavelength of the UV source. Using the holographic technique the Bragg wavelength of the FBG to be fabricated is adjustable across a wide range between near the UV wavelength to microwave limited only by the interferometer configuration.

The laser system used for FBG fabrication in this project consists of an injection seeded Nd:YAG laser, which is pulsed at 25 Hz. The output at 1.064 μm is frequency doubled into the green at 532 nm, and then used to pump a dye laser. The dye laser has a tuneable output, which is operated at around the 633 nm region. The output from the dye laser is then frequency doubled and mixed with some residual 1.064 μm light, which generates tuneable UV radiation in the 240-260 nm range, where fibres are most photosensitive[2.6] tuning the laser wavelength also allows fine tuning of the FBG to be fabricated[2.17].

A phase mask is used as the beam splitter and the two first order diffracted beams are used for each arm of the holographic interferometer. Both beams are reflected off separate mirrors and angled back onto the fibre resulting in an interference pattern on the fibre

corresponding to the Bragg wavelength, the angle of the intersecting beams governs the period interference of the fringes which in turn controls the Bragg wavelength of the FBG. The resulting interference pattern is shown in Fig 2.9.

During fabrication the formation of the FBG can be monitored by coupling the output from a broadband source into a directional coupler with the fibre where the FBG is to be fabricated, and attaching the other arm of the coupler to an optical spectrum analyser as shown in Fig. 2.10. The back reflection from the FBG can then be monitored so the correct parameters of the FBG can be attained.

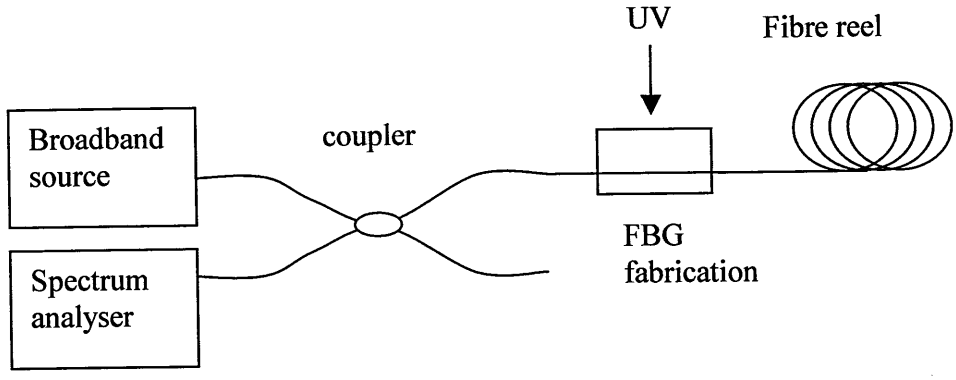

Fig. 2.10 Experimental set up for fabrication of FBGs

For the FBG fabrication used in this project the fibre in which the FBG was being fabricated was connected to the output port coupler, the reflected signal was directed to a monochromator and a 5nm region of the spectrum was monitored using an Ocean optics linescan CCD array. The fibre was prepared by having its jacket removed with fibre strippers so the UV radiation is less attenuated for irradiation of the core of the fibre. The angles of the mirrors and the distance to the fibre are then configured to match the required Bragg wavelength. The reflectivity of the grating was controlled by terminating the fabrication process when the required reflectivity had been obtained, resulting in reflectivities between 10% to around 80%. The FBGs were written into fibre which was hydrogen loaded prior to UV exposure to increase sensitivity.

2.3 Summary

Single mode and Hi-Bi optical fibres have proven to be revolutionary for the telecommunications industry. They also are invaluable for optical sensing and in particular interferometric sensing systems due to their ability to maintain polarisation and resist external interference by external forces.

FBGs act as wavelength selective filters, they can be fabricated at any wavelength and this wavelength can then be tuned non-permanently, post fabrication, by applied temperature or strain. Alternatively by monitoring the Bragg wavelength, the FBG can be used as a sensor.

When FBGs are fabricated in Hi-Bi fibre they have a double Bragg wavelength, one for each polarised eigenaxes of the fibre, the wavelength separation of the two Bragg wavelengths can then be altered by the application of transverse strain, to either reduce or increase birefringence depending on the direction from which the strain is applied.

References:

(2.1) K.C. Kao and G.A. Hockham, 'Dielectric fiber surface waveguides for optical frequencies', Proc. IEE, 1966, Vol. 113, pp. 1151-1158.

(2.2) M. Born and E. Wolf, 'Principles of Optics' 7th edn., Cambridge University Press, Cambridge, 1997.

(2.3) A.H. Badar, T.S.M. Maclean, B.K. Gazey, J.F. Miller and H. Ghafoori-shiraz, 'Radiation from circular bends in multimode and single-mode optical fibres', IEE Proceedings, 1989, Vol. 136, pp. 147-151.

(2.4) J.M. Senior 'Optical fibre communications: principles and practice', 2nd edn. Prentice Hall, 1992.

(2.5) K.O. Hill, Y. Fuji, D.C. Johnson and B.S. Kawasaki, 'Photosensitivity in optical fiber waveguides: Application to reflection filter fabrication', Applied Physics Letters, 1978, Vol. 32, pp. 647-649.

(2.6) Othonas and Kalli. 'Fiber Bragg gratings: fundamentals and applications in telecommunications and sensors' Artech House, London 1999.

(2.7) J. Stone, 'Photorefractivity in GeO_2-doped silica fibers', Journal of Applied Physics, 1987, Vol. 62, pp. 4371-4374.

(2.8) P. St. J. Russell, J.L. Archambault and L. Reekie, 'Fibre gratings' Physics World, October 1993, pp. 41-46.

(2.9) R. Kashyap, A. Swanton and D.J. Armes, 'Simple technique for apodising chirped and unchirped fibre Bragg gratings," Electronics Letts., Vol. 32, 1996, pp. 223-225.

(2.10) F. Ouellette, 'Dispersion cancellation using linearly chirped Bragg grating filters in optical waveguides', Optics Letts., Vol. 12, 1987, pp.847-849.

(2.11) R. Kashyap, R. Wyatt and P.F. McKee, 'Wavelength flattened saturated erbium amplifier using multiple side-tap Bragg gratings', Electronics Letts., Vol. 29, 1993, pp. 1025-1026.

(2.12) G. Meltz and W.W. Morey, 'Bragg grating formation and germanosilicate fiber photosensitivity,' International workshop on photoinduced self-organization effects in optical fiber, Quebec City, Quebec, May 10-11, proceedings SPIE, 1991, Vol. 15, pp. 185-199.

(2.13) W.L. Schultz, E. Udd, J.M. Seim, I. Perez and A. Trego, 'Progress on monitoring of adhesive joints using multiaxis fiber grating sensors', Smart structures and materials 2000: Industrial and commercial applications, Proc. SPIE, 2000, Vol. 3991, pp. 52-61.

(2.14) C.M.Lawrence, D.V. Nelson, E. Udd and T. Bennet, 'A fibre optic sensor for transverse strain measurement', Experimental Mechanics, Sept. 1999, Vol. 39, pp. 202-209.

(2.15) G. Meltz, W.W. Morey, and W.H.Glenn, 'Formation of Bragg gratings in optical fibres by a transverse holographic method' Optics Letters, 1989, Vol. 14, pp. 823-825

(2.16) P.J. Lemaire, R.M. Atkins, V. Mizrahi and W.A. Reed, 'High pressure H_2 loading as a technique for achieving ultra UV photosensitivity and thermal sensitivity GeO_2 Doped optical fibres', Electronics Letters, 1993, Vol. 29, pp. 1191-1193.

(2.17) M.L. Dockney, S.W. James and R.P. Tatam, 'Fibre Bragg gratings fabricated using a wavelength tuneable laser source and a phase mask based interferometer' Measurement science and technology. 1996, v. 7, pp. 445-448.

3: Semiconductor Lasers

The acronym LASER stands for Light Amplification by Stimulated Emission of Radiation. Einstein theoretically predicted the laser in 1917[3.1] when he proposed stimulated emission. The first laser action in a semiconductor was observed in 1962 by using a p-n junction diode[3.2]. Since then there has been a large research effort expended in the development of laser systems, and in their applications. The reason for this level of interest in the laser is its unique properties including coherence, brightness, directionality, monochromaticity and the ability to produce very short pulses of light. The most common and cheapest form of laser is the laser diode or semiconductor laser, which has a number of advantages that include:

1) Small size that enables it to be incorporated easily into other instruments.
2) Direct pumping by current injection. The small currents involved make it possible to drive with conventional transistor circuitry.
3) High efficiency, operating efficiency can exceed 50%.
4) High speed modulation of the injection current is possible.
5) Devices can be engineered into integrated optoelectronic circuits
6) Mass production is easily achievable with semiconductor based manufacturing technology developed for the electronics industry.
7) Outputs can be easily spectrally and spatially tailored to suit fibre-optic technology.
8) They are available in a wide range of wavelengths, from blue to far infra red.

3.1 The principles of operation of the semiconductor laser

In the following sections the principles of operation of the semiconductor laser will be addressed, its basic design and the improvements to its design since its inception. The laser needs to utilise stimulated rather than spontaneous emission for its narrow band

coherent output therefore conditions must be met that allow stimulated emission to dominate[3.2]. In order for stimulated emission to occur population inversion must take place so that the population of electrons on the upper energy level is much higher than the lower level. The process of creating this non-equilibrium distribution is known as pumping. The method used for pumping in a semiconductor laser is by direct application of an electric current. A semiconductor energy level diagram is shown in Fig 3.1

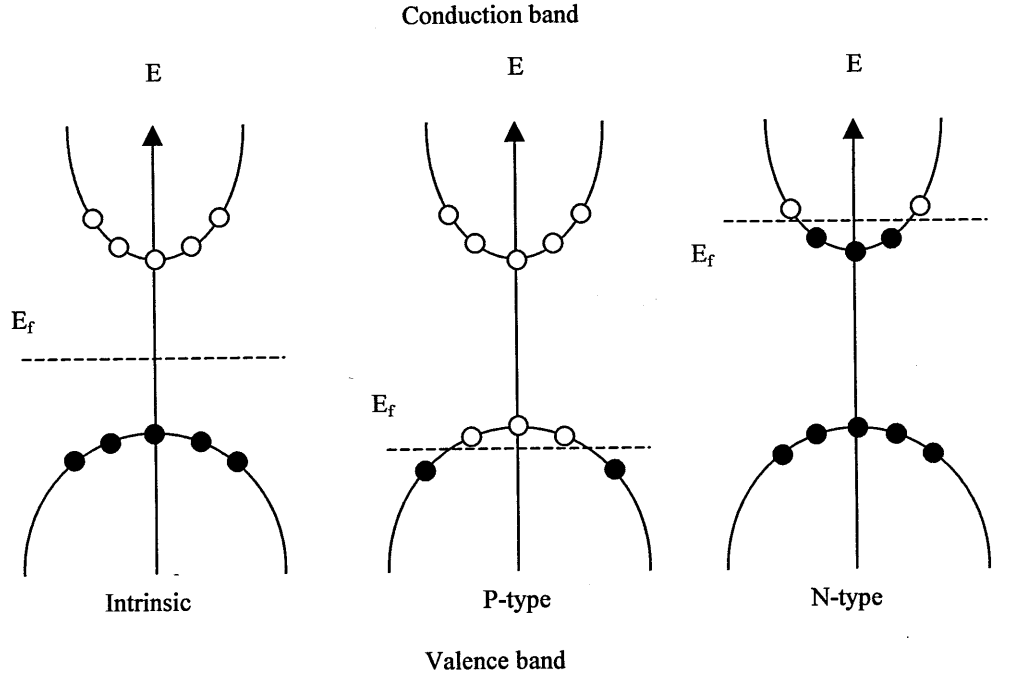

Fig 3.1 Semiconductor energy levels at 0K, E_f is the Fermi level, from left to right Intrinsic, p-type and n-type. The white dots are holes, the black dots are electrons.

At low temperatures all energy states in the valence band are occupied while all energy states in the conduction band are vacant. Thermal excites electrons across the bandgap leaving space in the valence band allowing electrical conduction to take place. Doping with a donor, n-type, impurity provides a surplus of electrons, pushing the Fermi level into the conduction band. Doping with an acceptor, p-type, produces an excess of holes pushing the Fermi level into the valence band. At higher temperatures there are Quasi-

Fermi levels for both the valence and conduction bands, allowing electrons to move up to the conduction band by absorption. Quasi-Fermi levels are illustrated in Fig. 3.2

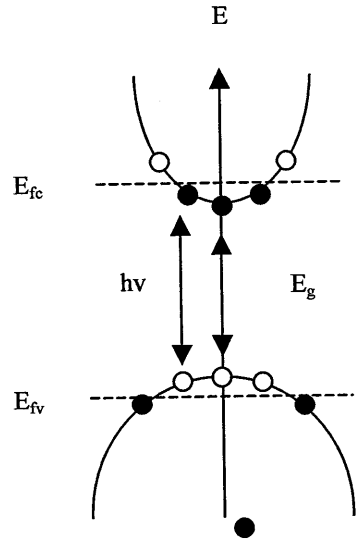

Fig. 3.2 Semiconductor energy levels when temperature is above 0K

The reverse transition results in the emission of a photon. Photons incident on the material with energy higher than the bandgap but lower than the separation of the quasi-Fermi levels can not be absorbed by the material but can induce the transition of an electron from the conduction to valence bands, creating a photon coherent with the incident photon, which leads to lasing.

3.1.1 The p-n junction

A semiconductor laser is formed between two layers of semiconductor material, one doped positively with an excess of acceptor impurities, holes, in the lattice and the other doped negatively with an excess of donor impurities, electrons. When the two types are brought together electrons diffuse across the junction form the n-type to the p-type and

holes from p-type to n-type. This brings the Fermi levels to the same levels for the two materials, further diffusion is prevented by this step and a depletion layer is formed. The depletion layer is free of mobile charge carriers, creating a potential barrier between the p and n regions. When an external positive voltage is applied to the p-type region the potential barrier and width of the depletion region are reduced. As the current is injected electrons can flow from the n-type material, and holes flow from the p-type material to the opposite region. This is illustrated by Fig. 3.3

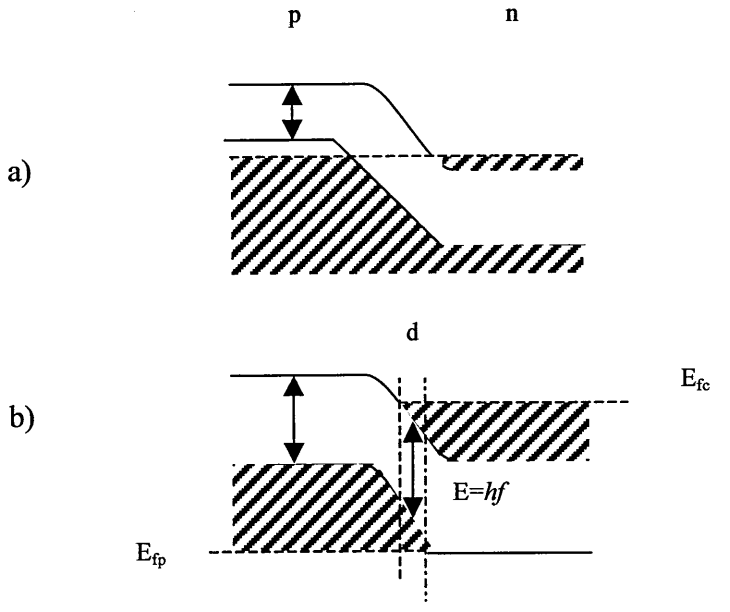

Fig. 3.3 p-n junction a) with no bias applied, b) with forward bias current applied. D is the overlap of the electron and hole population.

The two Fermi levels are separated with the forward bias, the potential barrier in the depletion region is reduced in height and there is overlap between the hole and electron populations and population inversion has occurred.

The forward bias applied to a p-n junction is shown in Fig 3.4

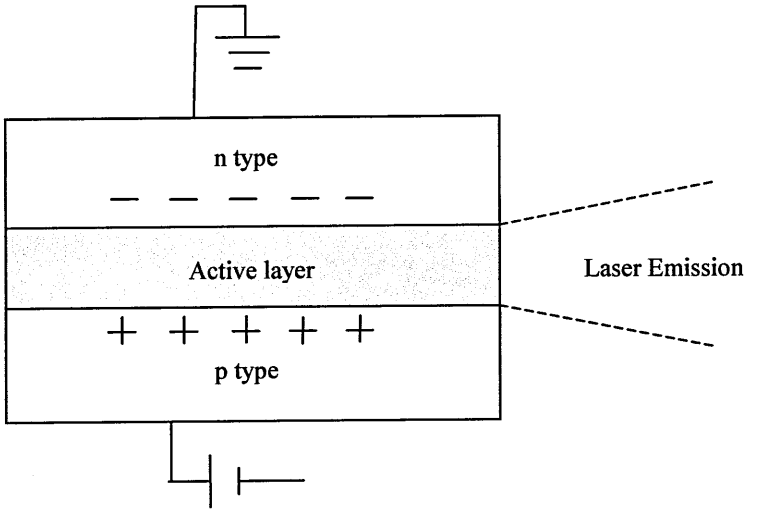

Fig. 3.4 The active region formed between p and n doped layers

As the carriers recombine across the depletion region emission of light is possible. The wavelength at which the particular semiconductor emits light at is governed by the band gap energy between the valence and conduction electron bands given by the equation (3.1) where E is energy, h is Planck's constant and ν is optical frequency.

$$E = h\nu \qquad (3.1)$$

Heterojunction structures are made of two different semiconductor materials, which differ in bandgap energy and refractive index. They are advantageous over p-n homojunctions as they require lower injection currents as there is a refractive index difference in the depletion region it increases radiation confinement as it is an optical waveguide[3.3]. Double heterojunction (DH) structures again improved optical confinement and reducing required injection currents lower again by a factor of 100[3.4]. Heterojunction

structures are capable of operation under pulsed conditions at room temperatures while DH structures are capable of continuous wave (CW) output at room temperatures due to their increased carrier and optical confinement. Fig 3.5 illustrates the operation of a double heterostructure junction laser diode. As well as increased optical confinement. The injected holes and electrons are confined in the active layer increasing population inversion for a given injection current.

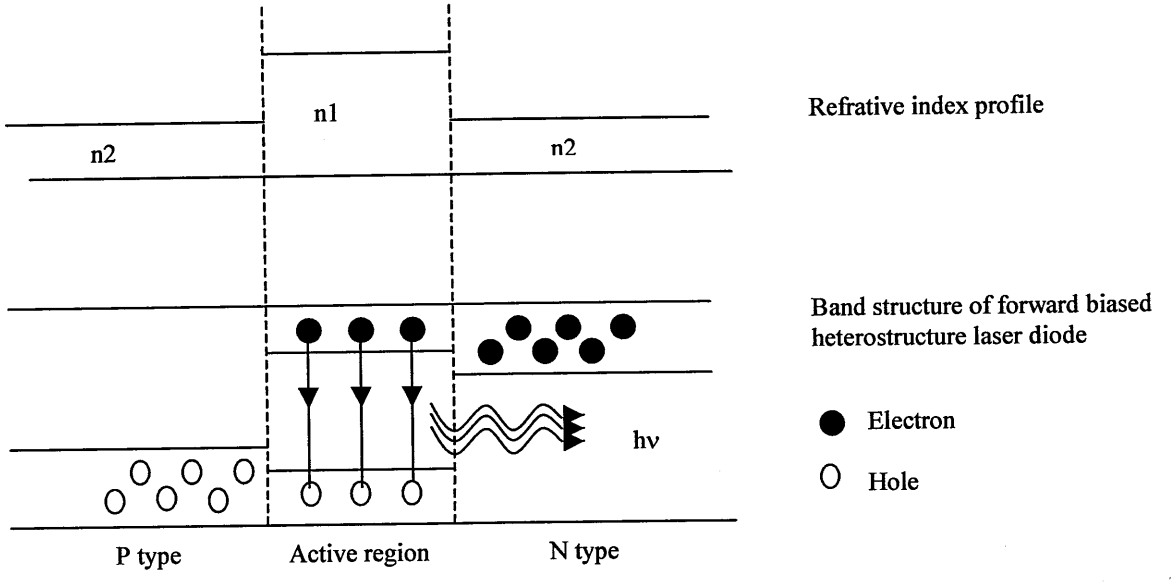

Fig 3.5 double heterostructure profile

Multiquantum-well structures[3.5] use a very narrow active layer of around 10 nm, which reduces the carrier motion. They demonstrate reduced threshold narrower linewidths, lower frequency chirp and less temperature dependence due to the better confinement of the optical mode.

3.1.2 The Fabry-Perot cavity

The amplification achieved by passing light of a compatible frequency through a forward biased p-n junction is often relatively small; around 10% per meter[3.4]. This can be improved by having highly reflecting surfaces on the ends of the pumped medium. The light then passes through the pumped medium multiple times. This form of optical cavity is called a Fabry-Perot resonator. When there is high optical intensity and a high degree of population inversion due to injection current pumping stimulated emission can dominate over spontaneous emission. The lasing threshold is marked by a sharp increase in the optical power output versus injection current input known as the I-P curve, as stimulated emission begins to dominate, shown in Fig. 3.6 below

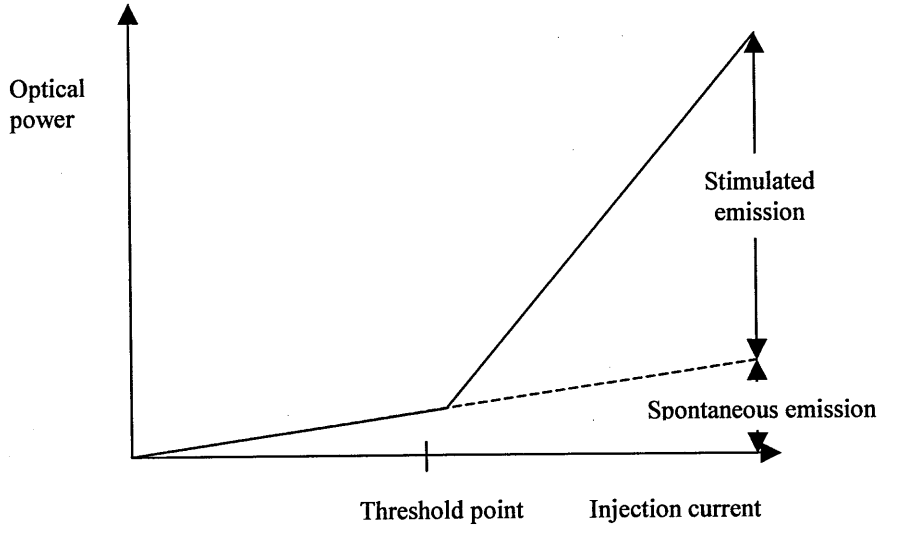

Fig 3.6 Injection current versus optical output power for a typical laser diode

The threshold current, I_{th}, can be predicted by Equation 3.2[3.1]

$$I_{th} = \frac{1}{\beta}\left[\bar{\alpha} + \frac{1}{2L}\ln\frac{1}{r_1 r_2}\right] \qquad (3.2)$$

β Is a gain factor coefficient constant governed by the material used, typically $21*10^{-3}$ [3.6]. $\bar{\alpha}$ is the loss coefficient per metre, r_1 and r_2 are reflectivities of the mirrored ends of the fibre, and L is the length of the active region. The stimulated emission minority carrier lifetime, meaning the time taken for an injected electron to be converted to a stimulated emission photon is much shorter than the lifetime of spontaneous emission. Therefore increases in injection current will result in a high quantum efficiency typically 50-100%, as stimulated emission has a much higher probability, making the output almost entirely stimulated emission. To provide feedback for the laser action two parallel end faces are prepared, usually by cleaving along crystal planes. Often special reflective coatings are not used as the Fresnel reflection is ~32% at an air/semiconductor interface, semiconductors typically have a refractive index of ~3.5 although reflective facets with highly reflective coatings, typically over 90%, improve efficiency and lower the lasing threshold.

Lasers emit a narrow spectrum of optical frequencies, which is a result of the properties of the laser material and of the resonant feedback cavity. Within a defined Fabry-Perot cavity length a discrete comb of wavelengths or resonant modes are allowed to lase. The frequency separation of these modes is given by the following equation [3.1].

$$\Delta\upsilon = \frac{c}{2nL} \qquad (3.3)$$

$\Delta\upsilon$, is the frequency spacing of the modes, n is the refractive index, c is the free space speed of light and L is the length of the laser cavity. Fig 3.7a) illustrates the comb of resonant modes of the feedback cavity. These modes are standing waves that reflect back in phase with themselves and so can be amplified by stimulated emission. The natural luminescent band of the materials used in forming the depletion region will have a distributed lineshape particular to those materials Fig. 3.7b) shows the combined result.

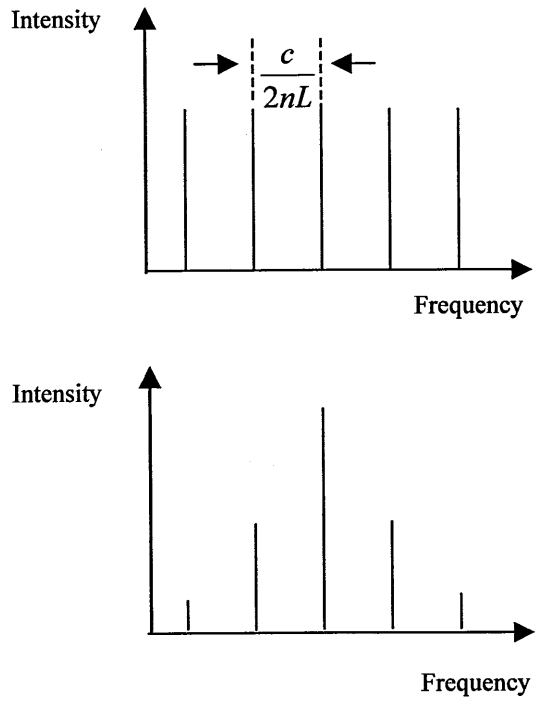

Fig. 3.7 a) Modes of the Fabry-Perot laser cavity. b) Modes combined with luminescence band of semiconductor material

For example, in a cavity of length 300 μm and of refractive index of 3.5, the longitudinal modes will be spaced by 142 GHz or approximately 0.3 nm at 800 nm. The width of the Fabry-Perot cavity is also important and a double heterojunction which comprises three layers, P-P-N, structure should have a narrow enough stripe geometry, typically 0.4 μm, to allow only the fundamental transverse mode to be supported, removing any high order transverse modes which could interfere with the longitudinal modes.

3.2 Semiconductor laser characteristics

The standard semiconductor laser has characteristics that are often relevant to the optical system into which the laser is being integrated. The following sections are concerned with these characteristics.

3.2.1 Linewidth and frequency shift

Single mode operation occurs when only a single longitudinal mode exists, therefore making the linewidth of the laser very narrow. However, linewidth and wavelength shift effects can affect performance further. The cavity amplifies standing waves; therefore changes in temperature will expand or contract the cavity and change the refractive index, which in turn will affect the wavelengths at which the cavity is resonant. The result is that changes in temperature will also shift the operating wavelength. Applying an electrical current to the amplifying medium also has an effect by changing the refractive index of the material. This is due to the strong coupling between the free carrier density and the index of refraction that is present in any semiconductor structure[3.7]. Therefore, even small changes in carrier density will produce a phase shift in the optical field, giving an associated change in the resonance frequency[3.1]. The change in the wavelength is typically 0.3 nm/°C, and 0.05 nm/mA. Therefore if a stable operating wavelength is required, careful control of current and temperature is required. Linewidth of lasing F-P structure laser diodes is often in the 30 MHz region [3.1] which corresponds to a coherence length of 10 m. However, this change in wavelength with injection current means the laser can be chirped under varying injection current conditions.

The linewidth of the laser also changes under different output powers, spontaneous emission is the dominant source of noise in laser diodes and is responsible for the variation in the phase of the laser output as well changing the gain of the active cavity which will alter the refractive index further increasing the phase noise which is the rate of deviation in phase and will shorten the coherence length of the laser[3.9]. Therefore as the output power of the laser increases spontaneous emission is less significant and laser linewidth narrows.

Laser diodes are also prone to phenomena known as spectral and spatial hole burning, both result in multi-mode operation and a decrease in side mode suppression ratio. Spectral hole burning is a reduction in the gain in a central lasing mode due to a depletion in electrons at that wavelength, which results in an increase in intensity of the side modes to that central mode. Semiconductor lasers are usually considered as homogeneously

broadened amplifiers but a large number of modes exist within the gain curve and the modes closer to the centre wavelength will experience greater gain saturation. Each electron transition at the lasing wavelength will cause a reduction in gain at that wavelength causing the spectral hole. The width of the spectral hole is the order of $1/\tau_{in}$ where τ_{in} is the intra band relaxation time[3.10] and is in the order of $1\text{-}3*10^{-13}$ for both GaAs and InGaAsP devices. The development of spectral hole burning as gain increases is show in Fig. 3.8, ΔG is the gain difference between adjacent optical modes λ_0 and λ_1.

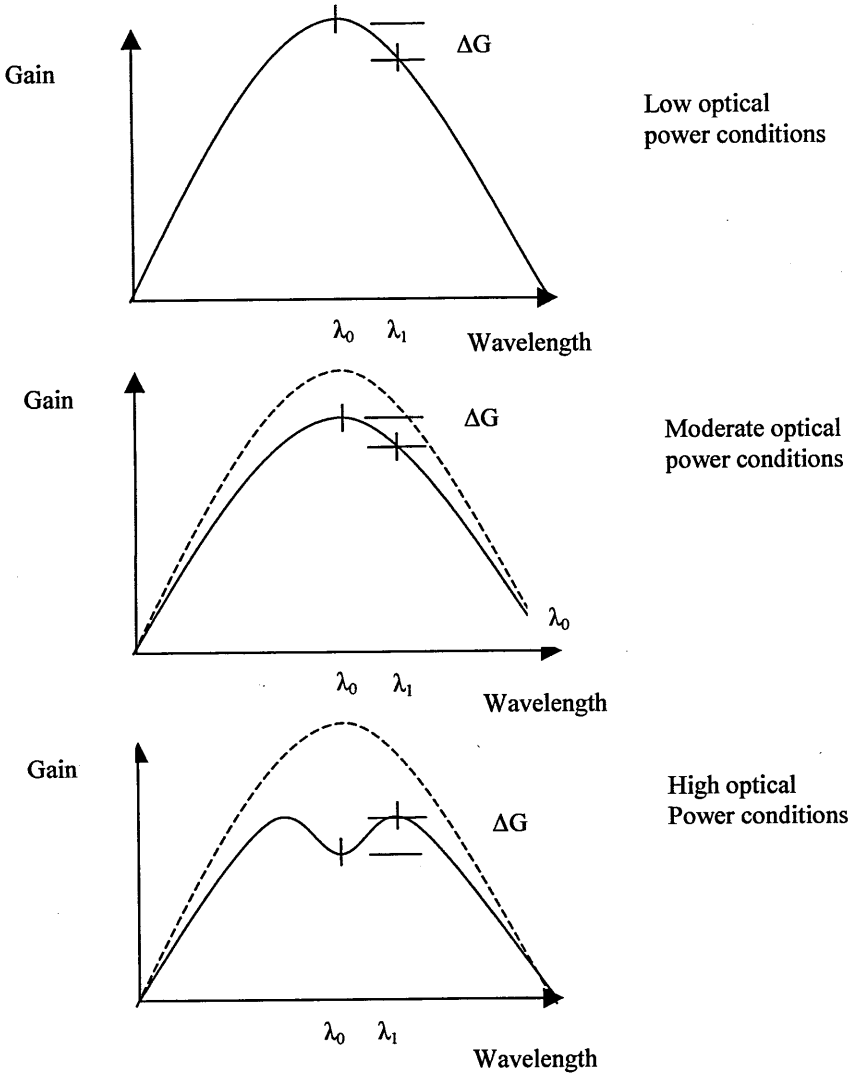

Fig 3.8 The effect of spectral hole burning under varying optical power conditions[3.7]

Spatial hole burning is caused by un-even carrier diffusion across the active cavity. Uneven carrier consumption can cause a reduction in gain in the centre of the active cavity and some standing waves are then subject to a different gain to other standing waves. When two waves propagate in the active medium they will interfere and increase this effect of gain saturation over a larger area within the amplifying medium. As with spectral hole burning, spatial hole burning the hole will deepen under increased optical intensity[3.11]. The carrier density and corresponding optical intensity in an active cavity is shown below in Fig. 3.9.

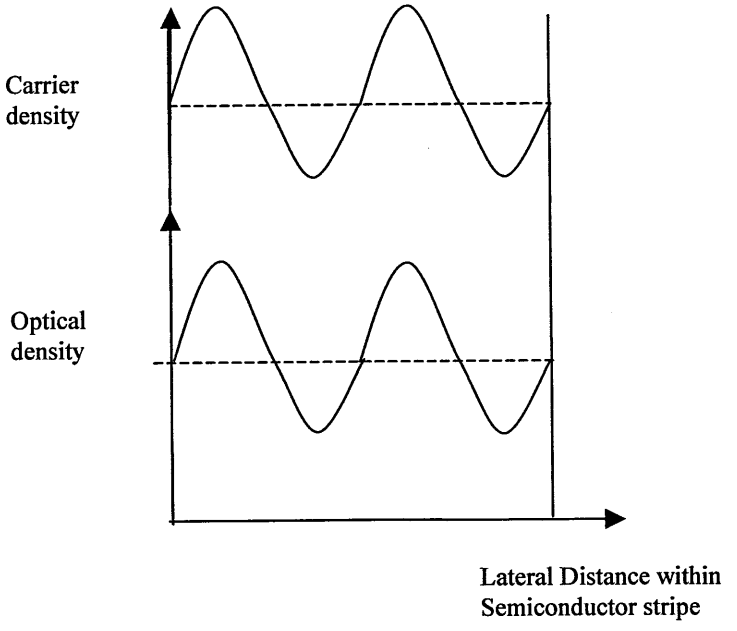

Fig 3.9 Optical intensity with carrier density within the active cavity of the laser diode

3.2.2 Mode hopping

As the injection current is increased a single mode laser diode can hop from one longitudinal mode to another. It is the result of increases in temperature of the device junction and injection current induced index change[3.1]. The change in refractive index with injection current is linear but mode hopping is not a continuous effect and will

suddenly occur between small changes in injection current. As well as frequency hops mode hops can also be observed as power fluctuations in the optical power verses injection current graph. Between mode hops, temperature and current change still cause drift in the wavelength as discussed in the previous section.

3.2.3 Noise in semiconductor lasers

Noise in laser diodes manifests itself in the forms discussed above, namely wavelength drift and mode hopping. Laser diode control systems have been developed with highly stable currents and thermoelectric cooling and can often reduce or remove these effects[3.1]. However, phase noise is intrinsic to all lasers, it is caused by random and discrete spontaneous emission that results in intensity fluctuations the spontaneous emissions are however an inevitable atomic aspect of the lasing process. Phase noise directly affects the coherence length and linewidth of the laser. As phase noise increases, linewidth will increase and the coherence length will decrease. Changes in intensity of the output of the semiconductor laser can be the result of temperature variations or spontaneous emission in the cavity, these fluctuations are referred to as relative intensity noise (RIN). Typically, RIN for a single mode laser diode would be - 130 to -160 dB/Hz, although RIN decreases as injection current is increased[3.12].

3.3 Techniques for achieving single mode operation and wavelength tuneability in semiconductor lasers.

Transverse modes can be controlled by strip geometry[3.1], the narrowing of the active cavity which decreases the probability of transverse modes, but longitudinal multi-mode operation can still exist. Therefore several techniques have been developed to make single mode and mode hop free operation of the laser more probable. Over the next sections these techniques will be introduced and their merits and detracting factors discussed. One

of the first methods was the use of a shortened laser cavity[3.13] (>50 μm), improving longitudinal mode selection due to the increased spacing between these modes. This technique met with little success due to the difficulty in handling such short cavities and their relatively low output power[3.14].

3.3.1 Cleaved coupled cavity lasers (C^3)

Cleaved coupled cavity (C^3) lasers employ two longitudinally separated active cavities as shown in Fig. 3.10, the gap between the cavities being in the region of a single wavelength. Cleaving a completed laser chip into two sections forms the C^3 laser[3.15]. Separately controlling the injection currents and temperature of each cavity along with temperature allowed side mode suppression of >30dB[3.16]. The laser can also be tuned by injection current over a range of 15nm within the injection current range although this occurs with discreet mode hops every 2 nm[3.17, 3.18]. The C^3 laser works on the principle that each cavity is a different size so therefore will have different spacing of cavity resonant frequencies. If a standing wave in each cavity matches then the corresponding wavelength will be amplified significantly more than unmatched wavelengths and therefore achieve a high side mode suppression ratio.

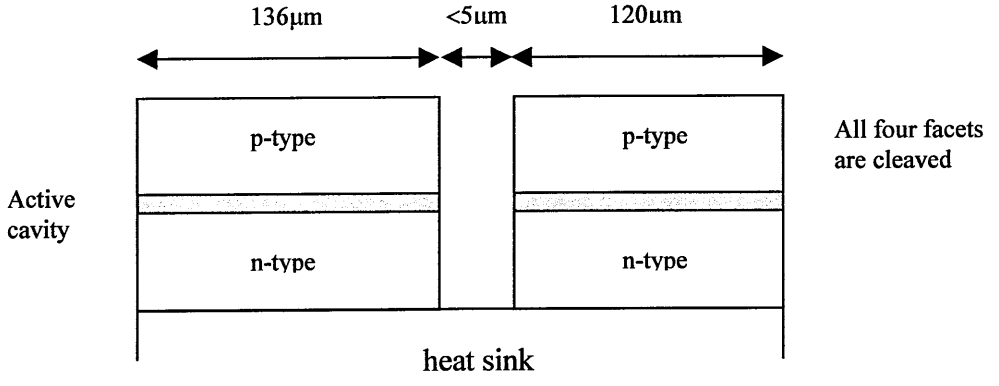

Fig 3.10 Cleaved coupled cavity laser

3.3.2 Distributed feedback (DFB) and distributed Bragg reflector (DBR) lasers

Two techniques employed to obtain single mode operation and tuneability are the use of DBR and DFB lasers. DFB[3.19] and DBR[3.20] lasers are both available commercially. In the DFB laser a Bragg grating is written into the gain cavity by etching, resulting in a periodic variation in refractive index along the cavity in the direction of wave propagation. Feedback of optical energy is achieved through Bragg reflection rather than by reflection from the cleaved facets. Therefore, the period of the corrugation determines the wavelength of the longitudinal mode emission. Fig. 3.11 is a schematic of the DFB laser.

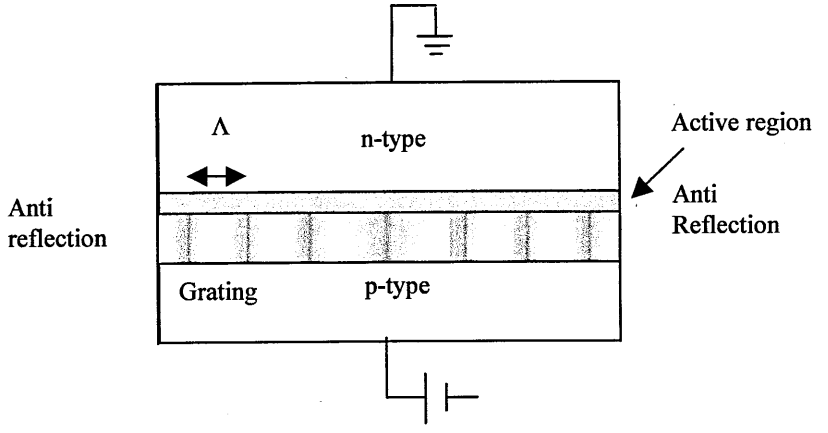

Fig. 3.11 Schematic of a DFB laser

DFBs feature a wavelength shift of λ/4 to facilitate lasing at the Bragg wavelength. To improve efficiency of these devices one facet of the laser often has lower reflectivity than the other facet. This also stops unwanted modes appearing as standing waves will not be allowed between the facets due to their low reflectivity. Narrower linewidths have been

obtained using these lasers, around 3 MHz[3.13] ($2*10^{-5}$ nm) significantly less than a standard Fabry-Perot diode linewidth[2.4] typically ~30 MHz.

The DBR laser has been less extensively researched. In this configuration the grating is etched at the cavity ends so distributed feedback does not occur in the active cavity but rather in the unpumped corrugated ends which act as wavelength selective mirrors. The reflected wavelength satisfies the Bragg condition and determines the operating wavelength of the laser. Fig. 3.12 is a diagram of the DBR laser.

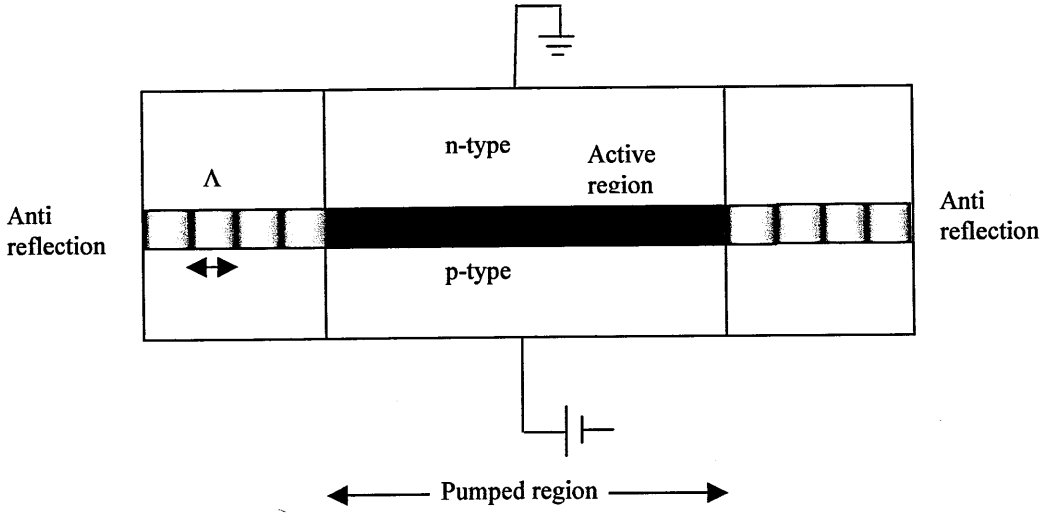

Fig. 3.12 Schematic of DBR laser

Both of these lasers are however significantly more expensive than the basic Fabry-Perot design due to the increased complexity of the wafer. Although single mode operation is achieved, these lasers still suffer from wavelength shift during variation of the injection current resulting in an output chirp, which is a frequency sweep of the output, during pulsed operation. In fact wavelength variation in these lasers has been shown to be greater than for standard laser diodes, responsivity of 100 pm/°C[3.67], in comparison with 30 pm/°C in a standard laser diode. This occurs as DFB lasers have the grating written

into the active cavity, which is subject to a refractive index change and therefore a change in the Bragg wavelength with varying injection current. However DFB lasers do not suffer from mode hops to the same effects as standard laser diodes.

3.3.3 External cavity lasers

External optical feedback is often unwelcome in laser's as it can easily destabilise the spectral and intensity properties of the laser. Optical feedback, however can sometimes be beneficial to laser diodes as a controlling element. It can enable the suppression of side modes[3.21, 3.22] by the same mechanism as the C^3 laser. Wavelength chirp can be reduced as the external cavity is not subjected to the same dynamic changes as the active cavity and linewidth also be narrowed by optical feedback.[3.23]. A degree of frequency tuning can also be achieved, ~1.2 GHz[3.24], depending on the phase condition and hence by varying the length of the external cavity.

3.3.4 External optical feedback

Much work has been done to investigate the effect that an external optical feedback has on the static, dynamic, noise, modulation and spectral characteristics of laser diodes. Therefore, most of these phenomena are well understood. This section will explain some of these effects and the following section will go on to categorise the regimes of operaton[3.25].

Reflected power corresponds to the power re-entering the laser including coupling losses. A pigtailed laser is shown in Fig. 3.13

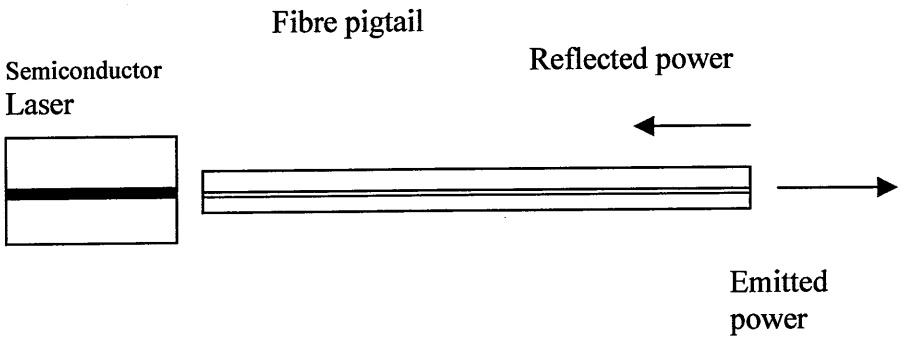

Fig 3.13 Schematic of the concept of feedback from an external reflector

The total feedback is then given by[3.7]:

$$F_{EXT} = \eta^2 \, \mathrm{Re} \tag{3.3}$$

F_{EXT} is the total feedback factor, the coupling efficiency is η, which is from laser to fibre, and Re is the Fresnel reflection at the end of the fibre. This assumes the polarization of the reflected light is identical to the polarization of the laser's emitted light. As the reflection is increased back into the laser cavity the laser threshold G_{th} is altered to G_N according to equation 3.4[3.26].

$$Gn = Gth - |C_e| \frac{\sqrt[2]{F_{EXT}}}{L} \cos(\phi_{ext}) \tag{3.4}$$

Where G_{TH} is the threshold gain of the laser diode without external cavity feedback, $|C_E|$ is the coupling efficiency between the laser and the external cavity and L is the cavity length of the laser diode. The threshold depends on the phase of the reflected light, ϕ_{ex} [3.26]

$$\phi_{ext} = 2\pi \upsilon \tau_{ext} \tag{3.5}$$

where ν is the optical frequency and the external cavity round trip time is $\tau_{ext.}$. Changes in ϕ_{EXT} can cause considerable changes in the required threshold gain[3.26].

The external cavity may introduce additional modes, due to the narrowing of mode separation in the longer external cavity. The linewidth enhancement factor, describing the effect of the carrier density on the refractive indices, must now be introduced, given by equation 3.6[3.27].

$$\alpha = -\frac{4\pi}{\lambda}\frac{\delta n / \delta N}{\delta g / \delta N} \tag{3.6}$$

Where α is the linewidth enhancement factor, λ is the lasing wavelength and δg/δN is the differential gain. The change in refractive index is over the whole length of the cavity L_S. δn/δN is the differential refractive index across the cavity. In an external cavity laser, only the semiconductor part of the device is active, reducing the effect of the proportional refractive index change over the entire cavity. Any change in threshold gain though will cause a change in refractive index of the laser cavity using the linewidth enhancement factor. A mode can exist in the external cavity when the phase condition of the round trip is $\Delta\phi_L = 0$ or multiples of 2π, $\Delta\phi_L$ being the phase difference between active cavity modes and external cavity modes, as defined in equation. 3.7 below

$$\Delta\phi_L = \frac{\tau_L}{\tau_{ext}}\left(2\pi\tau_{ext}(\upsilon - \upsilon_{th}) + C\sin\left(2\pi\upsilon\tau_{ext} + \arctan\alpha\right)\right) \tag{3.7}$$

$$C = \sqrt{F_{ext}}\frac{2|C_e|\tau_{ext}}{\tau_L}\sqrt{1+\alpha^2} \tag{3.8}$$

where C is a feedback parameter introduced in Reference (3.27). τ_L is the roundtrip time of the active laser cavity, υ_{th} is the frequency at which lasing occurs without external feedback. For weak feedback from the external cavity, C<<1, Eq 3.12 has just one solution for the optical frequency υ. For C>1 several solutions where $\Delta\phi_L = 0$ may exist. This implies multi-mode operation and mode competition. Spectral linewidth may be derived from Eq. 3.9

$$\Delta\upsilon = \frac{\Delta\upsilon_0}{\left[1 + C\cos(\phi_{ext} + \arctan\alpha)\right]^2} \tag{3.9}$$

Where $\Delta\upsilon_0$ represents the linewidth of laser diode with no optical feedback. There are no additional cavity modes as long as C<1, although, due to phase of the feedback, the linewidth may vary between minimum and maximum, as shown below in equations 3.10 and 3.11[3.26].

$$\Delta\upsilon_{min} = \frac{\Delta\upsilon_o}{(1+C)^2} \tag{3.10}$$

$$\Delta\upsilon_{max} = \frac{\Delta\upsilon_o}{(1-C)^2} \tag{3.11}$$

These equations are valid for low levels of feedback, C<<1, and show that for a value of C of around unity there can be an infinite linewidth. Numerical analysis performed on these equations showed a large linewidth broadening until C>1 when 2 external modes appear[3.28].

3.3.5 Feedback regimes

Numerical analysis[3.28] of single mode lasers with external feedback has identified a number of operating regimes when the laser diode is subjected to broadband optical feedback.

Regime 1: Variable linewidth

The first regime corresponds to C < 1, corresponding to ~ $F_{ext} < 10^{-7}$. The characteristic of this regime is that the linewidth is narrowed or broadened according to the phase of the feedback.

Regime 2: Mode hops

This corresponds to mode hopping between different external modes. Several solutions of $\Delta\phi_L = 0$ can exist simultaneously and the laser hops between the corresponding modes. This was observed in many initial experiments conducted in our laboratories via direct Fresnel reflections from beam splitters, fibre ends etc. Regime 2 occurs at C ~ 1-12, and $F_{ext} < 10^{-5}$.

Regime 3: Stable narrow linewidth

Under increased feedback conditions, the laser will enter regime 3. With an increasing amount of feedback, a strong variation of the gain threshold appears along with a reduction in the spectral linewidth. This results in stabilization of the mode with the largest linewidth reduction. A stable single longitudinal mode is observed at around C ≈ 12 ($F_{ext} < 10^{-4}$) and linewidth enhancement $\alpha = 2.5$[3.26]. Modes that satisfy $\Delta\phi_L = 0$ are stable when $d(\Delta\phi_L)/dv > 0$, however, there are also anti-modes or unstable modes where $d(\Delta\phi_L)/dv < 0$. The dominant mode has the maximum phase stability and minimum linewidth.

Regime 4: coherence collapse and chaos boundaries

Feedback is increased further and the 4th regime is characterised by strong instabilities. There are multiple external cavities, spectral linewidths of several 10's GHz and increasing intensity noise up to -130 db/Hz[3.26]. This increases until there is a complete loss of coherence, the so called chaotic state. Coherence collapse has been labeled a manifestation of chaotic dynamics[3.29]. This is unwanted for most uses of laser that require narrow linewidth operation. F_{ext} of around –40 dB of the emitted laser power are enough for the laser to enter coherence collapse and the laser linewidth can broaden from a few MHz to several GHz. This occurs at a value of $C > 40$ and F_{ext} of 10^{-4}

The point at which coherence collapse occurs is known as the critical feedback point, often called F_{extc} and corresponds to the feedback level at which the 4th state is entered. Numerical simulation by Schunk and Petermann[3.28] shows that the critical feedback level above which coherence collapses occurs increases as α decreases. This result was later confirmed by Tromborg et al[3.29]. These results suggest that the critical feedback level moves to infinity as α approaches 0. This further implies that coherence collapse could be absent from semiconductor lasers that have a very narrow linewidth. This has implications for the use of Quantum well lasers which have much smaller linewidth enhancement factors than standard laser diodes[3.28].

As well as an increase in linewidth, there is also an increase in relative intensity noise (RIN). The transition to coherence collapse can best be thought of by considering the threshold gain difference between the dominant mode with minimum linewidth and the mode with minimum threshold gain. With increasing feedback this threshold gain difference increases and eventually the laser will become unstable and the coherence will collapse. Equations[3.30] have been derived which will predict the critical feedback point and experimental investigations[3.31] indicate that complete coherence collapse or 'chaos boundaries' occur at feedback levels about 5 dB higher than the critical feedback level, therefore this could be thought of as a sub-regime within the 4th feedback regime.

Regime 5: External cavity dominance

The instabilities of the coherence collapsed regime cease when the external reflectivity becomes larger than the laser facet reflectivity. Anti reflection coatings can bring about this state as the facet reflectivity is brought close to 0. The laser facet reflectivity then acts as a small perturbation. The transition into this state has been measured experimentally[3.32] to correspond to F_{ext}~0.2 for a laser diode with antireflection facets.

3.3.6 Diffraction grating external cavity lasers.

Wavelength selective feedback allows more control over single mode behaviour. The following sections will concentrate on wavelength selective optical feedback. Bulk optic diffraction gratings have also been used as feedback sources for laser diodes[3.33, 3.34]. The diode laser is generally used with an anti reflection coating at one facet of the diode. The output from this end of the semiconductor chip is coupled on to the diffraction grating. The grating is wavelength selective and is needed since the extended cavity length results in reduced mode spacing, making multi mode operation likely if the optical feedback were broadband. The narrow spectral reflection from the diffraction grating enables the laser system to achieve linewidths as narrow 10 kHz[3.35, 3.36]. The grating can be rotated to tune the laser operating wavelength or a liquid crystal array can be utilised to pick out a wavelength at which the laser will see feedback[3.19, 3.34]. Fine tuning of the laser can also be achieved by adjusting the distance between the grating and the laser, thus adjusting the phase of the standing wave within the cavity [3.33]. This technique has also been used with a GRIN rod lens and a prism grating with a tuning range of around 40 nm and demonstrated mode hop free operation[3.34]. Systems have been experimentally demonstrated that show a tuneability of 240 nm, centred at 1550 nm[3.35]. Fig 3.14 is a system diagram of a typical semiconductor laser external cavity diffraction grating system.

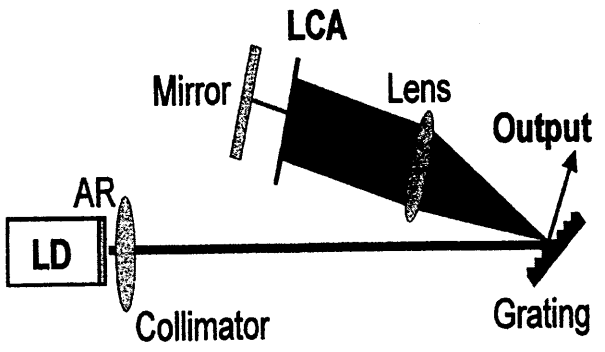

Fig 3.14 Bulk diffraction grating external cavity laser with LCA (liquid crystal array).Reproduced from Ref. (3.35)

The diffraction grating external cavity laser works on a principle that is a combination of the DBR and external cavity techniques. This allows dual benefits of the stability of the DBR laser and the tuneability of the external cavity laser. Diffraction grating lasers offer single longitudinal mode operation and have a wide wavelength tuning range. However they are expensive and can suffer from mechanical instabilities.

3.3.7 Fibre Lasers

Optical fibre can also be used as an amplifying medium of a laser by doping the core with rare earth ions. The most common fibre lasers uses an erbium doped fibre amplifier (EDFA) a pumping laser is required at 980 nm and lasing is produced in the 1550 nm region[3.2]. EDFAs have also been employed with FBGs to increase wavelength stability and reduce noise[3.38]. EDFAs are most commonly used in repeater stations in long haul telecommunications and use stimulated emission to amplify passing signals. FBG's are often used to reduce amplified spontaneous emission (ASE). However EDFAs can also be used with FBG's as the reflecting facets forming a wavelength selective cavity[3.39]. The erbium gain curve is relatively broad giving the laser a large linewidth up to 20 nm[3.39] which is broad enough to find application in white light interferometry techniques.

3.3.8 Summary of types of lasers

Table 3.15 is a summary of laser designs that can achieve tuneability and single mode operation.

Laser type	Advantages	Disadvantages
Standard F-P laser diode	Low cost	Unstable, Often multi-mode and suffers from mode hops
Cleaved coupled cavity lasers (C^3)	Single mode operation is possible.	Modes hops occur during wavelength sweeping
Distributed feedback (DFB) and distributed Bragg reflector (DBR) lasers	Single mode operation can be achieved. Some degree of tuneability. Linewidth reduction.	High cost. Limited wavelength tuning range. Suffer from wavelength drift under injection current variation
External cavity lasers	Single mode operation is achievable.	Narrow range of tuning.
Diffraction grating external cavity lasers	Wide tuning range, narrow linewidth	High cost, mechanical instabilities
Fibre Lasers	High power, some degree of tuneability.	High cost

3.4 Dual wavelength lasers

Dual wavelength lasers have been of considerable interest due to their applications for sensing systems for extended range sensing, miniature cavity interrogation, signal processing[3.40], and beat frequency and microwave generation in communication systems[3.41].

Specifically they are used for multiplexing of the wavelengths and generation of beat frequencies which are used to extend the range of interferometric sensors and encode information in communications systems. When two optical waves of different wavelength interfere they fall in and out of phase causing a periodic variation in amplitude. The oscillation rate of this amplitude variation is known as the beat frequency (or beat length

which is the corresponding spatial length) and is directly proportional to the difference between the wavelengths. The further apart the wavelengths the higher frequency at which they will fall in and out of phase. The extinction ratio of the beat frequency is the ratio between the maximum and minimum amplitudes of the beat frequency. Theoretically, for two equal amplitude signals that are strictly monochromatic and in the same state of polarisation, an extinction ratio of 100% should be achievable. The beat frequency is given below by (Eq. 3.12)[3.1]

$$\varpi_m \equiv \tfrac{1}{2}(\varpi_1 - \varpi_2) \tag{3.12}$$

$$\varpi \equiv 2\pi/\tau \tag{3.13}$$

ϖ_m is the beat frequency, ϖ is the angular temporal frequency and τ is the period of the wave. A derivation of the beat frequency is given in appendix A. With appropriate tuning of separation between wavelengths, a tuneable beat frequency signal can be created on a photodetector. The next section explains some of the applications of this heterodyning technique, which is the generation of a local oscillator of known frequency used to decode in the incoming signal, and some of the techniques used to generate beat frequencies.

3.4.1 Beat frequency applications

The advantage of using optical transmission to transmit microwaves for communications is the ease with which phase and amplitude of the signal can be controlled by adjusting path length of one the wavelengths or subtracting one wavelength[3.43]. The information can then be encoded by the phase or amplitude and the beat frequency used as a carrier signal. High speed direct modulation of the laser diode injection current can however lead to unwanted transients and harmonics that impose noise on the signal, due to extra optical reflections within the diode cavity that are out of phase with the modulation frequency. Direct modulation rates of over 10 GHz using these

techniques become increasingly problematic whereas with heterodyning two lasers the biggest problem is wavelength stabilisation between the sources[3.42]. During our own discussions with Alcatel they have been actively seeking out beat frequency generators of 10 GHz plus and millimetre wave radio communication networks. Radio communication networks could use these beat frequencies as sources because they have the potential to provide broadband customer services with tetherless connections and low cost. Applying this technique to radio systems rather than using local oscillators in the receivers gives more control over the radio emissions[3.42]. Other uses of beat frequency generation include testing response time on photodetectors by increasing the beat frequency and plotting the detector response.

3.4.2 Optical generation of microwaves

Early proposals for a system to create a tuneable optically generated microwave beat frequency used Stimulated Brillouin Scattering (SBS) in optical fibre. SBS can be described as a three wave interaction between an optical pump, an acoustic phonon and the scattered signal. Temperature effects the frequency separation of the back-scattered Brillouin line[3.44], a typical value would be ≈ 5.5 MHz/°C[3.45].

Direct modulation of the laser diode injection current can create a periodic amplitude variation but results in unwanted harmonics and transients caused by unwanted reflections in the chip, chirping of the wavelength under modulation[3.43]. Using an external modulator with a laser in continuous wave operation can result in 3dB losses and modulating at frequencies over 10 GHz can be problematic[3.43]. As a result heterodyning two wavelengths is often the favoured method for optical microwave generation and methods have been proposed for tuning the beat signal using multi quantum well DFB lasers[3.46, 3.41] varying the bias current in one of the lasers while leaving the other stationary. Low frequency extinction was estimated at around 24 GHz, and a tuneability of 24 GHz to 62 GHz was demonstrated. Beat frequencies have however, been experimentally demonstrated up to 40.6 THz[3.47] using laser diodes with external cavity diffraction gratings.

The use of a single laser is advantageous instead of heterodyning two lasers as it will reduce phase noise due to phase from the same source being correlated, whereas in two separate lasers the phase will fluctuate[3.48, 3.49]. A number of novel techniques have been used to achieve multiple wavelength lasers. Lai et al[3.50] used an Erbium doped fibre amplifier (EDFA) incorporating an optical isolator to produce a ring cavity system that emitted at 2 wavelengths 1560.76 nm and 1562.08 nm. A dual wavelength FBG EDFA has also been demonstrated[3.51]. Another dual wavelength FBG EDFA has been used in mode locked form with two separate wavelength FBG's to give picosecond lasers[3.52]. There have also been some cavities that have used highly birefringent fibre containing FBG's as the source of dual wavelength feedback[3.53, 3.54]. Other methods have been used to engineer similar dual wavelength performance from laser systems including diffraction grating external cavities[3.55, 3.56.3.57, 3.58] and DFB dual wavelength diodes[3.59, 3.60, and 3.61.]

3.5 Fibre Bragg grating external cavity lasers

The use of a fibre Bragg grating (FBG) in a wavelength selective external feedback cavity to a laser diode (FGEL) is a simple and effective method of controlling the behaviour of the output of the device. These systems demonstrate advantages over distributed Bragg reflector (DBR) or distributed feedback (DFB) devices in that the external cavity can simply be attached to ordinary Fabry-Perot laser diodes[3.62], the most common and cheapest form of laser diode with the widest wavelength range available. Therefore, the FGEL offers a way of modifying the performance of a low cost laser at low cost. Relative to waveguide gratings used on DFB and DBR lasers, FBG's also display better stability and wavelength accuracy due to their lower temperature sensitivity[3.62].

Modern dense wavelength division multiplexing (DWDM) telecommunication systems are becoming increasingly packed with communication channels, hence narrow linewidth tuneable sources are in demand to obtain the most from an optical communication network. Other optical systems including sensing schemes and spectroscopy may also benefit from these stabilised and narrow linewidth spectral attributes [3.62] as uncertainties in the measurand can be reduced.

3.5.1 Concept of Fibre Grating External Cavity laser diode.

The FGEL relies upon the output from a laser diode being coupled to a fibre containing an FBG. Light at the Bragg wavelength coupled back into the active cavity is amplified and forces lasing at the Bragg wavelength. Fig 3.16 shows a schematic of a typical configuration employing a FBG as a wavelength selective feedback element for a laser diode.

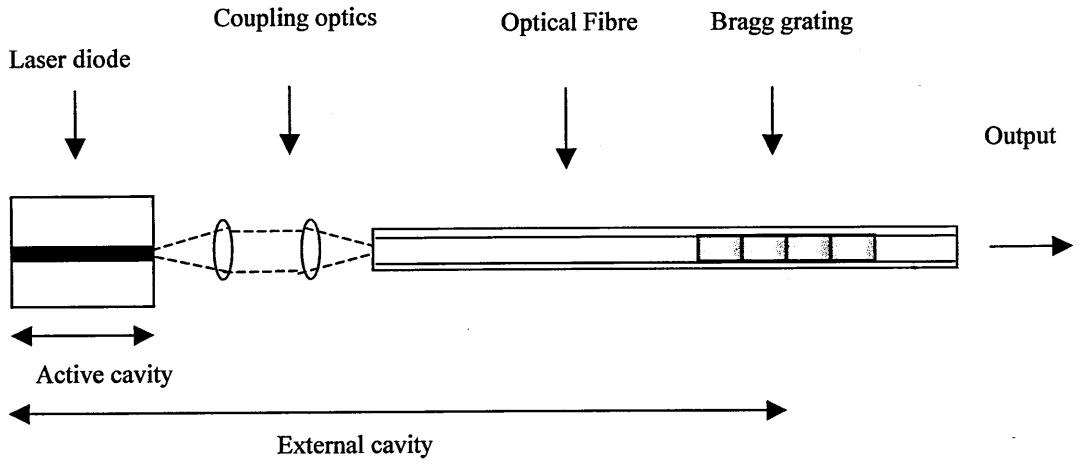

Fig 3.16 schematic of FGEL laser

The system has two cavities in this configuration, one cavity being the internal semiconductor cavity, the other being the coupling optics, the diode cavity and the single mode fibre ending at the FBG. The FGEL's principle of operation is similar in concept to the DBR discussed in section 3.3.2, the differences being that only one facet of the laser oscillator is wavelength selective and that the FGEL scheme is more cost effective and easier to manufacture.

3.5.2 Advantages of FGELs

External cavity lasers, as well as offering reduced linewidth[3.62] in comparison to standard laser diodes and DFB lasers, are less sensitive to the most common cause of wavelength shift in laser diodes, which are changes in temperature or drive current. A laser diode with a Fabry-Perot cavity structure will typically experience a wavelength shift of 0.3 nm/°C, and 0.05 nm/mA[3.1], dependent upon the materials from which the laser is constructed[3.1]. The wavelength shifts are a result of changes in the optical length of the cavity caused by temperature or carrier induced changes to the refractive index of the active medium. The wavelength shifts induced by a change δL_{sc} in the length of the active region, for a standard laser cavity and an external cavity laser, are given by the equations below [3.64]

$$\delta\lambda = \frac{\lambda \delta L_{sc}}{L_{sc}} \tag{3.14}$$

$$\delta\lambda = \frac{\lambda \delta L_{sc}}{L_T} \tag{3.14}$$

$\delta\lambda$ is the variation of output wavelength, L_T is the total cavity length and Lsc is the path length of the active region of the laser diode.

Since the injection current induced refractive changes take place only in the active region, the longer the length of the external cavity laser, relative to the internal cavity of the diode, the less sensitive the FGEL will be to injection current induced changes in the wavelength of the laser output. This will result in a reduction in the concomitant wavelength shift by a factor Lsc/L_T. The optical fibre, which acts as part of the cavity, has a lower sensitivity to environmental changes, making this hybrid laser more stable in response to temperature and current changes than either a DFB or DBR laser, typically 15 pm/^{0}C, with a cavity length of 30 mm, compared with 100 pm/^{0}C for a DBR laser[3.65]. One of the most practical applications of this stability is that a very low level of chirp is

induced when the laser is being modulated. This resistance to chirp can be further increased by increasing the external cavity length or shortening the semiconductor path length. This latter technique was used to demonstrate experimentally increased wavelength change resistance to temperature variation[3.66]. The manufacture of laser diodes with a cavity of less than 50 μm is problematic though[3.67], making the use of longer external cavities attractive. An external cavity fibre grating laser which used a lens tipped fibre[3.68] was shown to have 5 times less sensitivity in wavelength drift to temperature when compared to a DFB laser between mode hops. Sensitivity to change in injection current was also improved by a similar factor when compared to a DFB laser.

Another important benefit of the FGEL laser is its mode hop free operation. Standard Fabry-Perot laser diodes exhibit mode hopping across the operational range of temperature and current[3.69]. Under conditions of varying operating temperature and drive current, the output from a FP cavity laser diode may exhibit stable single longitudinal mode operation or multimode operation. The required conditions for single mode operation vary from device to device, but the use of a FBG to stabilise the laser diode onto the Bragg wavelength reduces mode hopping significantly[3.69]. In 1995, Timofeev et al[3.66] used a shortened cavity laser diode (150 μm). Using return to zero modulation, in which the injection current is cut-off between pulses, the external cavity laser diode demonstrated a near linear response in the input injection current versus optical power output curve due to the FGEL virtually eliminating mode hopping problems. This is an improvement with respect to the mode hop induced power fluctuations observed in a laser diode without external FBG cavity.

When the diode cavity is 25% of the length of the standard diode, the inter mode spacing will be increased by a factor of 4. As can be seen from Eq. 3.3 the shorter the cavity the greater the distance between adjacent modes. Therefore, no mode hops were seen over the current variation range in the test with the shorter cavity. Linewidth was also narrowed although output power levels were not as high due to the reduced length of the amplification medium[3.66].

The FGEL laser may be tuneable as is the bulk diffraction external grating laser, it is also relatively robust and does not suffer from the mechanical instabilities inherent to

bulk diffraction external grating lasers. There are many applications of lasers in which the ability to tune the wavelength is desired. This may be readily achieved with the FGEL, as there are a number of techniques that can be used to alter the Bragg wavelength e.g. via the application of strain or via temperature control of the grating as discussed in Chapter 2. Another advantage of the FGEL is that the Bragg wavelength may be defined at the manufacture of the FBG. This can increase the yield on the semiconductor wafer, making manufacturing more efficient as low cost Fabry-Perot cavity structures may be forced to operate at a desired wavelength by fabrication of an appropriate FBG external cavity, potentially allowing all of the chips on a wafer to be used. This is an advantage over DFB lasers, which have to be individually tested before packaging to ensure that they match the required specifications, leading to a high degree of wastage[3.64]. A chirped FBG may also be used to tune the output of the laser, by applying a pulsed injection current to the diode the timing of the optical feedback can be used to pick out a particular wavelength in space and time for each pulse to operate on[3.70].

The threshold current has also been shown to reduce with the addition of an external cavity. As illustrated in Eqs. 3.2 and 3.4, injection current threshold reduces as optical feedback and reflectivity into the active cavity increases. Higher coupling efficiency to the fibre and a higher reflectivity FBG with a narrow bandwidth together will reduce lasing threshold. In 1991, Bird[3.71] demonstrated the reduction in lasing threshold brought about by optical feedback from an external cavity laser diode, as shown in Fig. 3.17. The grating was attached by splicing a FBG on to an AR tapered fibre lens, which reduces coupling losses and reflections. The FBG had a reflectivity of around 40% and a FWHM of around 0.1 nm, the Cavity length was approximately 8 mm.

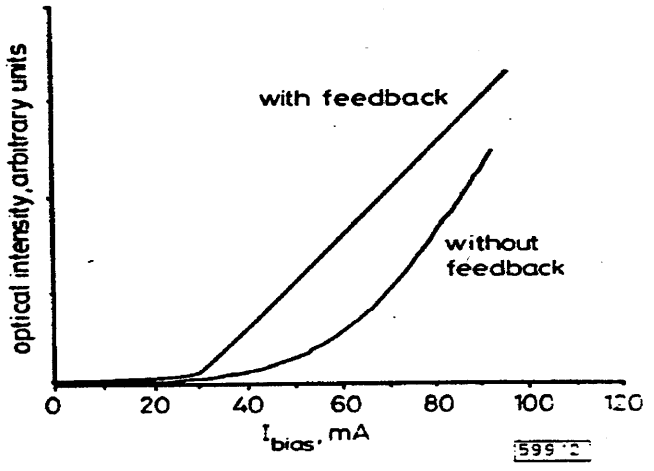

Fig. 3.17 L-I curve of a laser diode with and without an FBG external cavity[3.71]

3.5.3 Anti-Reflection coated laser diodes

The standard laser diode is highly efficient in comparison with other types of lasers[3.1]. However, when used with an external cavity this means much of the light reflected from the external cavity cannot enter the active cavity. The majority of research on external cavity lasers has used an anti reflection coating on the emitting facet of the laser chip. Facet reflections have been reduced to as low as $\sim 10^{-3}$. However, problems have been observed with Fresnel reflections (typically 4%) from the cleaved face of the fibre, as discussed in the section on feedback regimes. These may be removed by angle polishing the face of the fibre[3.72] with an angle of as little as 3°. Angle polishing the diode facet may also reduce the reflectivity from front of the active cavity[3.72]. The experimental demonstrations of an angle cleaved laser diode were tested against a similar system with a flat diode facet. The technique exhibited improved performance over AR coatings, by limited mode hopping and power transition non-linearities. A near linear L-I curve was observed, whereas for the non angled output power jumps of up to 30% occurred corresponding to mode hops of 0.6 nm.

There are however, benefits of the reflecting facets of the diode. The cleaved facets of the semiconductor chip have reflectivities of 30%, and are parallel, thus working to form a low loss cavity. The reflectivity of the semiconductor facets is broadband, thus reducing the amplitude of any unwanted external reflections going back to the active cavity of laser which could easily destabilize the laser. This means that AR coated FGELs are particularly susceptible to the influence of reflections from outside the external cavity. This can be avoided by the use of an optical isolator to stop any external reflections into the external cavity and active cavities of the diode. AR coated lasers are also expensive and require a high quality coupling to the fibre to be effective. Non-AR coated laser diodes employed in external cavity systems suffer from competition between the modes of the two cavities[3.73].

3.5.4 Early FGELs

The first interest in external cavity configurations employing side etched fibre Bragg reflectors's was in the mid 1980's[3.74]. The linewidth narrowing performance was comparable with external air cavities or bulk diffraction gratings. A 2m long fibre cavity and a low reflectivity FBG was demonstrated and later the same year another external cavity FBG laser was presented[3.75] and substantially narrower linewidths were obtained using shorter cavity lengths (0.11 m compared to 2 m) and a high reflectivity FBG (90%) in the external cavity. The Bragg wavelength of the grating was temperature controlled and no mode hopping was observed until a change of 40°C, when the FBG mode hopped by 1.3 nm.

Table 3.18 Chart detailing the early external cavity Bragg lasers that have been published.

Reference	Year	Wavelength	Linewidth	Side mode suppression ratio	FBG reflectivity	Cavity length	AR coating	comments
(3.74)	1986	1300nm	60kHz	20dB	Low	2m	No	First paper proposing linewidth reduction for FGELs
(3.75)	1986	1500nm	10kHz	25dB	<90%	0.11m	No	Further improvement on linewidth reduction capabilities of FGELs
(3.70)	1991	1550nm	<50kHz	>30dB	40%	60mm	Yes	First non etched FBG FGEL
(3.77)	1992	1550nm	NA	NA	63%	NA	Yes	Proposed as source for soliton systems, threshold reduction reported
(3.66)	1995	1553nm	NA	45dB	65%	50mm	Yes	FGELs shown to have improve resistance to mode hopping under varying injection current conditions
(3.78)	1996	1530nm	NA	NA	24%	10mm	Yes	Experimental results report increased temperature stability for FGELs

NA: Not available

3.5.5 Multiple wavelength FGELs

FGELs have been used for beat frequency generation by using separate external cavities on different laser diodes[3.77]. Each grating was temperature tuned to give a tuneable beat frequency. This had previously been done with DFB lasers but due to the narrower linewidth of FGEL laser the generated beat frequency had a narrow linewidth of 50 kHz.

A novel method of producing switchable wavelength pulses was also proposed by oscillating the injection current of the laser diode to match the resonant cavity frequency of one of the FBGs which are at different spectral and spatial locations in the cavity[3.78].

A 'wavelength uncommitted laser'[3.79] was presented in which gratings were packaged within FC-PC connectors and used in conjunction with AR coated laser diodes. A selection of easily changeable gratings were available for the device, the wavelengths used spanning 1480 nm – 1573.6 nm. This represented the first changeable rather than tuneable external cavity laser, which demonstrated high quality CW performance. Side mode suppression ratio of 50 dB at a power output of 1 mW was achieved. Fibre switches could also be used to select different wavelengths[3.80] as they have low insertion loss (<1dB) and low optical cross talk (<40dB).

3.5.6 Other uses of FBG external cavity lasers

Other uses of the external cavity lasers include mode locking and coherence collapse. An external cavity FBG can be used in actively mode locked systems[3.78]. In these systems, there is a strong need for AR coating on the semiconductor facet, as the grating must be the only form of feedback. Mode locking is initiated by modulating the injection current at the characteristic frequency of the optical cavity, the round trip time. There is an example of this system being used in this configuration to produce a soliton source[3.76]. Hybrid systems consisting of DFB lasers and external cavities have been employed but as yet there are no reports of the use of FBG's[3.76.] Chirped gratings may also be used to tune the frequency of the mode locked pulses[3.70].

Coherence-collapsed systems are used without AR coating[3.30], as the object of operation is to destroy the coherence of the source. The most common way of constructing these systems is to place the feedback grating beyond the coherence length of the diode thus making the feedback incoherent with the source. High frequency noise increases and the low frequency noise normally characterized by mode hops decreases, stabilising the power greatly. Another common use of this is pump sources for EDFAs[3.81].

External cavities have also found application as vibration sensors[3.82, 3.83] and displacements of the external feedback source as small as 10^{-4} mm where detected.

3.6 Summary

Semiconductor lasers are low cost which has made them the subject of much research and used in ever expanding applications. There are however some problems with their performance such non-linearity in power output, wavelength drift, multi-mode operation and mode hopping. These problems can result in errors in the signal in a communications system or uncertainties in the measurand in a sensing system. Therefore a number of techniques have been developed to counter these characteristics, they include DBR and DFB laser configurations which are expensive and can still suffer from wavelength drift. The external cavity diffraction grating laser was proposed as a solution, it is capable of a wide tuning range but also can be expensive and suffer from mechanical instability. FGEL lasers however are lower cost and meet requirements of single mode operation, high efficiency during production, reduced threshold, wavelength stability, tuneability and narrow linewidth. They can be used for a number of applications including multiple wavelength generation for synthetic wavelengths and beat frequencies.

3.7 References:

(3.1) J.M. Senior 'Optical fibre communications: principles and practice', 2nd edition, Prentice Hall, London, 1992.

(3.2) O. Svelto, 'Principles of lasers' Plenum press, New York 1998.

(3.3) R.N. Hall, G.E. Fenner, J.D. Kinsley, T.J. Stolys and R.O. Carlson, 'Coherent light emission from GaAs p-n junctions', Physics Review Lett., 1962, Vol.9, pp. 366-368.

(3.4) J. Wilson and J.F.B. Hawkes 'Lasers principles and applications' Prentice hall international series in Optoelectronics 1987.

(3.5) W.T. Tsang, 'Extremely low threshold AlGaAs modified multiquantum-well heterostructure lasers grown by MBE', Applied Physics Lett., 1981, Vol. 39. pp.786-794.

(3.6) H. Kressel and J.K. Butler, 'Semiconductor lasers and Heterojunction LEDs', Academic Press, London, 1977.

(3.7) K. Petermann, 'Laser diode modulation and noise', Kluwer academic publishers, Dordrecht Holland, 1988.

(3.8) Landau, L.D. and Lifshitz, E.M. 'Electrodynamics of continous media', Pergamon Press, London, 1960.

(3.9) C.H. Henry, 'Theory of the linewidth of semiconductor lasers', IEEE J. of Quantum Electronics, 1982, Vol. QE-18, pp. 259-264.

(3.10) Nishmura, Y. and Nishmura, Y. 'Spectral hole-burning and nonlinear gain decrease in a band-to-level semiconductor laser'. IEEE J. of Quantum electronics, 1973, Vol. QE-9, pp. 1011-1019

(3.11) Chanin, D.J. 'The effect of gain saturation on injection laser switching', J. Applied Physics, 1979, Vol. 50, pp. 3858-3860.

(3.12) P. Hill, R. Olhansky, J. Schalfer and W. Powazinik, 'Reduction of relative intensity noise in 1.3μm InGaAsP semiconductor lasers', Applied Physics Letts., 1987, Vol. 50, pp. 1400-1402.

(3.13) Bowers, J.E. and Pollack, M.A. 'Semiconductor lasers for telecommunications', in Optical Fiber Telecommunications II, Miller, S.E and Kaminow, I.P. (Eds.), 1998, Academic Press, pp. 509-568.

(3.14) K. Kobayashi and I. Mito, 'Single frequency and tuneable laser diodes', J. Lightwave Technology, 1988, Vol. 6, pp. 1623-1633.

(3.15) W.T. Tsang, N.A. Olson and R.A. Logon, 'High-speed direct single frequency modulation with large tuning rate in cleaved-coupled-cavity lasers', Appl. Phys. Lett., 1983, Vol. 42, pp. 650-651.

(3.16) L.A. Coldren, G.D. Boyd, J.E. Bowyers and C.A. Burrus, 'Reduced Dynamic linewidth in three-terminal two-section diode lasers', Appl. Phys. Lett., 1985, Vol. 46, pp. 125-127.

(3.17) N.K. Dutta, 'Optical sources for lightwave systems applications', in E.E Basch (Ed.) in Optical-Fiber Transmisson, H.W. Sams & Co, New York, 1987.

(3.18) Y. Susematsu and S. Arai, 'Integrated optics approach for advanced

semiconductor lasers', Proc. IEEE, 1987, Vol. 75. pp.1472-1487.

(3.19) D.R. Scifres, R.D. Burnham and W. Streifer, 'Distributed feedback single heterojunction diode laser', Appl. Phys. Lett., 1974, Vol. 25, p. 203.

(3.20) W.T. Tsang and S. Wang, 'GaAs-AlGaAs double-heterostructure injection laser with distributed Bragg reflector', Appl. Phys. Lett., 1978, Vol. 28. p. 596.

(3.21) K.R. Preston, K.C. Woolard, and K.H. Cameron, 'External cavity controlled single longitudinal mode laser transmitter module', Electron. Lett., 1981, Vol. 17, pp. 931-933.

(3.22) L.A. Coldren and T.L. Koch, 'External cavity laser design', J. Lightwave Technol., 1984, Vol. LT-2, pp. 1045-1051.

(3.23) C. Voumard, 'External-cavity-controlled 32MHz narrow-band cw GaAlAs-diode lasers', Opt. Lett., 1977, Vol. 1, pp. 61-63.

(3.24) R.S. Vodhanel and J.S. Ko, 'Reflection induced frequency shifts in single-mode laser diodes coupled to optical fibres', Electronics Lett., 1984, Vol. 20, pp. 973-974.

(3.25) K. Petermann, 'Laser diode modulation and noise', 1988. Kluwer academic publishers, London

(3.26) K. Petermann, 'External optical feedback phenomena in semiconductor lasers' IEEE J. of selected topics in Quantum Electronics, 1995, Vol. 1, June 1995.

(3.27) G.A. Acket, 'The inflence of feedback inensity on longitudinal mode

properties and optical noise in index-guided lasers' IEEE J. Quantum Electronics, 1984, Vol. QE-20 pp.1023-1032.

(3.28) N. Schunk and K. Petermann, 'Numerical analysis of the feedback regimes for a single mode semiconductor laser with external feedback' IEEE J. of Quantum Electronics 1988, Vol. 24, pp. 1242-1247.

(3.29) B. Tromborg and J. Mork, 'Stability analysis and the route to chaos for laser diodes with optical feedback'' IEEE Photonics Technology Lett., 1990, Vol. 26 pp.642-654.

(3.30) J.S.Cohen 'The critical amount of feedback for coherence collapse in semiconductor lasers', IEEE J. of Quantum electronics, 1991, Vol. 27 pp 10-12.

(3.31) S.L. Woodward, 'The onset of coherence collapse in DBR lasers' IEEE Photonics Technology Lett., 1990, Vol. 2, pp. 391-394.

(3.32) R.W. Twach 'Regimes of feedback effects in 1.5μm distributed feedback lasers' IEEE J. of Lightwave Technol., 1986, Vol. LT4 pp. 1655-1661.

(3.33) W.V. Severin and H.J. Shaw, 'A single-mode fiber evanscent grating reflector', IEEE J. of Lightwave Technol., 1985, Vol. 3, pp. 1041-1048.

(3.34) J. Wittmann and G. Gaukel, 'Narrow linewidth laser with a prism grating: GRINrod lens combination serving an external cavity', Electronics Lett., 1987, Vol. 23, pp. 524-525.

(3.35) H. Tabuchi and H. Ishikawa 'External grating tunable MQW laser with wide tuning range of 240nm' Electronics Lett., 1990, Vol. 26, pp. 742-743.

(3.36) N.K. Dutta,, T. Cella, A.B. Piccirilli, R.L. Brown, 'Integrated external cavity lasers', Conf. On Lasers and Electro-optics, 1987, CLEO '87 (USA), MF2.

(3.37) J. Struckmeier, A. Euteneuer, B. Smarsky, M. Breede, M. Born, M. Hoffmann, L. Hildebrand and J. Sacher 'Electronically tunable external cavity laser diode' Optics Lett, 1999, Vol. 24, pp. 1573-1574

(3.38) L. Reekie, 'Tunable single-mode fiber laser,' J. of Lightwave Technology, 1986, Vol. LT4, pp. 956-957.

(3.39) S.Y. Ko, M.W. Kim, D.H. Kim, S.H. Kim, J.C. Jo and J.H. Park, 'Gain control in erbium-doped fibre amplifiers by tuning centre wavelength of a fibre Bragg grating constituting resonant cavity' Electronics Lett., 1998, Vol. 34, pp. 990-991.

(3.40) A.D. Kersey and A. Dandridge, 'Dual-wavelength approach to interferometric sensing', Proc. SPIE, 1987, Vol. 798, pp. 176-181.

(3.41) X. Wang, W. Mao, M. Al Minia, S.A Paapert, J. Hong and G. Li 'Optical generation of Microwave/Millimetre-Wave signals using two section gain coupled DFB lasers', IEEE Photonics Technology Lett., 1999, Vol. 11 pp. 1292-1294.

(3.42) R.A. Griffin, P.M. Lane and J.J. O'Reilly 'Dispersion tolerant subcarrier data modulation of optical millimeter wave signals' Electronics letters, 1996, Vol. 32, pp. 2258-2260.

(3.43) M. Hickey, R.Marsland and T. Day 'Generating microwaves with laser diodes' Lasers & Optronics, 1994, July, pp. 15-17.

(3.44) G. P. Agrawal, 'Nonlinear Fiber optics' Academic press, 1989, London.

(3.45) D.Culverhouse, F. Farahi, C.N. Pannell, D.A. Jackson, 'Stimulated Brillouin scattering : a means to realise tunable microwave generator or distributed temperature sensor' Electronics Lett., 1989, Vol.25, pp. 915-916.

(3.46) R. Hai, B. Zhe, K. Demarest, C. Allen and J. Hong 'Generation of ultra high speed tuneable rate optical pulses using strongly gain coupled dual wavelength DFB laser diodes' IEEE Photonics Techonology Lett., 1999, Vol.11 pp. 518-520.

(3.47) N. Onodera 'Optical beat frequency generation up to 40.6THz by mode locked semiconductor lasers' Electronics Lett., 1996, Vol. 32, pp 1727-1729.

(3.48) U. Gliese, T.N. Nielsen, M. Bruun. E. Lintz-Christiansen, K.E. Stubjaer, S.Lindgren and B. Bromberg. 'A Wideband Heterodyne optical phase locked loop for generation 3-18 GHz microwave carriers' IEEE Photonics Technology Lett. 1992, Vol. 4, pp. 936-938.

(3.49) J.J. O'Reilly, P.M. Lane, R. Hiedemann and R. Hofstetter 'Optical generation of very narrowlinewidth mm wave signals' Electronics Lett., 1992, Vol. 28, 2309-2311.

(3.50) Y.C. Lai, C. Lu, W. Zhang, J.A.R. Williams, L. Zhang and I. Bennion 'Generation of microwave signal with very narrow linewidth from a dual mode fibre grating DFB laser' IOP Applied optics and opto-electronics conference 17-21 September, Loughborugh 2000, pp. 23.

(3.51) Y.Z. Xu, H.Y. Tam, W.C. Du and M.S. Demokan, 'Tunable Dual-Wavelength-

Switching Fiber grating laser' IEEE Photonics Tech. Lett., 1998, Vol. 10, pp. 334-336.

(3.52) Y. Zhou and C. Shu, 'Wavelength-tunable active modelocking of a novel fiber laser including fiber gratings' proc. CLEO Europe, 1998, pp.280.

(3.53) J. Hernandez-cordero, V.A. Kozlov, A.L.G. Carter and T.F. Morse, 'Fiber Laser Polarization tuning using a Bragg grating in a Hi-Bi Fiber', IEEE Photonics Technology Lett., 1998, Vol. 10, pp.941-943.

(3.54) O.Deparis, R. Kiyan, S.A. Vasilev, O.I. MedledKov, E.M.Dianov, O. Pottiez, P. Megret and M. Blondel, 'Polarization maintaing Fiber Bragg gratings for wavelength selection in actively mode-locked Er-Doped Fiber lasers', IEEE Photonics Technology Lett., 2001, Vol. 13, pp. 284-286.

(3.55) B. Zhu, K.O. Nyairo and I.H. White, 'Dual-wavelength Picosecond Optical Pulse generation using an actively Mode-Locked Mulichannel grating cavity laser' IEEE Photonics Technology Lett, 1994, Vol. 6, pp. 348-351.

(3.56) C.L. Wang, Y.H. Chuang and C.L. Pan, 'Two wavelength interferometer based on a two colour laser diode array and the second order correlation technique', Optics Letters, 1995, Vol. 20, pp. 1071-1073.

(3.57) C.L. Pan and C.L. Wang, 'A novel dual-wavelength external cavity laser diode array and its applications' Optical and Quantum Electronics, 1996, Vol. 28, pp. 1239 – 1257.

(3.58) Y.H. Wong, C.W Hsu and C.C. Yang, 'Characteristics of a Dual-Wavelength Semiconductor Laser Near 1550nm', IEEE Photonics Technology Lett., 1999, Vol. 11, pp. 173-175.

(3.59) L.P.Barry, J.M. Dudley, B.C. Thomsen and J.D. Harvey, 'Frequency-resolved optical gating measurement of 1.4THz beat frequencies from dual wavelength self-seeded gain-switched laser diode' Electronics Letts., 1998, Vol. 34, pp. 988-990.

(3.60) S.D. Roh 'Single and tunable Dual wavelength operation of an InGaAs-GaAs Ridge waveguide distributed Bragg Reflector laser' IEEE Transactions on Photonics Lett. 2000, Vol. 12, pp. 16-18.

(3.61) A. Hsu, S.L. Chuang and T. Tanbun-Ek, 'Tunable Dual-Mode operation ina chirped grating distributed feed back laser', IEEE Photonics Technology Lett., 2000, Vol. 12. pp. 963-965.

(3.62) R. Kashyap, 'Fiber Bragg Gratings' Academic press, London, 1999.

(3.63) L. Xiao, 'Low frequency wavelength modulation spectroscopy using an external cavity diode laser' SPIE. Vol. 3862, 1999 International conference on industrial lasers pp 556-559.

(3.64) J-L Archambault and S.G.Grubb, "Fiber gratings in Lasers and Amplifiers" J. of Lightwave Technology" 1997, Vol.15, 1378-1391.

(3.65) P. Chanclou, M. Thual, A. Laurent, J. Lostec and M. Gadonna, 'Wavelength Selector External Cavity Laser Diode by Fiber Switch', Optical Fiber Technology, 2000, Vol. 6, pp. 329-343.

(3.66) F.N. Timofeev, P. Bayvel, L Reekie, J. Tucknott, J.E Midwinter and D.N Payne, 'Spectral characteristic of a reduced cavity single-mode semiconductor fibre grating laser for applications in DWDM systems' in proc. 21st European

conf. Optic. Commun. (ECOC 95) pp.477-480.

(3.67) Wilson, J. Hawkes, J.F.B. 'Lasers principles and applications' 1987, Prentice hall international series in Optoelectronics, London.

(3.68) M. Ziari. J-M. Verdiell. J-L. Archambault, A. Mathur, H. Jeon, R-C. Yu and T.L Koch, 'high speed fibre grating coupled semiconductor wavelength division multiplexed laser' Proc. Conf. Lasers electro-opt (cleo '97), pp. 27.

(3.69) S.P. Reilly, S.W. James and R.P. Tatam, 'Tunable and switchable dual wavelength lasers using optical fibre Bragg grating external cavities', Electronics Lett., 2002, Vol. 38, pp. 1033-1034.

(3.70) P.N. Kean, 'Dispersion-modified actively mode-locked erbium fiber laser using a chirped fiber grating' Electronics Lett., 1994, Vol. 30, pp.2133-2135.

(3.71) D.M. Bird 'Narrow line semiconductor laser using fibre grating' Electronics Lett., 1991, Vol. 27, pp 1115-1116.

(3.72) R.J. Campbell 'Wavelength stable uncooled fibre grating semiconductor laser for use in an all optical WDM access network' Electronics Lett., 1996, Vol. 32, pp 119-120.

(3.73) J.-F. Lemieux, A. Bellemare, C. Latrasse and M. Tetu, 'Step-tunable (100GHz) hybrid laser based on Vernier effect between Fabry-Perot cavity and sampled fibre Bragg grating' Electronics Lett., 1999, Vol. 35, pp. 904-905.

(3.74) E. Brinkmeyer, W. Brennecke, M. Zurn and R. Ulrich, 'Fibre bragg reflector for mode selection and line narrowing of injection lasers', Electronics Lett., 1986, Vol. 22, pp.134-135,

(3.75) C.A. Park, C.J. Rowe, J. Buus, D.C.J. Reid, A. Carter and I Bennion, 'Single mode behaviour of a multi mode laser with a fibre grating external cavity' Elecronics Lett., 1986, Vol. 22, pp. 1132-1133.

(3.76) P.A.Morton, V. Mizrahi, S.G. Kosinski, L.F. Mollenauer, T. Tanbun-Ek, R.A. Logan, D.L Coblentz, A..M. Sergent and K.W. Wecht, 'Hybrid soliton pulse source with fibre external cavity and bragg reflector' Electronics Letts., 1992, Vol.28, pp. 561-562.

(3.77) F.N. Timofeev, S. Bennet, R. Griffin, P. Bayvel, A.J. Seeds, R. Wyatt, R. Kashyap and M. Robertson, 'High spectral purity millimetre-wave modulated optical signal generation using Fibre grating lasers', Electronics Lett., 1998, Vol. 34. pp. 668-669.

(3.78) Shenping Li, K.T. Chan, Y. Liu, L. Zang and I. Bennion, 'Multiwavelength picosecond pulses from a self- seeded Fabry-Perot Laser diode with a fiber External Cavity Using Fiber Bragg gratings', IEEE Photonics Tech. Lett., 1998, Vol. 10, pp. 1712-1714.

(3.79) R. Kashyap. 'Wavelength uncommitted lasers' Electronics Lett., 1994, Vol. 30, pp.1065-1066

(3.80) P. Chanclou, M. Thual, A. Laurent, J. Lostec and M. Gadonna, 'Wavelength Selector External Cavity Laser Diode by Fiber Switch', Optical Fiber Technology, 2000, Vol. 6, pp. 329-343.

(3.81) P. Tavares 'high bit rate synchronization of RZ Signals using external cavity DFB lasers' Proc. SPIE. 3572, 1999, pp 405-409.

(3.82) C. Mignosi, R.P. Griffiths, M. Bordovsky, C.N. Morgan and I.H. White, "Novel optical vibration sensor using external cavity feedback" Proc. SPIE Vol. 3626, 1999, pp. 14-22.

(3.83) O.L. Quanm. 'External cavity semiconductor laser sensor' Proc. SPIE. 1999, Vol. 3897. pp 692-699.

4: The Fibre Bragg Grating External Cavity Laser

This chapter will present results on the characterisation of a 5420 laser diode manufactured by SDL, to highlight some of the problems associated with the performance of a standard laser diode, and will then contrast these results with those obtained from the characterisation of the same laser diode with an external cavity.

4.1 SDL laser diode

The laser diode used for the construction of the dual wavelength laser is a SDL 5420 laser diode. The laser has it has a peak output power of 150 mW and the spatial profile of the output is diffraction limited which aides coupling efficiency of the optical power into single mode optical fibres. It combines index guided and quantum well structures, and, like most Fabry-Perot structure diodes the output suffers from spectral broadening, mode hopping and wavelength drift. Table 4.1 illustrates the manufacturers quoted performance characteristics[4.1]

Table 4.1 Manufacturers predicted performance characteristics of the SDL 5420 laser diode[4.1]

Laser characteristic	Typical value	Units
Max CW output power	150	(mW)
Centre wavelength	809+/-4	(nm)
Max operating current	230	(mA)
Threshold current	35	(mA)
Slope efficiency	0.75	(mW/mA)= $P_0/(I_{op}-I_{th})$
Temperature coefficient of wavelength	0.3	(nm/^{0}C)
Single mode operation	Single mode operation is possible with this laser at certain values of temperature injection current and optical feedback	

4.1.1 Characterisation of laser diode

Characterisation of the laser diode was required to facilitate an assessment of the effect of the application of an FBG external cavity. The anticipated effects of the addition of an external cavity include reduction of threshold conditions, smoothing of the L-I graph due to a reduction in mode hops. Mode hopping with change in injection current is a well known effect [4.2]. The experimental set-up is shown in Fig 4.2

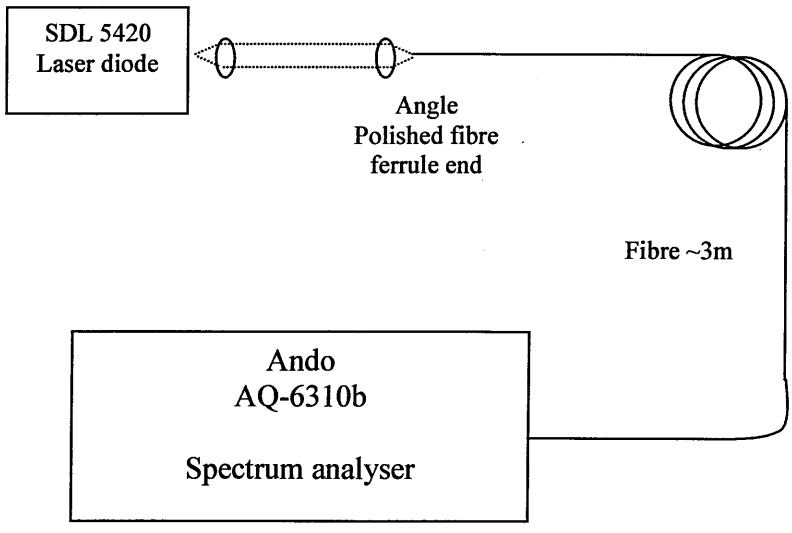

Fig 4.2 Experimental configuration for the analysis of SDL 5420 output

As external optical feedback can destabilise the laser[4.3], a polished fibre end angled at 8° to the normal was prepared. Lenses with correct focal length and anti reflection coatings were used to couple light into a single mode optical fibre to minimise any back reflections. An OFR PAL-TE-850, which is a commercially available diode to fibre coupler used. Coupling efficiency was adjusted to <5% of laser power, preventing de-stabilising external reflections. The distal end of the optical fibre was then angle cleaved and attached to the Ando optical spectrum analyser, which has a spectral resolution of

0.1 nm, using an FC ferrule connector. Using this experimental configuration the lasing threshold and the stability of the operating wavelength could be observed as the injection current was adjusted. Fig 4.3 shows the evolution of the spectral output of the laser with increasing injection current when the temperature was stabilised at 21°C ±0.1.

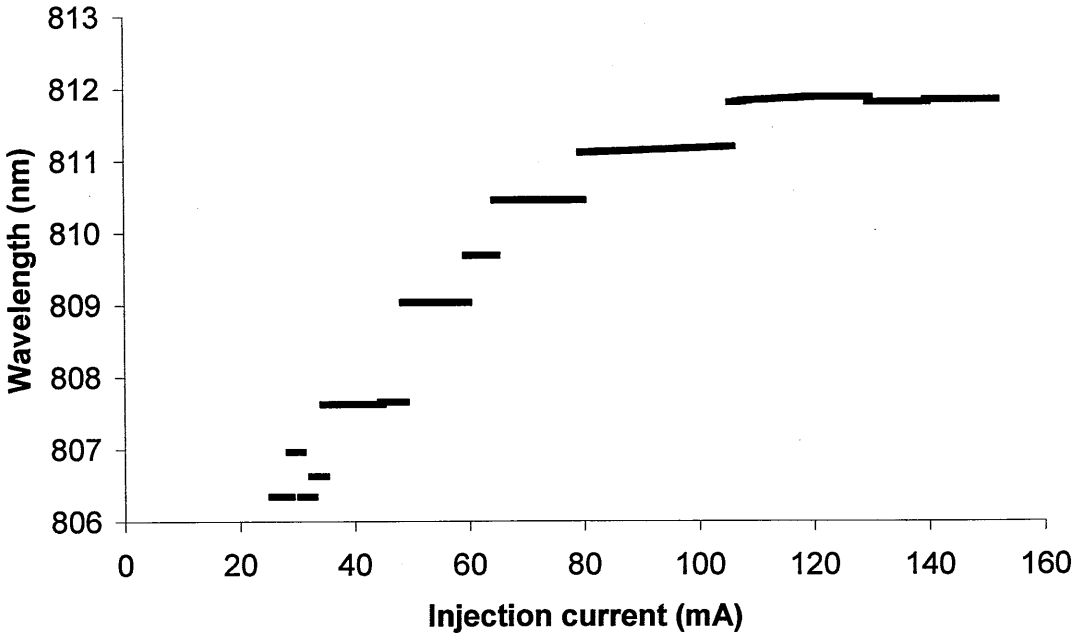

Fig. 4.3 Spectral output of the SDL 5420 laser with varying injection current. The temperature was stabilised at 21°C ±0.1.

The mode hops and multimode operation commonplace in the spectrum of standard laser diodes are evident. This is due to the change in refractive index within the laser cavity. As the refractive index and temperature changes, the wavelength of the dominant mode shifts, this manifests itself in mode hops as well as wavelength drift and multiple mode operation states. It is an undesired effect for optical sensing systems, specifically interferometric systems, as errors can be introduced into the recovered values of the measurand due to the instability of the laser. Sensors often require calibration to the wavelength of the laser If a mode hop or wavelength drift occurs then it is ambiguous whether the measurand has changed or the laser wavelength has changed. Mode hops can

also cause power fluctuations in the laser output[4.1]. In the same way that wavelength changes can create uncertainties in the sensor unexpected changes in the optical power of the laser will mean ambiguities in the measurand. Fig 4.3 was taken when the temperature of the laser diode was stabilised at 21°C ±0.1. However, mode hopping and multimode operation were observed across a broad range of temperatures.

An L-I measurement was also taken by monitoring the laser output power as a function of injection current. The experimental set up used to monitor this is illustrated in Fig 4.4. As in the measurement of the laser, anti reflection coated lenses and an angle polished ferrule end where used to reduce potentially destabilising reflections.

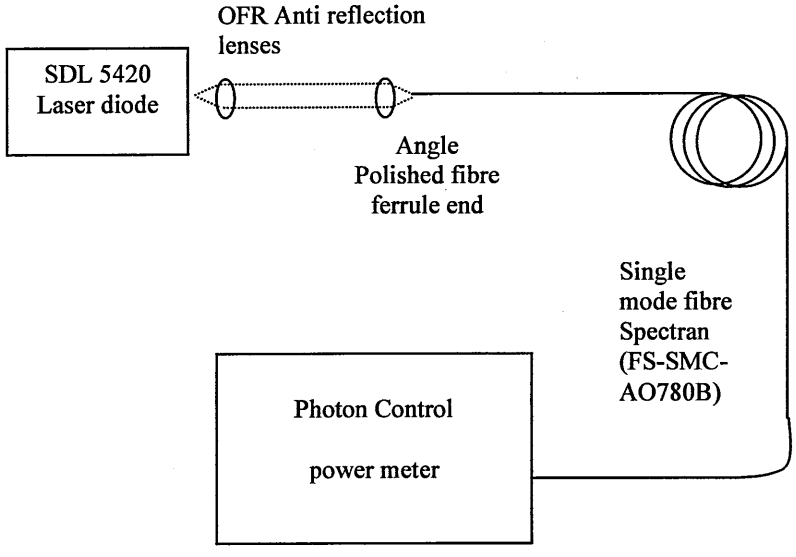

Fig 4.4 Experimental set up for measurement of L-I graph

The L-I graph, Fig 4.5, illustrates that the output power is not linear with injection current due to mode hops and multi-mode operation. It is noticeable how some of the major deviations from the linearity of the L-I graph occur at points of significant mode hops on Fig 4.5, ~ 105 mA and 65 mA.

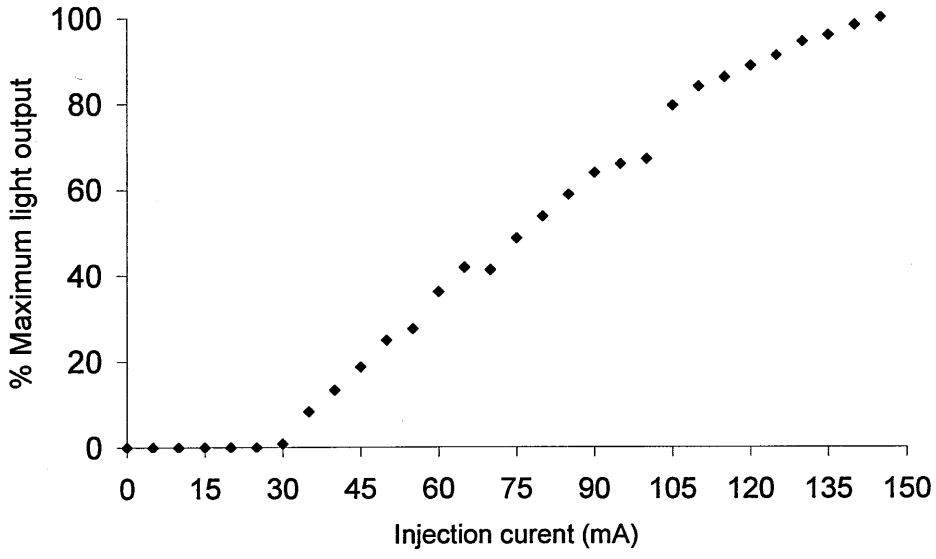

Fig 4.5 L-I graph of SDL 5420

The deviations in the output power of the laser are the result of mode hops as the injection current changes the refractive index of the active cavity. The temperature of the diode was stabilised to 21°C ±0.1.

4.2 Laser diode with External cavity FBG

A FBG external cavity laser was prepared with as narrow bandwidth FBG as possible, as short an external cavity as could be permitted and as high a reflectivity as could be permitted. Practically, however, during fabrication reflectivity is related to FBG bandwidth, the higher the reflectivity the broader the FBG would be and priority was given to having a narrow FWHM FBG.

The same experiments performed in section 4.1.1 are repeated on an SDL 5420 laser diode with a FBG external cavity. The performance of the external cavity laser was evaluated, and effects observed including threshold reduction, wavelength and power stabilisation. The FBG used had a peak reflectivity at 808.9 nm, a FWHM of 0.15 nm, measured by illuminating the FBG with the laser diode in pre-threshold mode and

measuring the spectrum on an Ando AQ-6310b. The FBG was fabricated in Spectran (FS-SMC-AO780B) using the hydrogen loading method described in chapter 2.

The output form the laser diode was coupled to the fibre with a OFR PAL-TE-850, which achieved a coupling efficiency of ~35%, quantified by taking a relative measurement to the laser diode's maximum power output. The fibre used had a ferrule end which was angle polished to 3° to reduce unwanted back reflections. Fig 4.6 is a schematic of the FGEL, the external cavity length is approximately 65 mm.

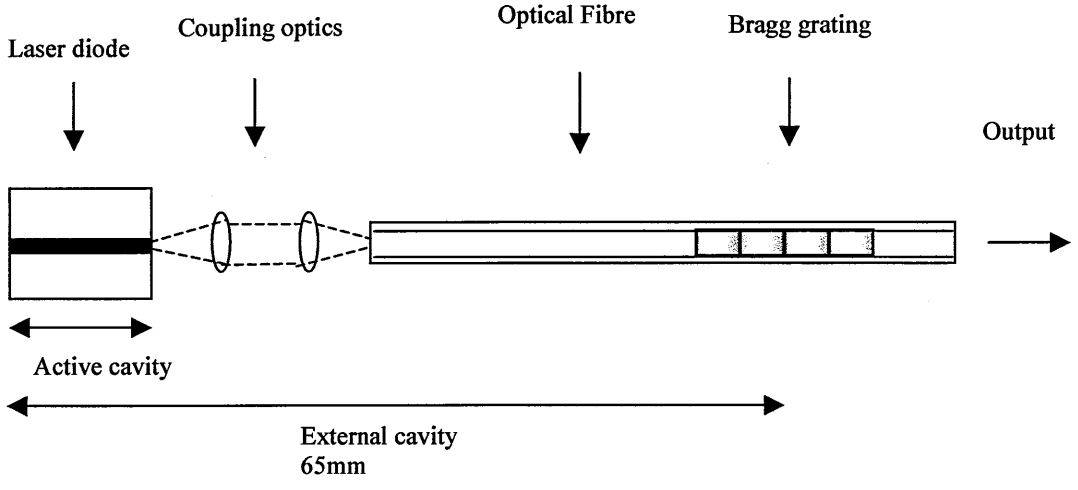

Fig 4.6 SDL 5420 with external cavity FBG in Spectran single mode fibre

Fig. 4.7 shows results of the measurements of wavelength as a function of injection current on the laser with an FBG external cavity. The FBG can be seen to reduce mode hopping, thus stabilising the wavelength of the laser under conditions of changing injection current, and also to reduce the injection threshold to 15 mA, from the preliminary measurement of 27 mA was observed.

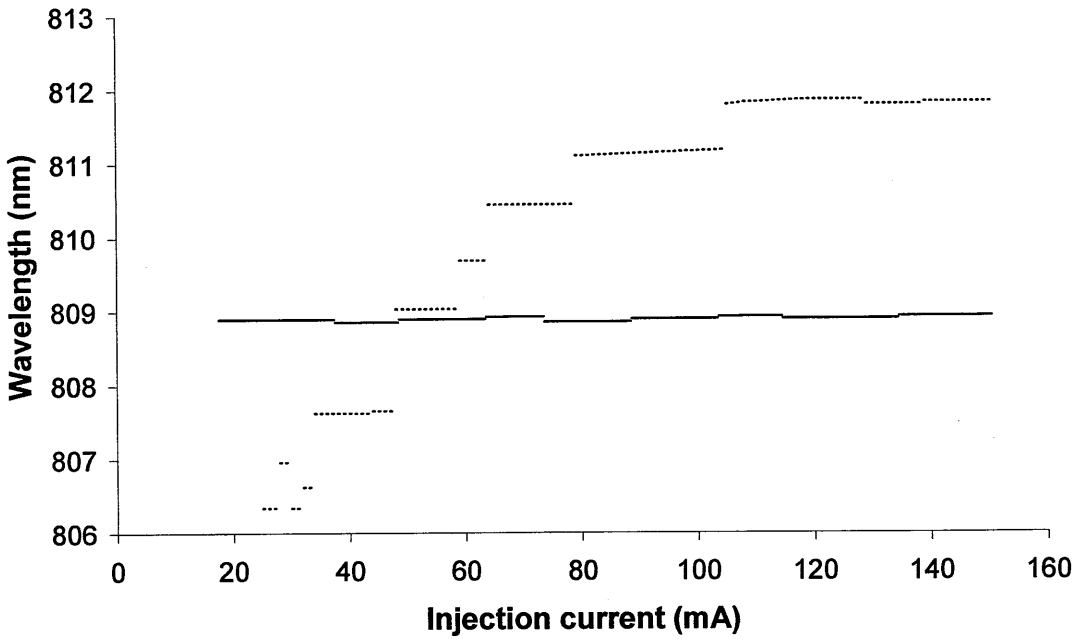

Fig. 4.7 Wavelength stability of FGEL laser in comparison with same diode with no external cavity. The solid line is the FBG external cavity laser, the dotted line is the laser diode with no external cavity. The temperature was stabilised at 21°C ±0.1.

The L-I graph is also re plotted in Fig. 4.7 for the SDL 5420 diode with an external cavity to illustrate the stability of the external cavity laser. Although output is not linear the kinks are significantly less prominent than those seen in the output of the diode when no external FBG cavity is attached. This is directly related to the increased wavelength stability of the diode with the external cavity. The slight variation in the wavelength of the external cavity laser comes from the spectrum analyser's read out function, it is unnoticeable on the display trace and less than half the resolution of the Ando AQ 6310b optical spectrum analyser, 0.1 nm.

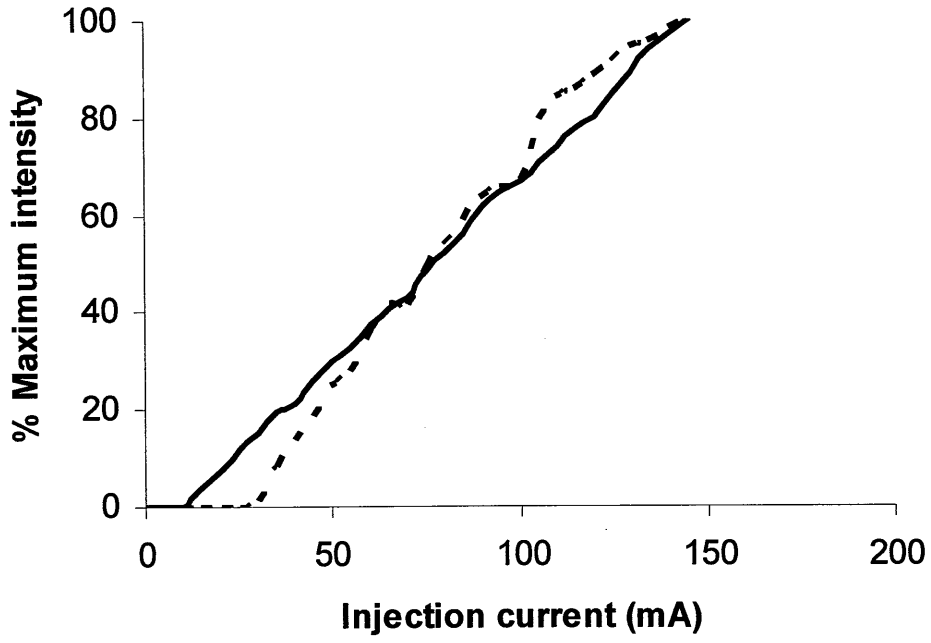

Fig 4.8 Comparison of L-I graphs of SDL 5420 diode with and without an external cavity FBG. The solid line is the FBG external cavity laser, the dotted line is the stand alone laser diode. The temperature was stabilised at 21°C ±0.1.

4.3 Linewidth measurement

One of the benefits of FGEL lasers is reduced linewidth, with linewidths of 10 kHz[4.3] reported. This is a considerable improvement on standard Fabry-Perot laser diodes which typically have linewidths of around 20 MHz, equating to a coherence length of around 15 m. Linewidth is an important characteristic for lasers, narrow linewidths are often desired in, for example, densely populated communication channels and heterodyne beat frequency generation where a narrower linewidth will result in a narrower spectrum beat frequency. Also, as a narrower linewidth is intrinsically linked to a longer coherence length, increasing the range of an interferometric sensor in, for example, optical frequency domain reflectometry[4.2].

A linewidth measurement was undertaken on the SDL laser diode using a delayed self-heterodyne technique[4.4] in which part of laser output itself is used as a local oscillator. The technique offers a linewidth resolution proportional to the distance of the delay line used in the experiment. The principal is illustrated in Fig. 4.8. The output of the laser is divided into two paths, branches A and B. Branch A is subjected to a time delay, τ_d, by routing it through a length of single mode fibre, which must be longer than the coherence length of the laser, as the output must be uncorrelated with its own delayed signal. Branch B is subjected to a frequency shift, π_s, which must be higher than the spectral width to be measured to reduce correlation. The two branches are then combined, the resulting signal is measured on an electronic spectrum analyser. As the mixed signal is uncorrelated it will display a FWHM 3 dB wider than the original spectrum due to both signals being equally noisy. Assuming the spectrum is Lorentzian[4.5] a typical laser diode lineshape, the FWHM is twice its original value and can be measured by radio frequency measurement of the combined signal output.

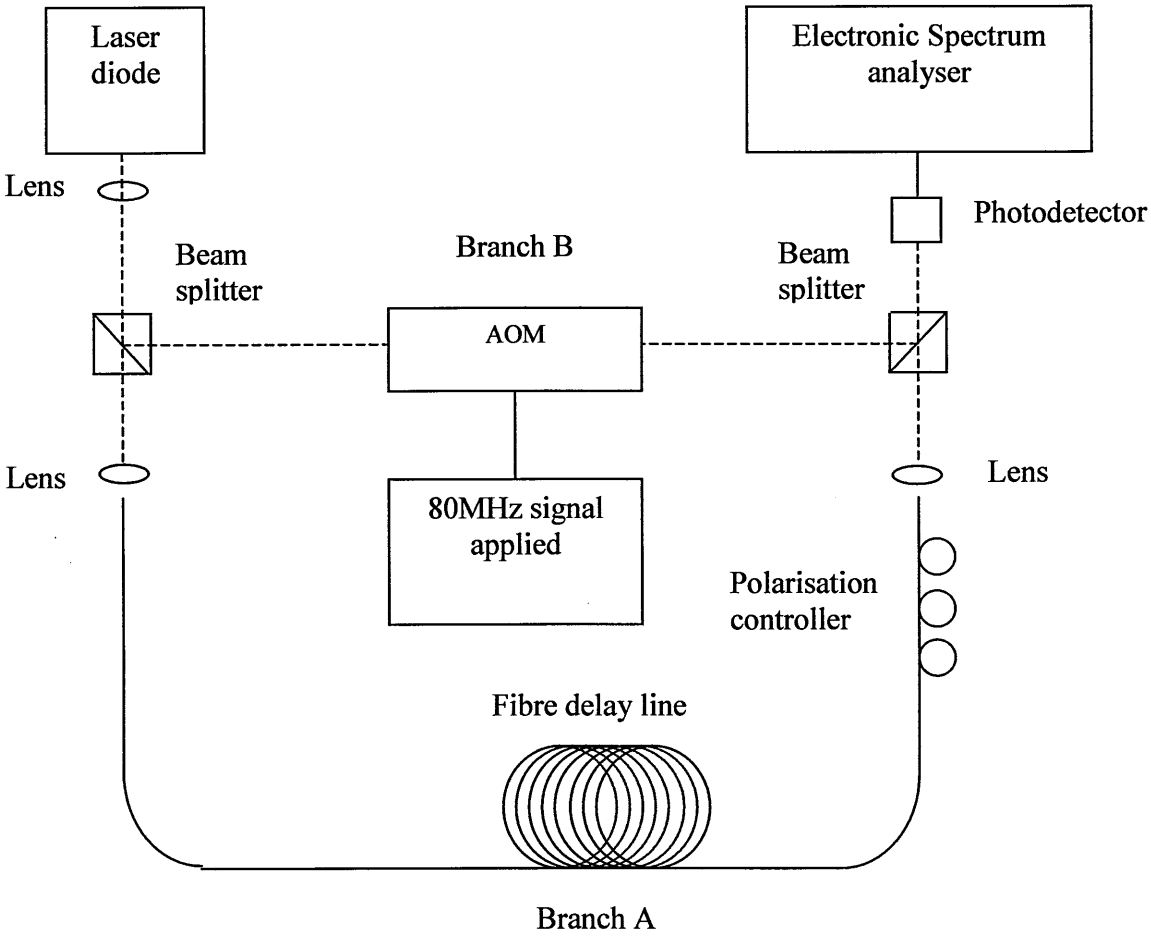

Fig. 4.9 Experimental configuration for measurement of laser linewidth, AOM: Acousto-optic modulator.

A fibre polarisation controller was used on the delayed path to ensure there was no loss of the beat signal. The 1st order beam of a acousto-optic modulator, (Isomet 1205c-2) was used to frequency shift the local oscillator branch by 80 MHz, enough to separate the two branches in wavelength by larger than the expected linewidth which is around 30 MHz for semiconductor lasers. The acousto-optic modulator was driven by an RF signal

generator (Isomet D301b) and tuned by the application of a DC signal. Beam splitters were 50/50 split ratio non-polarising and 400 m of Spectran FS SMC AO 780B fibre was used to provide the delay line which corresponds to a τ_d of 2μs and hence an achievable resolution of around 500 kHz. A Hamamatsu C4777 8B-005 photodetector with a frequency bandwidth up to 100MHz and a photosensitivity of $-2.5*10^5$ V/W, converted the optical signal into an electrical signal which was then sent to the spectrum analyser (Hewlett-Packard 8591a controlled via GPIB by a PC using Labview™ software).

Fig. 4.10 Shows the measured linewidth of the laser diode. At the FWHM point (-3 dB) a spectral spread of ~ 5 MHz is seen which gives a true linewidth of around 2.5 MHz equivalent to a coherence length of around 110m presuming a Lorentzian laser line shape.

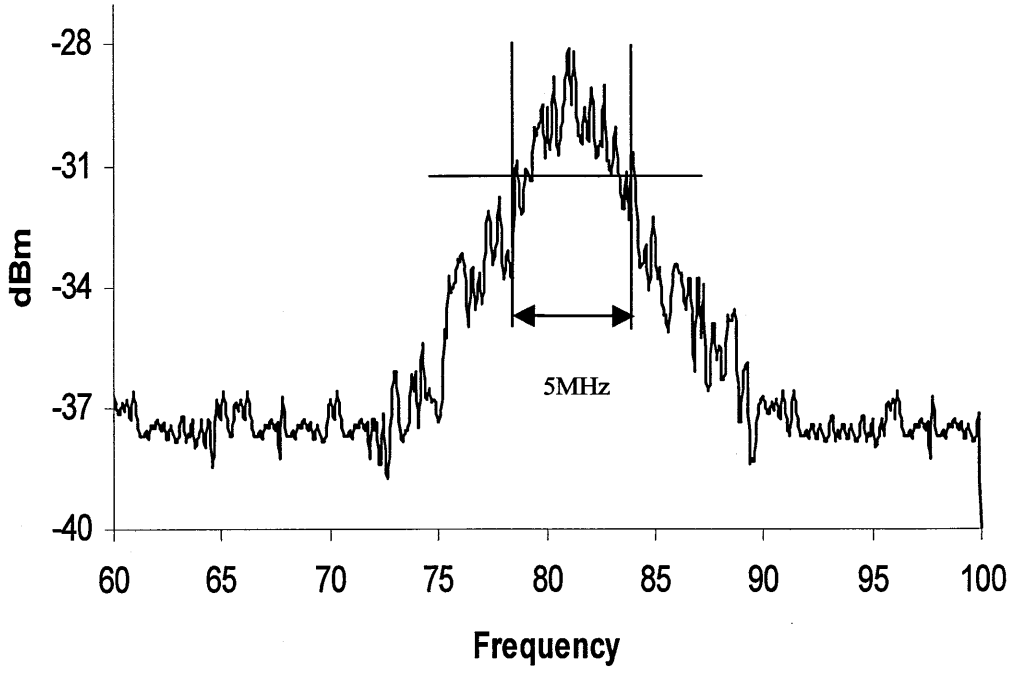

Fig. 4.10 Linewidth of the SDL 5420 laser diode as displayed on the Hewlett-Packard 8591a electrical spectrum analyser

Throughout most of the injection current range however the laser diode operated on more than one wavelength. Several windows exist however during which a side mode

suppression ratio of 15 dB was achieved, the above linewidth measurement was taken with an injection current of 71 mA and a temperature of 20°C.

4.2.1 Linewidth Reduction using an external cavity fibre Bragg grating

The use of a FBG as an external cavity has been shown to reduce the linewidth of a laser diode[4.4]. A FBG, depicted in its transmission spectrum in Fig. 4.10, was fabricated in Spectran SM fibre at 804.5 nm with a FWHM bandwidth of ~ .12nm and a reflectivity of ~16%. A coupling efficiency of around 30% was achieved when coupled to a SDL 5420 laser diode and the FBG formed an external cavity approximately 35 mm long. A schematic of the laser is shown in Fig 4.12

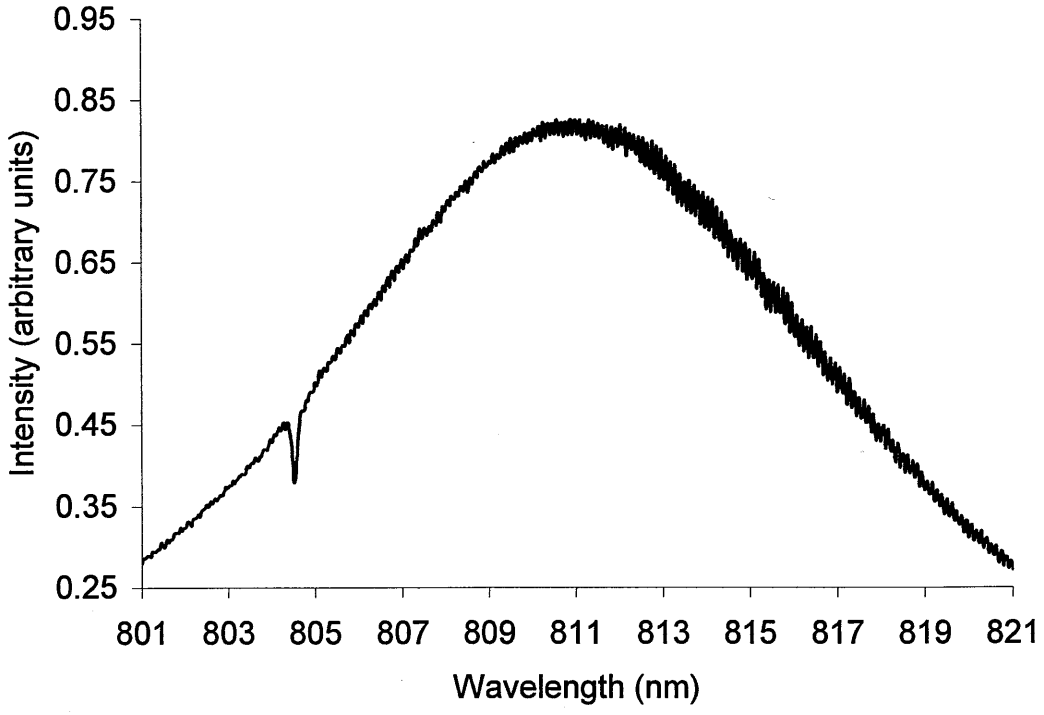

Fig. 4.11 Transmission spectrum of FBG used in linewidth measurement.

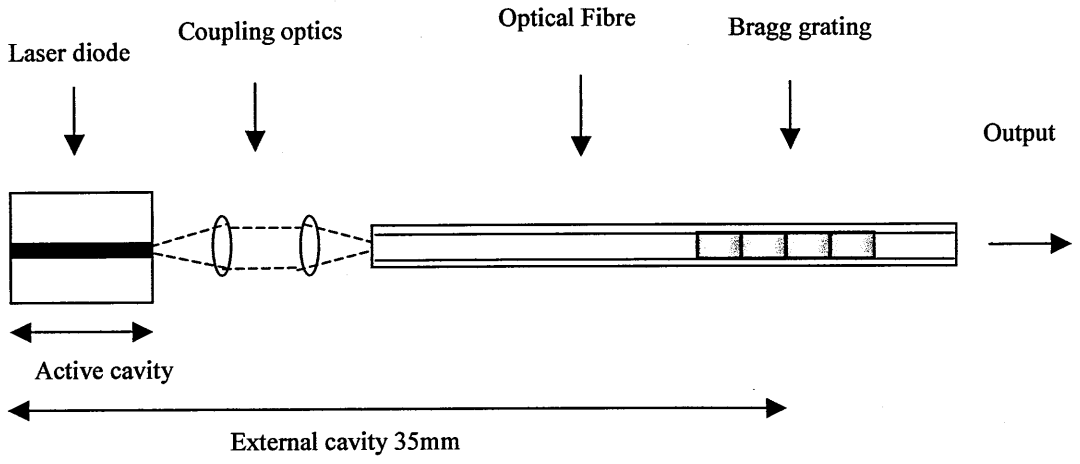

Fig. 4.12 FGEL laser system used in linewidth measurement experiment.

A threshold current reduction from 34 mA to 18 mA was observed, the laser was seen to operate on a stabilised single longitudinal mode over the full range of the injection current. Its spectrum is shown in Fig. 4.12.

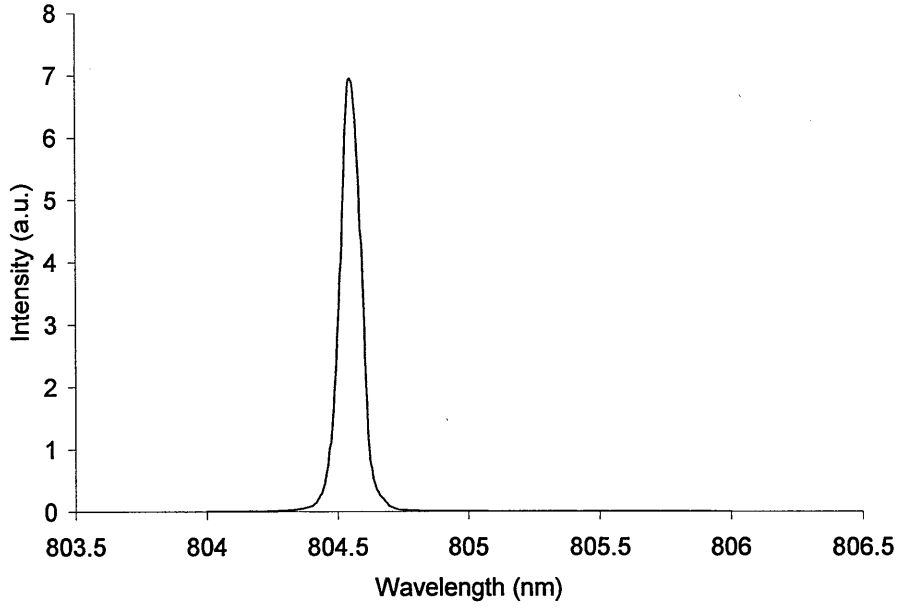

Fig. 4.13 Spectral Output of FBG laser diode

The same experimental set up was used as for the laser linewidth measurement without external cavity as was shown in Fig. 4.8.

Results show a linewidth of <500 kHz, Fig 4.13), limited by the fibre delay line, equivalent to a coherence length of over 600 m, a significant reduction on the ~ 2.5 MHz linewidth demonstrated by the laser diode with no external cavity.

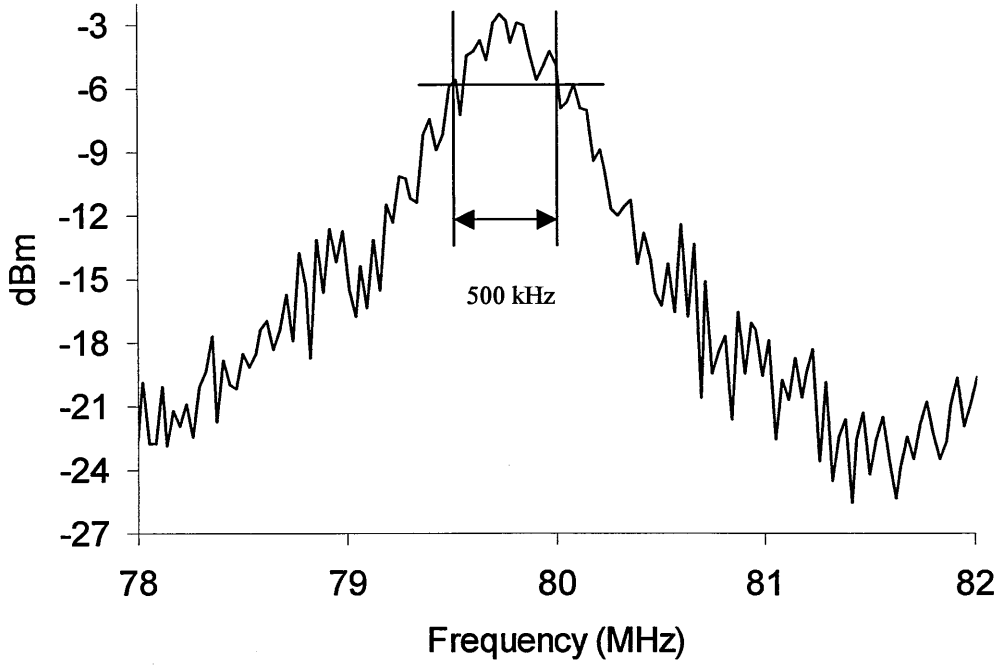

Fig. 4.14 Linewidth of the SDL 5420 laser diode with external FBG cavity as displayed on the Hewlett-Packard 8591a electrical spectrum analyser

4.4 Summary

The SDL 5420 laser diode has been characterised and it was shown that it suffers from many of the same problems as standard laser diodes, such as mode hopping, multimode operation and an uneven L-I curve. The addition of a FBG external cavity demonstrated that mode hopping and multi mode operation can be significantly reduced, making laser diodes more reliable sources for both communication and sensing systems. Threshold current has also been shown to be reduced, increasing the dynamic range of the modulated laser diode. Non-linearity and kinks in the L-I graph as also been show to be reduced.

References

(4.1) SDL product catalogue, 96/97, First edition. SDL inc. 80 Rose orchard way, San Jose CA, 95134-1365, USA

(4.2) J.M. Senior, 'Optical fiber communications: principles and practice', 2nd Edition, Prentice Hall, London, 1992

(4.3) K. Petermann, 'External optical feedback phenomena in semiconductor lasers' IEEE J. of selected topics in Quantum electronics, 1995, Vol. 1, No. 2, June 1995.

(4.4) C.A. Park, C.J. Rowe, J. Buus, D.C.J. Reid, A. Carter and I Bennion, 'Single mode behaviour of a multi mode laser with a fibre grating external cavity' Electronics Lett., 1986, Vol. 22, pp. 1132-1133.

(4.5) T. Okoshi, K. Kikuchi and A. Nakayama, 'Novel method for high resolution measurement of laser output spectrum' Electronics Lett., 1980, Vo. 16, pp. 630-631.

(4.6) E.E. Hinkley and C. Freed, 'Direct observation of the Lorentzian line shape as limited by quantum phase noise in a laser above threshold', Physics Review Lett., 1969, Vol. 23, pp. 277-280.

(4.7) J-L Archambault and S.G.Grubb, "Fiber gratings in Lasers and Amplifiers" J. of Lightwave Technology" 1997, Vol.15, pp. 1378-1391.

5 External cavity FBG semiconductor laser based on Hi-Bi fibre

In this chapter a novel external cavity laser is demonstrated experimentally. It is based on a FBG fabricated in highly birefringent (Hi-Bi) fibre and offers the ability to switch between modes that are separated in polarisation and wavelength. FBGs fabricated in Hi-Bi fibre have been proposed previously as feedback sources for fibre laser's[5.1, 5.2, 5.3] primarily to control the state of polarisation of the laser and aid the lasers long term stability[5.4].

5.1 The Hi-Bi FGEL

The Hi-Bi FGEL laser configuration is based on the use of FBGs fabricated in Hi-Bi fibre and exploits the difference in the wavelength of the Bragg reflections of light populating the orthogonally polarised eigenaxes of the fibre. Feedback from a FBG written in Hi-Bi fibre then results in the laser operating on two longitudinal modes that are separated in both wavelength and polarisation. The wavelength separation of the orthogonally polarised Bragg reflections can be calculated using the Bragg and birefringence equations below[5.4].

$$L_B = \frac{\lambda}{n_{effx} - n_{effy}} \tag{5.1}$$

$$\Delta\lambda_{Bg} = 2\Delta n_{eff}\Lambda \tag{5.2}$$

Where L_B is the beat length, λ is the operating wavelength, n_{effx} and n_{effy} are the effective refractive index of the fibre in each orthogonal axis; Δn_{eff} is the difference in refractive indices between n_{effx} and n_{effy}, $\Delta\lambda_{Bg}$ is the difference in Bragg wavelengths and Λ is the

period of the FBG. Therefore, a Hi-Bi fibre with a beat length of ≈ 1.6mm will produce a corresponding wavelength separation of 0.3 nm, A variation in refractive, Δn, of $0.5*10^3$, between the orthogonally linearly polarised modes of the reflection from the FBG. The fibre used in the experiment was bow-tie, Fibercore (HB 750), with a cut-off wavelength of 750 nm, a cladding diameter of 125μm and a numerical aperture of 0.15. The fibre was hydrogen loaded for 7 days in a pressure vessel at 130 bar to increase photosensitivity in the fibre prior to fabrication. The FBG was subsequently fabricated using a wavelength tuneable UV source and phase mask based interferometer[5.5] as described in chapter 2. The FBG was fabricated 250mm from the end of the fibre. The fibre was glued into a ferrule and subsequently angle polished at 3° to reduce unwanted reflections from the fibre end back into the active laser cavity that could de-stabilise the laser[5.6]. The FBG had a reflectivity of 40% and a bandwidth of 0.15 nm (FWHM). However due to the FBG being fabricated in Hi-Bi fibre, the FBG displayed two centre wavelengths one at 807.1 nm the other at 806.8 nm. As shown in Fig 5.1

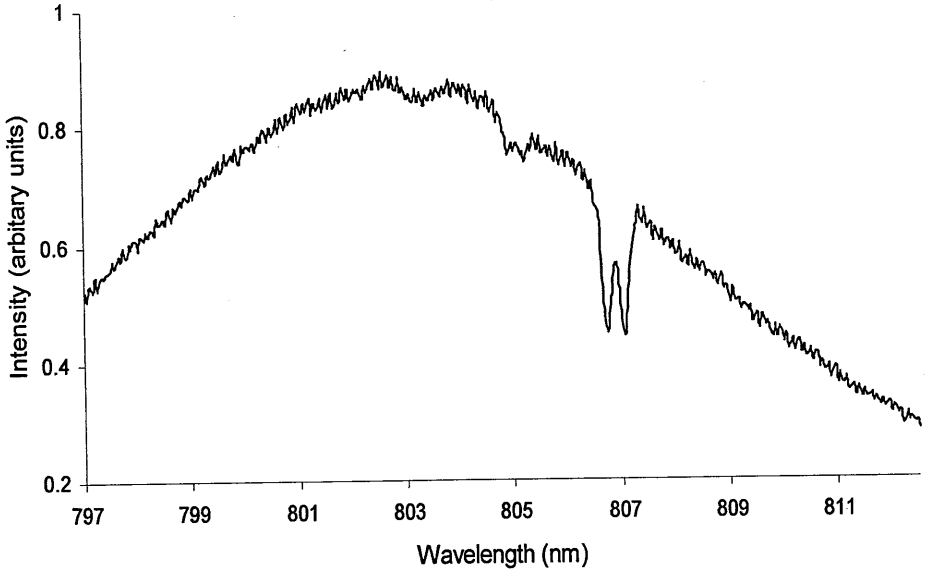

Fig. 5.1 Spectrum of the Hi-Bi FBG used in the external cavity

Light was coupled into the fibre using anti reflection (AR) coated lenses to further reduce unwanted reflections. A 150 mW, SDL 5420, non-AR coated 809 nm laser diode was coupled to the angle polished end of the fibre. The laser diode was driven with an

injection current of 60 mA and the operating temperature was stabilised at 21^0C ±0.1. A coupling efficiency of 40% was achieved. The optical length of the external cavity was 320 mm. A half wave plate was used to adjust the orientation of the polarisation of output of the laser with respect to the eigenmodes of the fibre. Transverse load applied to the FBG was used to adjust the birefringence and thus the separation of the Bragg wavelength of the reflection from each eigenaxes of the fibre. The load was applied by positioning the FBG, which has its coating removed, between two glass slides alongside an identical fibre to ensure even distribution of the load to the fibre. This allows the switchable laser to then be tuned by application of the load. The experimental configuration is shown in Fig. 5.2a & b.

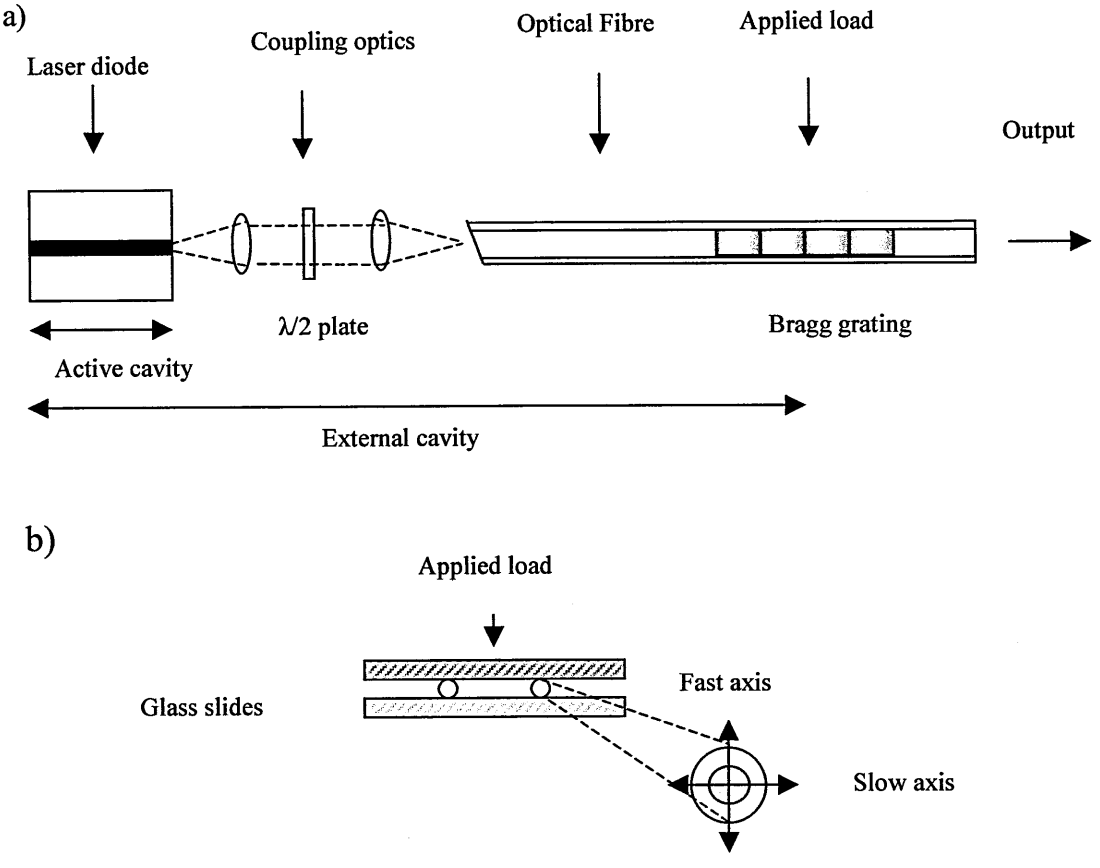

Fig. 5.2 a: Experimental arrangement for the Hi-Bi polarisation and wavelength switchable laser. b: Transverse strain apparatus. The slow axis of the fibre is orientated orthogonally to the direction of applied strain as shown in the diagram of the cross section of the fibre. A weight is placed on the top glass slide to induce transverse strain.

5.2 Wavelength switching

The FBG feedback was seen to reduce the laser threshold to 16mA, when light was coupled into the slow axis. The corresponding threshold current when coupled to the fast axis was 18mA. The spectrum was observed using an Ando AQ-6310b optical spectrum analyser with a resolution of 0.1 nm. As the λ/2 wave plate was rotated the proportion of light coupled into each eigenmode was varied, allowing lasing on a longitudinal mode corresponding to either eigenmode, or allowing both modes to lase simultaneously. The spectral output of the laser under different conditions of polarisation coupling is shown in Fig 5.3. The wavelength separation of the two modes is 0.3 nm, equal to the change in Bragg wavelength between each eigenmode. This matches the separation expected from a FBG written in Hi-Bi fibre with a beat length of 1.6 mm at 810 nm.

Fig. 5.4 plots the relative intensity of each mode under different states of polarisation coupling. The laser can be seen to switch the wavelength and polarisation of its output. The laser operates in 3 regimes. In regions A and C the laser operates on a single longitudinal mode that is orthogonally polarised for each region. In region B both orthogonally polarised modes co-exist, since the eigenaxes of both modes are equally populated. A rotation of the waveplate by 45^0 is required to alter the polarisation by 90^0. As the waveplate is rotated to a point ~ 41° from being orientated in line with the slow axis, a transition occurs, feedback increases and lasing threshold is passed. Simultaneously an opposing effect is occurring in the slow axis and at ~ 49° feedback decreases to a point where lasing will cease. The switching effect between wavelengths is reciprocal when the waveplate is turned in the other direction.

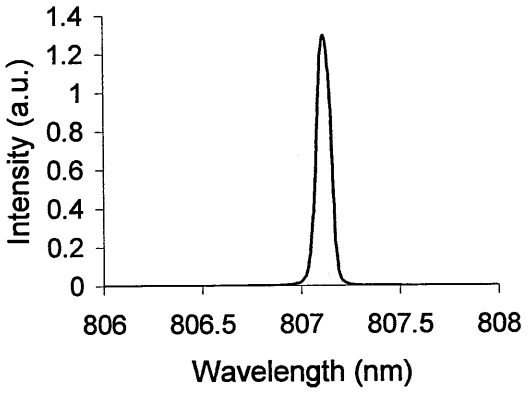

λ/2 wave plate rotation angle 0°
Coupling into slow axis

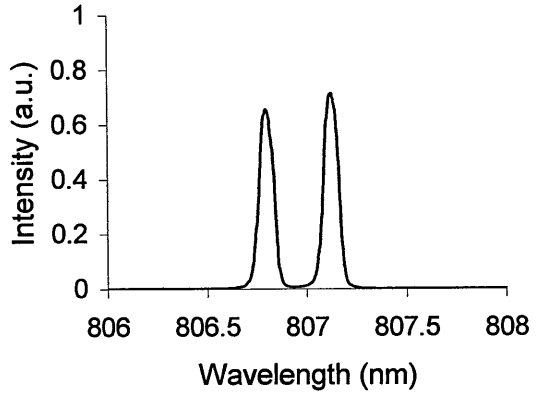

λ/2 wave plate rotation angle 22.5° (45° state of polarisation rotation)
Coupling into both axis

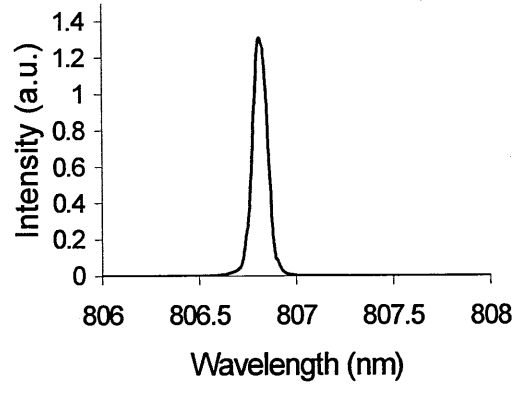

λ/2 wave plate rotation angle 45° (90° state of polarisation rotation)
Coupling into the fast axis

Fig 5.3 Spectrum of Hi-Bi laser as the λ/2 wave plate is rotated through 45°

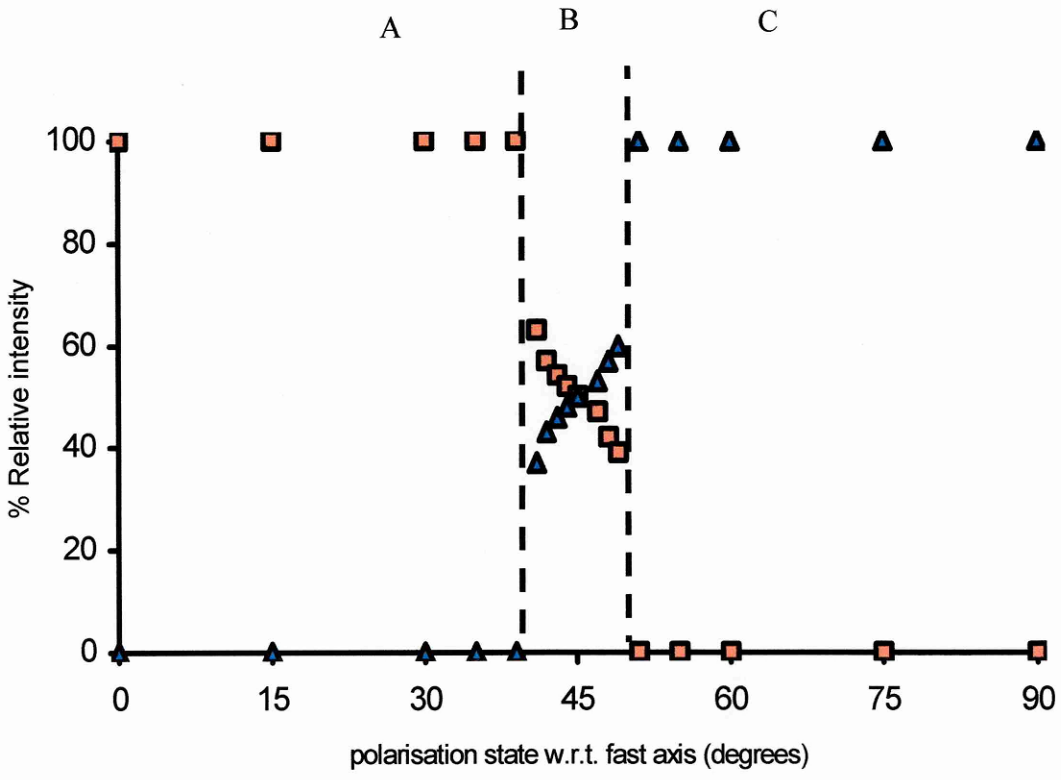

Fig. 5.4 SDL 5420 laser diode with Hi-Bi fibre FBG external cavity. The relative intensity of the orthogonally polarised modes as the plane of polarisation of the output of the laser is rotated. The square points represent the relative intensity of the fast axis mode, and the triangular points are the relative intensity of the slow axis mode.

▲ *Fast axis* ■ *Slow axis*

5.3 Wavelength tuning by transverse strain

As discussed in section 2.2.3, the application of transverse load to a FBG fabricated in Hi-Bi fibre will cause a change in birefringence of the fibre, which will in turn alter the difference between the Bragg wavelengths reflected from either eigenmode[5.7]. Tuning of the wavelength separation between the modes of the fibre may thus be achieved by transversely loading the FBG. A series of increasing weights were used to transversely load the fibre, using the apparatus shown in Fig 5.1b. The FBG was in parallel with another fibre of the same type whose coating had also been removed to ensure that load is applied from an orthogonal direction. A cross section of this experimental configuration is shown in Fig 5.1b.

Applying the load parallel to the fast axis reduces the birefringence of the fibre, causing the wavelength separation of the two modes to decrease. Fig. 5.5 shows the dependence of the lasing wavelengths upon the applied transverse load. Loads of up to 0.34 N/mm were placed on the fibre, and a linear dependence of the wavelength separation upon the applied load was observed.

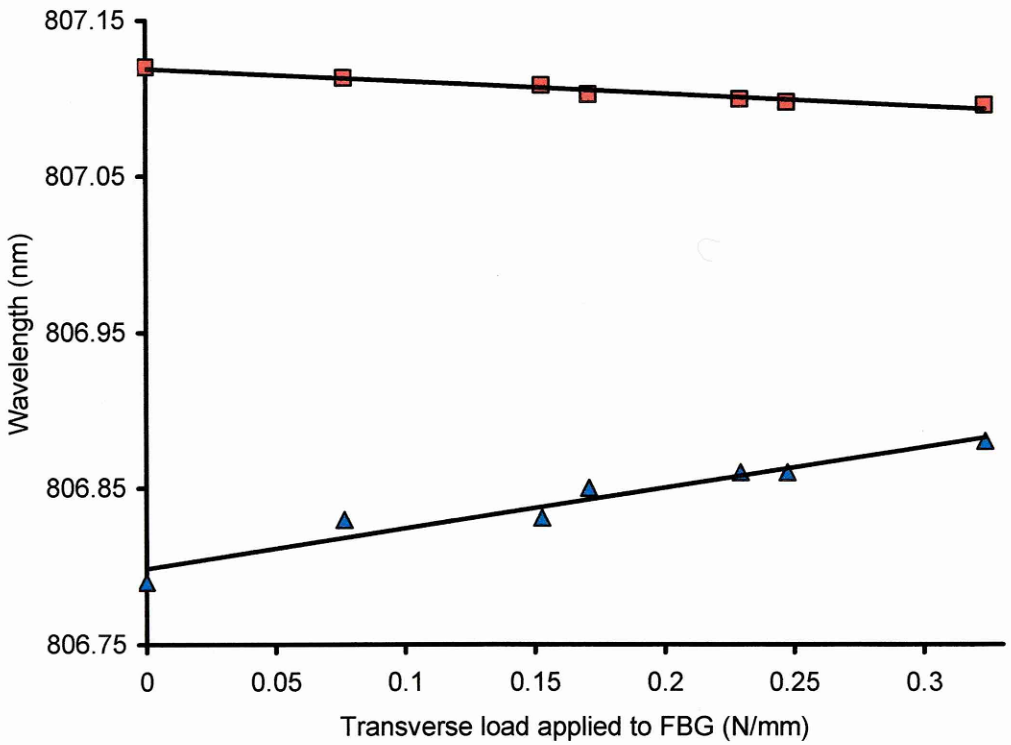

Fig. 5.5 The dependence of the lasing wavelengths upon the applied transverse load.

■ Slow axis ▲ Fast axis

5.4 Benefits and potential applications of the external cavity FBG semiconductor laser based on Hi-Bi fibre

The external cavity Hi-Bi laser offers new methods of switching and tuning the spectral output of a stabilised laser diode[5.8]. This chapter has experimentally demonstrated a stabilised wavelength switch of 0.3 nm dependant on birefringence of the fibre used to fabricate the FBG. As the polarisation of the laser switched by 90° there is also a concomitant switch in wavelength. The transverse loading of the FBG varied the separation of the modes between 0.3 nm and 0.2 nm, which corresponds to a beat length tuneable from 2.17 mm to 3.25 mm, and a beat frequency tuneable between 138 GHz and 92 GHz.

Using the Hi-Bi laser as a beat frequency source would require the use of a polariser, orientated at 45° to either axis at the output of the laser, selecting a component of each orthogonally polarised mode. If a component exists in both polarisation states it will create a potentially tuneable beat frequency. This has applications in, for example, the signal processing of miniature Fabry-Perot cavities[5.9].

Using an electro-optic liquid crystal device to define the polarisation of the light coupled into the fibre would permit the laser to be controlled electronically.

The methods presented here have advantages over alternative techniques such as distributed feedback and distributed Bragg reflector laser diodes as they are spectrally stable and will not shift wavelength, in response to a varying injection current[5.10]. Also, they are advantageous due to the increased control of tuneability FBGs have and the significantly lower cost, in that the technology can be applied to the simplest low cost non AR laser diode.

5.5 Summary

The Hi-Bi laser demonstrated stable operation on two orthogonally polarised longitudinal modes. The laser could be switched between modes by the rotation of a waveplate, allowing the output of the laser to be switched in both the polarisation and wavelength domains. Alternatively the laser could operate simultaneously on two modes. Transversely loading the fibre allows the wavelength separation of the two modes to be controlled. These characteristics could find use in polarisation and wavelength domain multiplexed sensing schemes. As wavelength separation between switchable modes of the laser is defined by fibre birefringence it is easily calibrated which has applications in multiple wavelength signal processing techniques[5.8]. The transverse loading of the FBG varied the separation of the modes between 0.3 nm and 0.2 nm, which corresponds to a beat length tuneable from 2.17 mm to 3.25 mm, and a beat frequency tuneable between 138 GHz and 92 GHz.

References

(5.1) J. Hernandez-Cordero, V.A. Kozlov, A.L.G. Carter and T.F. Morse, 'Fiber Laser Polarization tuning using a Bragg grating in a Hi-Bi Fiber', IEEE Photonics Technology Lett., 1998, Vol. 10, pp.941-943.

(5.2) O. Deparis, R. Kiyan, S.A. Vasilev, O.I. Medledkov, E.M. Dianov, O. Pottiez, P. Megret and M. Blondel, 'Polarization maintaing Fiber Bragg gratings for wavelength selection in actively mode-locked Er-Doped Fiber lasers', IEEE Photonics Technology Lett., 2001, Vol. 13, pp. 284-286.

(5.3) Y.C. Lai, C. Lu, W. Zhang, J.A.R. Williams, L. Zhang and I. Bennion 'Generation of microwave signal with very narrow linewidth from a dual mode fibre grating DFB laser' IOP Applied optics and Opt-electronics conference 17-21 September, Loughborough 2000, pp. 23.

(5.4) T.F. Carruthers, I.N. Duling III and M. L. Dennis, 'Active-passive modelocking in a single-polarization erbium fiber laser', Electronics Letts., 1994, Vol. 30, pp. 1051-1053.

(5.4) J.M. Senior, 'Optical fibre communications: principles and practice' 2nd edition, Prentice Hall international series in optoelectronics, UK, 1992.

(5.5) M.L. Dockney, S.W. James and R.P. Tatam, 'Fibre Bragg gratings fabricated using a wavelength tuneable laser source and a phase mask based interferometer' Measurement Science and Technology. 1996, Vol. 7, pp. 445-448.

(5.6) K. Petermann 'External optical feedback phenomena in semiconductor lasers' IEEE J. of selected topics in Quantum electronics, 1995, Vol. 1, pp. 480-489.

(5.7) C.M. Lawrence, D.V. Nelson, E. Udd and T. Bennet, 'A fiber optic sensor for transverse

strain measurement' Experimental mechanics, 1999, Vol. 39 (3), pp. 202-209.

(5.8) S.P. Reilly, S.W. James and R.P. Tatam 'Tuneable and switchable dual wavelength lasers using optical fibre Bragg gratings external cavities', Electronics Lett., 2002, Vol. 38, pp. 1033-1034.

(5.9) A. Ezbiri and R.P. Tatam 'Passive signal processing technique for miniature Fabry-Perot interferometric sensor with a multimode laser-diode source', Optics Letts., 1996, Vol. 20, pp. 1818-1820.

(5.10) F.N. Timofeev, I.A. Kostko, P. Bayvel, O. Berger, R. Wyatt, R. Kashyap, I.F. Lealman and G.D. Maxwell, '10Gbit/s directly modulated, high temperature-stability external fibre grating laser for dense WDM networks', Electron. Lett., 1999, Vol. 35, pp. 1737-1739.

6 External cavity FBG semiconductor laser based on multiple FBGs

In this chapter a novel external cavity laser is demonstrated experimentally. The external cavity comprises two spatially separate fibre Bragg gratings fabricated in mono-mode optical fibre. The central wavelengths of the two FBGs are tuneable independently, allowing the laser to be used for tuneable beat frequency generation. A three FBG external cavity laser is also demonstrated experimentally, which can potentially generate simultaneously three tuneable beat frequencies.

6.1 Multiple wavelength FGEL lasers

Dual wavelength lasers have been the subject of considerable research interest for several applications including interrogation of miniature cavity sensors[6.1] and as an illuminating source for broad FBG sensors to reduce uncertainty in the measurand[6.2]. They have also found application as sources capable of producing beat signals at microwave frequencies, which is desirable for electronic signal processing systems[6.2,6.3]. Beat frequencies have been generated previously using separate laser cavities[6.2,6.3]. However, systems employing separate cavities can suffer from phase noise and drift, making a single cavity dual wavelength laser preferable for producing stable beat frequencies. In this chapter two novel FBG external cavity laser configurations are demonstrated experimentally. Both use the light reflected from the FBGs to force the laser to operate at the two Bragg wavelengths. The central wavelengths of the FBGs are independently tuneable allowing the generation of a tuneable beat frequency.

6.2 The Dual FBG External cavity laser

This laser configuration employs two spatially separate FBGs. The FBGs were fabricated in single mode fibre at two different wavelengths, forcing the laser to lase on two longitudinal modes. The experimental configuration is outlined in Fig. 6.1.

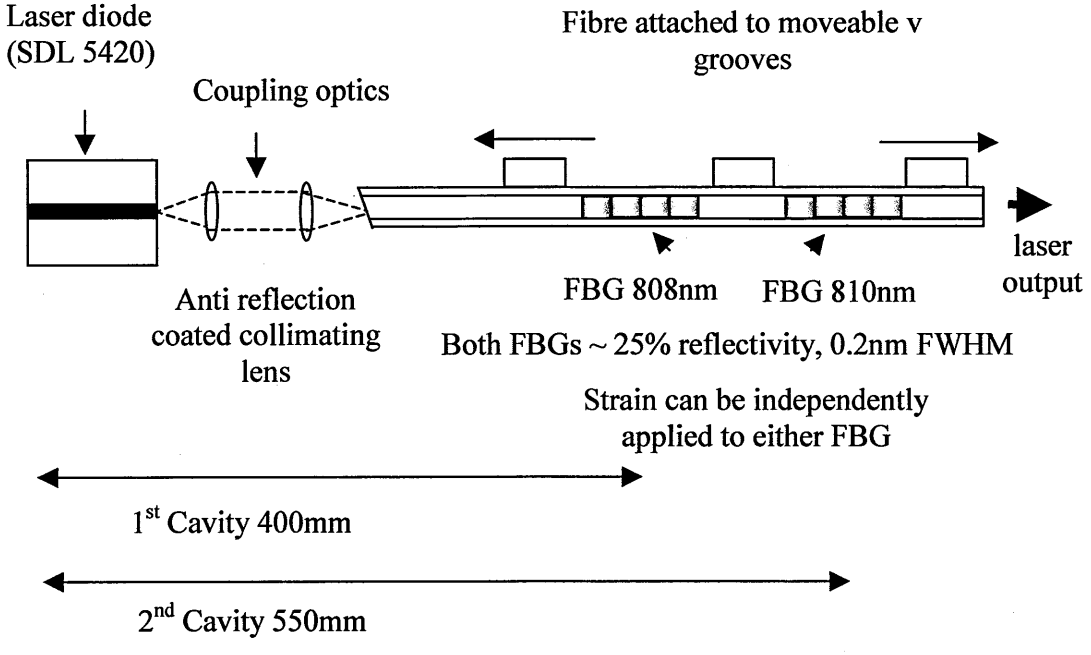

Fig 6.1 Experimental configuration for the dual FBG external cavity laser.

The two FBGs were not co-located, allowing strain to be applied independently to each FBG, making both FBGs centre wavelengths, and hence the two modes of the laser independently tuneable. The interference between these two longitudinal modes can be used to create a beat signal, the frequency of which is a function of the separation in wavelength of the two modes, as discussed in Appendix A. Thus the beat frequency that may be generated using the output from this laser is tuneable. The FBGs were fabricated with a physical separation of approximately 150 mm. The FBGs were fabricated in hydrogen loaded fibre, Spectran (FS-SMC-A0780B), using the technique outlined

earlier[6.4]. The Bragg wavelengths were separated by 2nm, the FWHM of each FBG was ≈ 0.2 nm and reflectivity was ≈ 25%. The intra cavity end of the fibre was angle polished to prevent de-stabilising reflections. The coupling efficiency from the diode into the fibre was ≈ 35%. The first FBG, fabricated at 808 nm, formed an external cavity approximately 400 mm in length, the second FBG at 810 nm formed a cavity approximately 650 mm long. The two FBGs are labelled FBG1 and FBG2 respectively. The spectrum of the FBGs is shown in Fig 6.2

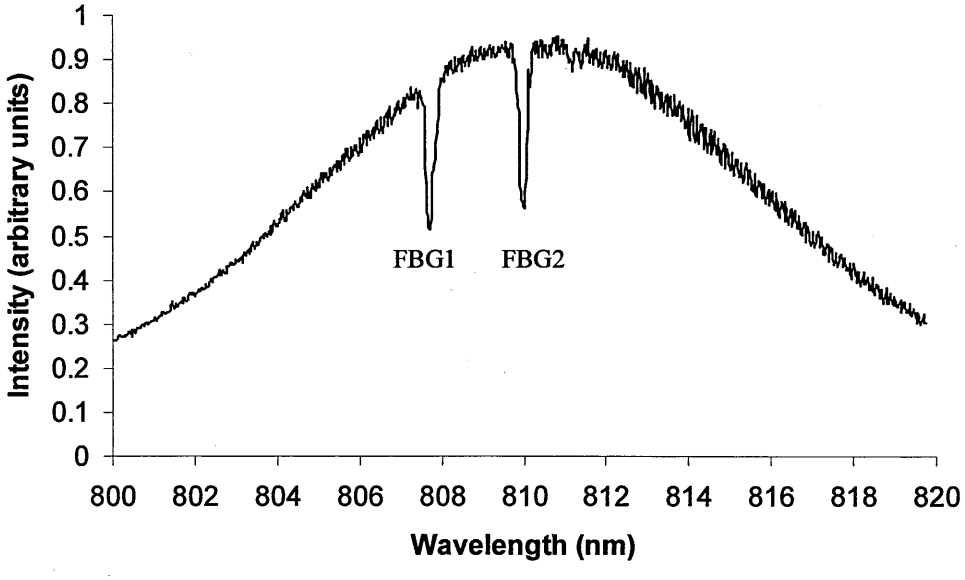

Fig 6.2 Spectrum of FBG1 and FBG2 spatially separated in SM fibre.

The laser was observed to operate on two longitudinal modes corresponding to the centre wavelength of each FBG. The spacing of the modes decreased as an axial strain was applied to the first FBG, the wavelength separation of the two longitudinal modes is shown in Fig. 6.3. The relative power in each mode could be tuned with injection current and temperature as these parameters will introduce a shift in the luminescence spectrum of the diode. However at a temperature of 21°C ±0.1, FBG1 demonstrated a lowered threshold ~ 18 mA while the FBG2 threshold was ~ 23 mA. Throughout the full range of the injection current the difference in power between the two modes was no more than 20%.

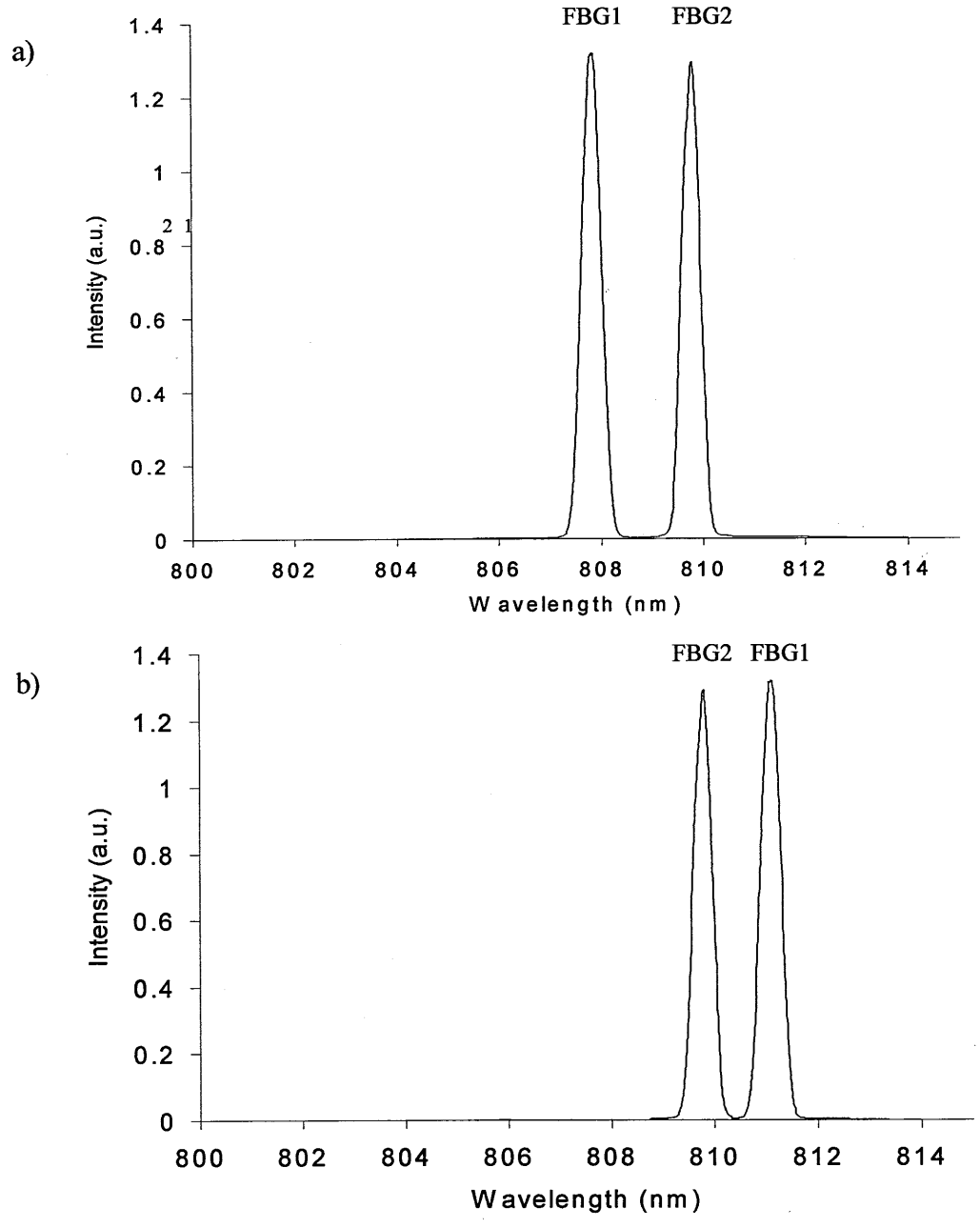

Fig 6.3 Comparison of spectral output of the dual FBG external cavity laser under the same conditions of injection current and temperature when an axial strain of magnitude 5300με is applied to FBG 1 in b)

When the two modes are separated by less than ≈ 0.3 nm, mode competition effects collapsed both modes into a single mode as the FBGs spectrally came closer to each other, forming a single longitudinal mode laser, shown in Fig. 6.4. As the modes became spectrally closer, FBG2 decreased in amplitude, to around 50% of FBG1, until a separation of around 0.3 nm when FBG2 collapsed into FBG1. The single longitudinal mode of FBG1 continued to dominate the spectrum until the central wavelength of the FBGs were tuned so that their spectral separation exceeded 0.3 nm, when the second mode reappeared. This 0.3 nm separation generated the lowest beat frequency achieved, ≈ 130 GHz with a corresponding synthetic wavelength of 2.3 mm. The maximum beat frequency was >2.28 THz, which has a corresponding synthetic wavelength of <0.131 mm. Operation was mode hop free over the entire injection current range as demonstrated by Fig. 6.5, where a dual FBG external cavity laser is compared to the same laser diode at the same operating temperature, 21°C, but with no optical feedback. A threshold current reduction of around 30% was observed for the mode at 810 nm, corresponding to FBG2. The 808 nm, FBG1, mode was seen to have a higher threshold than the diode with no feedback. The modes were observed to be stable over a period of several hours.

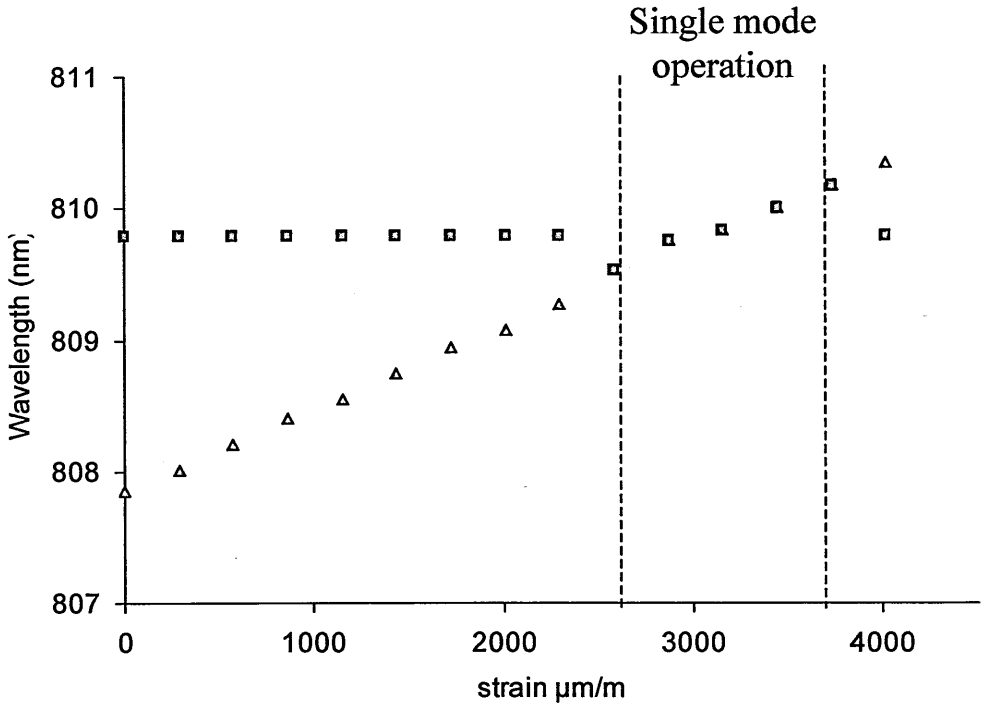

Fig. 6.4 the centre wavelengths of the two modes as the first FBG1 fabricated at 808 nm is strained. The region marked with dotted lines illustrates the range of applied strain where the laser operates on a single longitudinal mode.

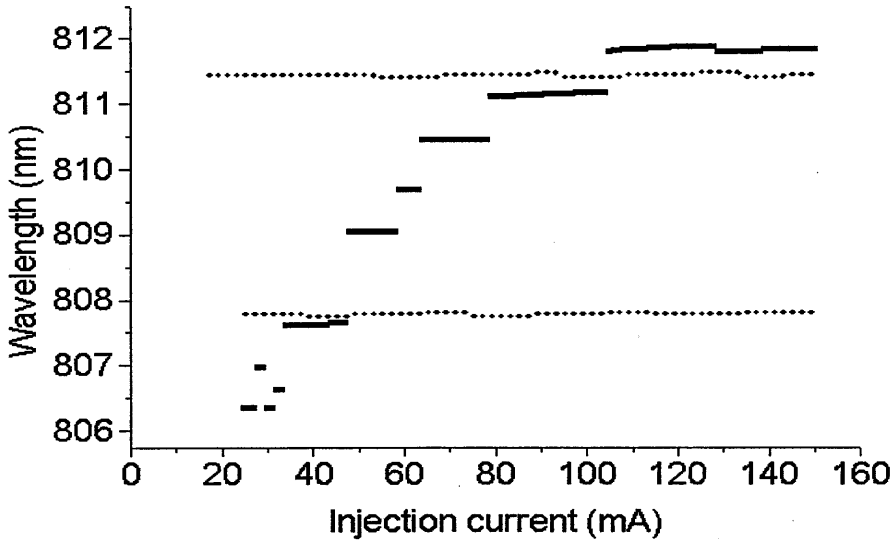

Fig. 6.5 The spectral stability of the modes of the dual FBG laser in comparison with the same laser diode stabilised to the same temperature with no optical feedback. The solid line represents the wavelength of the laser diode with now feedback and the dotted line represents both modes of the dual FBG feedback

6.3 The three wavelength FBG external cavity laser

An FBG external cavity laser incorporating three FBGs was also fabricated. It comprises the same experimental set up as the dual FBG laser but with an extra FBG

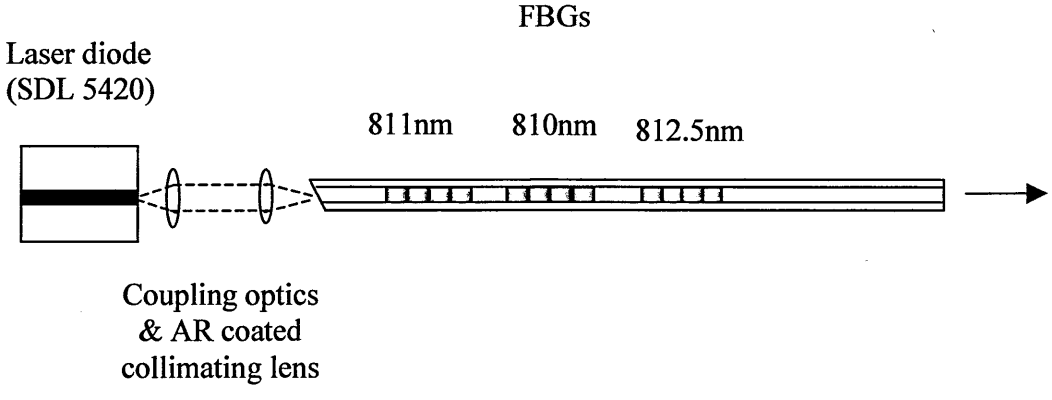

Fig. 6.6 Experimental configuration of three wavelength laser.

As the three FBGs were not co-located, strain could be applied independently to each, making all modes independently tuneable. The interference between three modes can be used to create a beat signal, which will have three frequency components. If two of the FBGs are tuneable, all three beat frequencies will be tuneable.

The FBGs in the triple FBG laser were fabricated with a physical separation of approximately 1 mm, in a tuneable system however FBGs would be spaced further apart to allow for the tuning apparatus. The FBGs were fabricated in hydrogen loaded fibre, Spectran (FS-SMC-A0780B), with the same technique as outlined earlier[6.4]. The Bragg wavelengths were separated by 1-1.5nm, the FWHM of each FBG was ≈ 0.3nm and reflectivity was ≈ 15-25%. The end of the fibre was angle polished to prevent de-stabilising reflections. The coupling efficiency was ≈ 35%. The first FBG, fabricated at 811 nm, formed an external cavity approximately 100 mm in length, the second FBG at 810 nm formed a cavity approximately 115 mm long. The third FBG fabricated at 812.5 nm formed a third external cavity approximately 130 mm in length. The spectrum of the laser was then measured on an Ando AQ-6310b

The spectrum of the laser is shown in Fig. 6.7. Operation was mode hop free over the entire injection current range as demonstrated by Fig. 6.8. Where the three FBG external cavity laser is compared to the same laser diode under the same conditions, 21°C ±0.1, but with no optical feedback. This was observed to be stable over a period of several hours. It can be seen however that all three modes do not exist over the full range of the injection current due to the shift in gain spectrum within the active cavity of the laser diode as the injection current is increased.

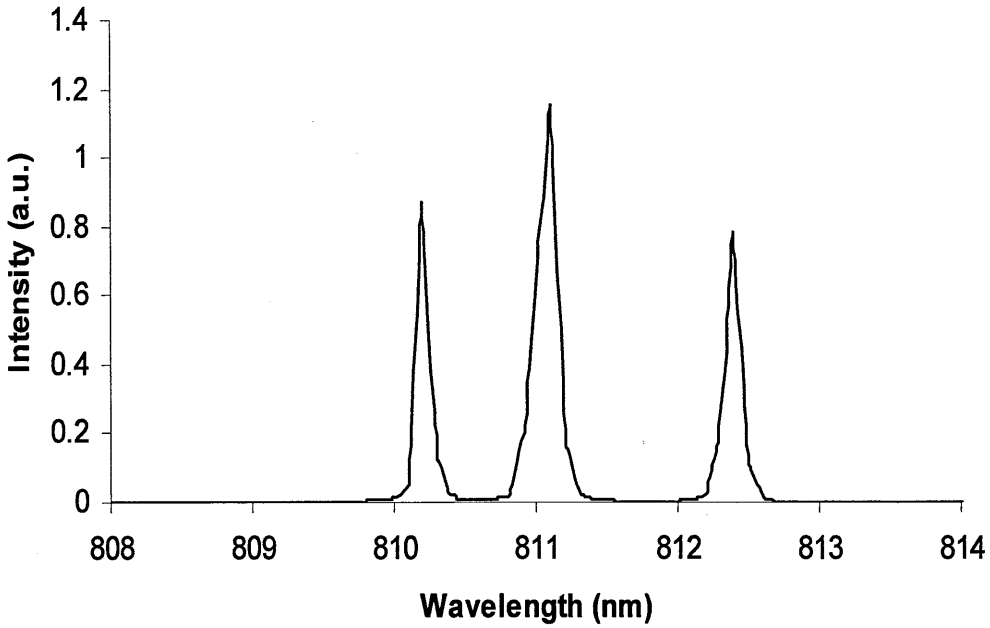

Fig.6.7 Spectral output of three FBG external cavity laser

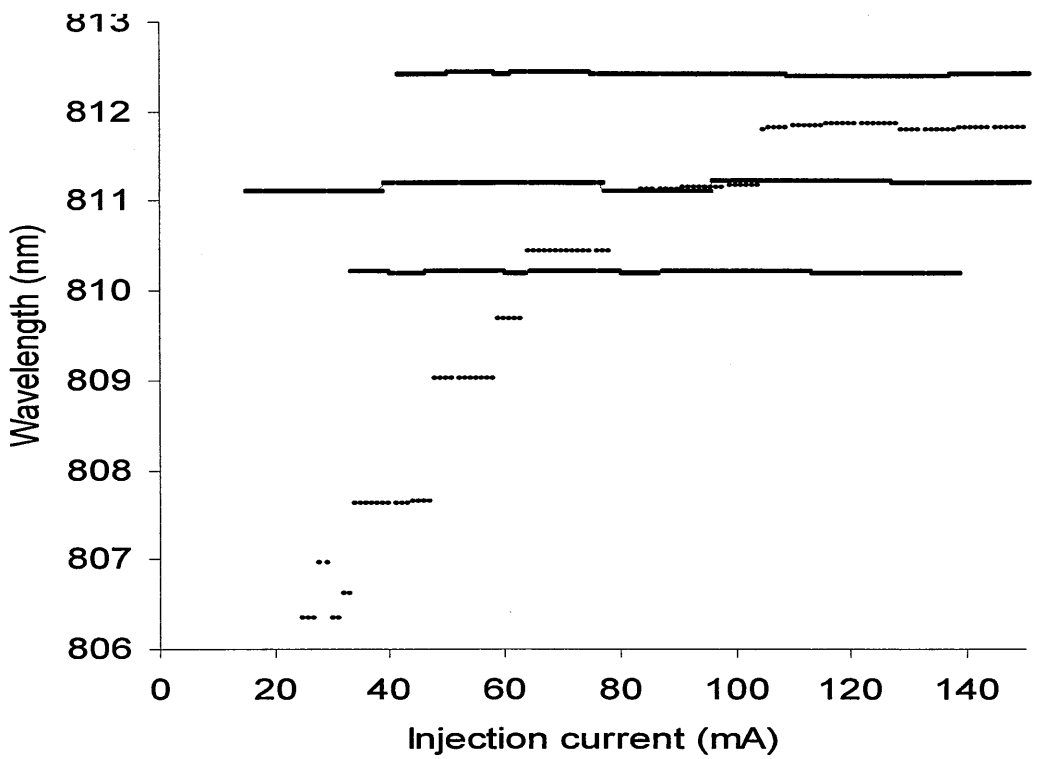

Fig. 6.8 The spectral stability of the modes of the three FBG laser in comparison with the same laser diode operating at the same temperature, but with no optical feedback.

6.4 Summary

Two novel external cavity lasers have been demonstrated. Both lasers were shown to be mode hop free and a high degree of stability was observed over several hours. The dual FBG laser system employing spatially and spectrally separated FBGs allowed independent tuning of the two longitudinal modes. The lowest beat frequency achieved was ≈ 130 GHz with a corresponding synthetic wavelength of 2.3 mm. It is thought that this frequency can be lowered significantly by the use of narrower bandwidth FBGs. As the overlapping of the FBG spectrums would occur at when the FBG were at a greater spectral proximity.

The three FBG laser was also experimentally demonstrated that can potentially generate three simultaneously tuneable beat frequencies. There is potential for more FBGs to be added to create more wavelengths, limited by the luminescence band of the diode.

References

(6.1) A. Ezbiri and R.P.Tatam 'Passive signal processing technique for miniature Fabry-Perot interferometric sensor with a multimode laser-diode source', Optics Letts., 1996, Vol. 20, pp. 1818-1820.

(6.2) A. Wilson, S.W. James and R.P.Tatam, 'Time-division-multiplexing of In-fibre Bragg gratings using a pulsed laser diode source', Presented at 12th Optical Fibre sensors conference, OFS-12, Williamsburg VA, USA, Nov. 1997

(6.3) N. Onodera, 'THz optical beat frequency generation by mode locked semiconductor lasers', Electron. Lett. 1996, Vol. 32, pp. 1013-1015.

(6.4) F.N. Timofeev, S. Benett, R. Griffin, P. Bayvel, A.J. Seeds, R Wyatt, R. Kashyap, and M. Robertson, 'High spectral purity millimetre-wave modulated optical signal generation using fibre grating lasers', Electron. Lett. 1998, Vol. 34, pp. 668-669

(6.5) M.L. Dockney, S.W. James and R.P. Tatam, 'Fibre Bragg gratings fabricated using a wavelength tuneable laser source and a phase mask based interferometer' Measurement science and technology. 1996, Vol. 7, pp. 445-448.

7 Interrogation of miniature Fabry-Perot interferometric sensors

In this chapter a dual FBG external cavity laser is used to demonstrate experimentally an interrogation technique for miniature Fabry-Perot sensor cavities. Prior to the presentation of these results, miniature Fabry-Perot sensor cavities are introduced and the reduction in errors of the measurand by dual wavelength interrogation techniques discussed.

7.1 Optical fibre sensors

Fibre optic sensors offer a number of advantages in comparison to electrical sensors[7.1]. The light weight and relatively small size of optical fibre sensors are complemented by their strong immunity to electromagnetic interference, eliminating the need for heavy and costly shielding. The result has been widespread interest in applying this technology to many different fields. As optical fibre sensors are made of glass they can tolerate wide temperature ranges, and high levels of vibration and shock. Optical fibre sensors all work on the principal that the measurand will induce a measurable change in the properties of the light recovered from the fibre sensor, such as phase, intensity and wavelength. They can be broadly divided into two categories. Intrinsic sensors allow the measurand to affect the light while in the fibre. In extrinsic optical fibre sensors the interaction between the light and the measurand occurs outside the fibre, and therefore the fibre is often a delivery mechanism to and from the sensor

7.2 Fabry-Perot Interferometers

Fabry Perot cavities are formed between two partially reflecting surfaces, they are based on the same principles as laser Fabry-Perot cavities discussed in chapter 3. All

passes through the interferometer are combined together. The principle of Fabry- Perot multiple beam interference is illustrated in Fig 7.1

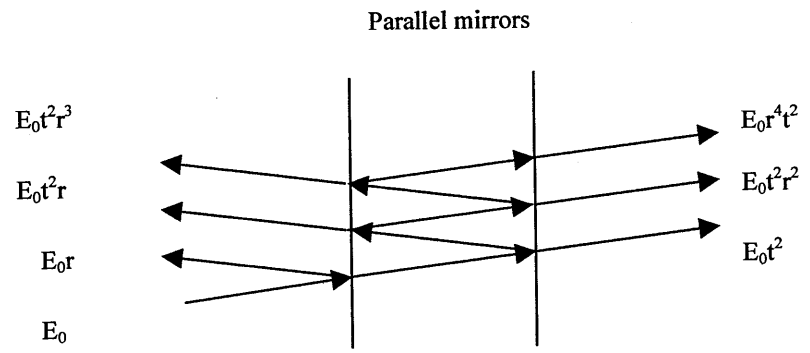

Fig 7.1 Ray paths in a Fabry-Perot interferometer, the incident ray has an amplitude of E_0, r and t are coefficients of reflection and transmission respectively.

However if the distance between cavity facets can be varied then the device becomes a Fabry-Perot interferometer, a spectroscopic device with potentially high resolution. The Fabry-Perot interferometer is a multiple beam interferometer and as such the irradiance of the reflected and transmitted waves are described respectively by Eqs (7.1) & (7.2)[7.2].

$$I_r = I_i \frac{[R/(1-R)]^2 \sin^2(\delta/2)}{1+[R/(1-R)]^2 \sin^2(\delta/2)} \tag{7.1}$$

$$I_t = I_i \frac{1}{1+[R/(1-R)]^2 \sin^2(\delta/2)} \tag{7.2}$$

Where R is the reflectance of the mirrors, when the mirrors absorb or transmit some of the energy they are less reflective and the resolution of the interferometer reduces. I_r, I_t and I_i are the irradiances of the reflection, transmission and incident light respectively and

δ is the optical phase shift. However when reflectance is low enough these Fabry-Perot cavities can be thought of as two beam interferometers

7.3 Miniature low finesse Fabry-Perot interferometric sensors

Many interferometric sensing systems require a reference arm. This can be a potential problem as the reference arm could easily be exposed to unwanted different environmental perturbations in comparison with the sensing arm, introducing ambiguities into the recovered measurand. This problem is heightened when the sensor is used for remote applications. In contrast to two beam interferometers like the Mach-Zehnder or Michelson the low finesse fibre Fabry-Perot interferometer (LFFFPI)[7.3] uses the same arm for reference as the measurand, bypassing the problem of different perturbations in the reference arm. The characterisation of LFFFPI's responses to measurands has been published detailing their exploitation as sensors[7.4,7.5,7.6]. The small size of the sensors makes then ideal for embedding in structures and also makes them useful for highly localised measurements.[7.7] The LFFFPI also has an extrinsic version show in Fig 7.2

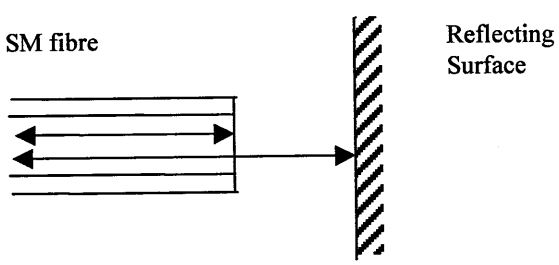

Fig 7.2 Extrinsic Fabry-Perot interferometric sensor

The cavity is formed between two low reflecting surfaces and can essentially be thought of as a two beam device. The cleaved end of the fibre acts as the first reflecting surface while the second reflecting surface, which is the measurand, re-injects light back into the fibre core[7.4]. If the cavity is shorter than the coherence length of the illuminating source

then an interferometric output is obtained and its transfer function is a series of cosine fringes. A fibre Fabry-Perot sensor of this kind has been used as an accelerometer[7.3] The sensor was shown to have twice the sensitivity of a Mach-Zehnder, due to twice passing the length of the cavity. The LFFFP sensor was capable of detecting phase shifts of $4*10^{-5}$ rad at 100 Hz, which translates to a sensitivity of $\geq$ 200 rad/g although the sensor did suffer from polarisation effect due to its long cavity length. High finesse Fabry-Perot cavities have also been shown to contribute to a factor of two improvement in sensitivity over two beam interferometry schemes[7.6]. The LFFFP sensor has also found applications detecting vibration and acoustic measurements[7.4], strain[7.3], voltages and magnetic fields[7.5] and temperature for medical applications[7.6]. Very short gauge sensors have also been investigated in both intrinsic and extrinsic forms[7.4]. These very short cavities, ~ 20 μm to 3 mm provide very localised measurements and also have low phase noise. The LFFFP has limitations however in multiplexing a number of sensors and it has a large unambiguous range.

7.4 Signal processing schemes

An ambiguity that exists with interferometric sensing is the problem of the varying sensitivity over a full cycle of the interferometer. Over a full cycle of 2π the interferometer passes two points of maximum sensitivity 180° apart and two points of minimum sensitivity midway between the points of quadrature, illustrated by Fig 7.3. A variety of techniques have been developed to address this problem of varying sensitivity. An outline of the techniques available is presented in the proceeding sections

7.4.1 Extended range interferometry

In addition to the problem of varying sensitivity, interferometric sensors also suffer from the unambiguous range being limited to 2π radians. Fringe counting systems have been developed but there are some optical solutions such as dual wavelength interferometry, where the two wavelengths generate a synthetic wavelength, which is the wavelength of the beat frequency, providing an increased unambiguous range for the

interferometric sensor. The closer the two illuminating wavelengths the larger the extended range of the sensor. The synthetic wavelength is derived in Appendix A.

Another technique is white light interferometry[7.7]. The sensor is interrogated by a broad band source and an interference pattern is generated by varying a balancing arm of the interferometer. An extended range white light interferometer could move the balancing arm further too constantly maintain maximum fringe visibility, thus monitoring the balancing arm can recover the measurand.

7.4.2 Passive homodyne signal processing schemes

Passive homodyne systems have been developed by producing a psuedo dual wavelength laser. Two wavelengths can be tuned to have a constant $\pi/2$ phase difference[7.8] for the specific length of cavity being interrogated, this ensures that when one output has faded the other is at quadrature. This can be realised by applying a square wave injection current of appropriate amplitude thus producing two alternating wavelengths due to the change in wavelength with injection current, as described in chapter 3. The output of the first wavelength from the interferometer is of the form:

$$I_c = I_{0c}[1 + V\cos(\phi)] \tag{7.3}$$

The second wavelength, due to the different injection current has an output from the interferometer of the form:

$$I_s = I_{0s}\left(1 - V\cos\left(\phi - \frac{\pi}{2}\right)\right) = I_{0s}[1 - V\sin(\phi)] \tag{7.4}$$

These two wavelengths, at constant $\pi/2$ phase difference are illustrated in Fig. 7.3

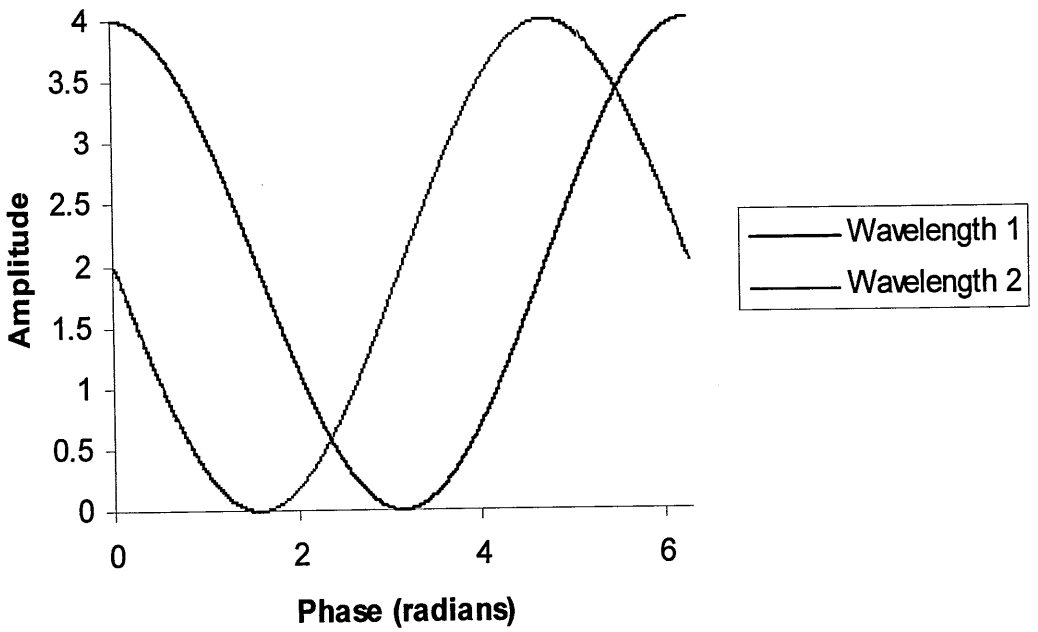

Fig 7.3 Theoretical output of the interferometer from two wavelengths with a spectral difference that will induce a 90° phase difference.

The phase difference between the two wavelengths recovered from the sensor cavity can then be derived from:

$$\phi = \tan^{-1}\left(\frac{I_s - I_{0s}}{I_c - I_{0c}}\right) \tag{7.5}$$

For the phase to be accurate in equation 7.5, both wavelengths must be sampled above the Nyquist rate of the phase change of the measurand. The technique of switching the injection current between two values to create two wavelengths is however limited by the wavelength separation between the two injection current values, typically 1 nm for a 20 mA variation in injection current, which would require a sensor cavity size of ~80 μm for the two wavelengths to be in quadrature. Also the interference pattern is likely to have a poor extinction ratio due to the wavelengths being at different powers and discontinuous nature of the switched signal. It is possible to use two separate lasers but there must be high wavelength stability between the sources.

7.5 Dual wavelength interrogation of a Miniature low finesse Fabry-Perot interferometric sensors

The fibre Fabry-Perot interferometer has the transfer function[7.2]:

$$I = I_0 \frac{2R_0(1-\cos(\phi))}{1+R_0^2-2R_0\cos(\phi)} \tag{7.6}$$

Where R_o is the reflectivity of the mirrors, I_0 is the DC intensity of the illuminating light and ϕ is the phase between interfering waves. In the low finesse interferometer however the transfer function can be thought of as a two beam interferometer and can be approximated by:

$$I = I_0(1+V\cos(\phi)) \tag{7.7}$$

Where V is the visibility, the ratio of brightness of the interference fringes. If the sensor is interrogated by two different wavelengths λ_1 (frequency υ_1) and λ_2 (frequency υ_2) the difference in phase between the two fringe patterns is then given by[7.15]:

$$\Delta\phi = 4\pi nl\left(\frac{v_1-v_2}{c}\right) \approx \frac{4\pi nl(\lambda_1-\lambda_2)}{\lambda_1^2} \tag{7.8}$$

The two wavelengths are then multiplexed using WDM which gives two separate interference patterns. The phase shift, $\Delta\phi$, can then be adjusted to reach quadrature by either tuning the sensor cavity or by tuning the separation in wavelength between the two illuminating wavelengths. Therefore, if the required phase difference is $\pi/2$, as would be the case in maximising quadrature, the corresponding required cavity length, l, is given by:

$$l \approx \frac{\lambda_1^2}{8n(\lambda_1 - \lambda_2)} \tag{7.9}$$

Therefore at a $\pi/2$ phase shift between the wavelengths, the output of the interferometer the two fringe patterns take the form:

$$\begin{aligned} i_1 &= I_1(1 + V\cos(\phi)) \\ i_2 &= I_2(1 + V\sin(\phi)) \end{aligned} \tag{7.10}$$

I_1 and I_2 are the optical powers at each wavelength

7.6 Errors in cavity interrogation

The equations presented in the preceding section are appropriate for a low finesse Fabry-Perot (F-P) interferometer as in fibre there is a low reflectivity, ~4%, at the air-fibre interface. This limits the effect of multiple reflections; however they do contribute an error to the phase of the interferometer. This difference between considering a multiple beam interferometer error means Eq. (7.6) becomes Eq. (7.11)[7.15]

$$\begin{cases} i_1 \approx I_0 \dfrac{2R_0}{1+R_0^2}\left(1 - \dfrac{(1-R_0)^2}{1+R_0^2}\cos(\phi) - \dfrac{2R_0}{1+R_0^2}\cos^2(\phi)\right) \\ i_2 \approx I_0 \dfrac{2R_0}{1+R_0^2}\left(1 - \dfrac{(1-R_0)^2}{1+R_0^2}\sin(\phi) - \dfrac{2R_0}{1+R_0^2}\sin^2(\phi)\right) \end{cases} \tag{7.11}$$

$$\tan(\phi') = \left(\frac{1 - \dfrac{2R_0}{1+R_0^2}\sin(\phi)}{1 + \dfrac{2R_0}{1+R_0^2}\cos(\phi)}\right)\tan(\phi) \tag{7.12}$$

Subtracting the phase, φ, from the error included phase signal gives:

$$\phi'-\phi=\left(\left(\frac{1-\frac{2R_0}{1+R_0^2}\sin(\phi)}{1+\frac{2R_0}{1+R_0^2}\cos(\phi)}\right)-1\right)\frac{\sin(2\phi)}{2} \tag{7.13}$$

This results in a maximum error of ~0.06rad (3.4°)[7.15] over the phase range 0-π.

As the interferometer path length is changed under the application of the measurand the interference fringes are shifted away from quadrature. This is another intrinsic error but it can be quantified. A change in the cavity length, *dl*, produces an alteration in the phase $d(\Delta\varphi)$ between the interferometric outputs of both wavelengths, given by:

$$\frac{d(\Delta\phi)}{dl}=\frac{4\pi\Delta v}{c} \tag{7.14}$$

Corresponding to a single wavelength:

$$\frac{d(\phi)}{dl}=\frac{4\pi v}{c} \tag{7.15}$$

The relative phase change is:

$$\frac{d(\Delta\phi)}{d(\phi)}=\frac{\Delta v}{v}\approx\frac{\Delta\lambda}{\lambda} \tag{7.16}$$

This demonstrates the linear incremental drift in phase between the two wavelengths, the resulting error can be written in the form ε'φ, where:

$$\varepsilon' = \frac{d(\Delta\phi)}{d\phi_1} \approx \frac{\Delta\lambda}{\lambda_1} \tag{7.17}$$

This manifests itself in the overall interferometric signals of the two wavelengths by Eq. 7.19[7.15]

$$\begin{cases} i_1 \approx I_0 \dfrac{2R_0}{1+R_0^2}\left(1-\dfrac{(1-R_0)^2}{1+R_0^2}\cos(\phi)-\dfrac{2R_0}{1+R_0^2}\cos^2(\phi)\right) \\ i_2 \approx I_0 \dfrac{2R_0}{1+R_0^2}\left(1-\dfrac{(1-R_0)^2}{1+R_0^2}\sin(\phi+\varepsilon+\varepsilon'\phi)-\dfrac{2R_0}{1+R_0^2}\sin^2(\phi+\varepsilon+\varepsilon'\phi)\right) \end{cases} \tag{7.18}$$

$\varepsilon'\varphi \approx 4.5*10^{-3}$ is the added error for an infra red laser with $\Delta\lambda$= 3nm resulting in a phase error in the interferometer of .02 rad. The error, ε, for the possible miscalibration of the system, is the largest potential error compared with the measurand induced errors of drifting out of quadrature and multiple reflection errors. An error of 10% in calibration can result in an error of 0.2 rad[7.15].

7.7 Miniature Fabry-Perot interferometric sensor with a Dual FBG external cavity semiconductor laser

It is possible for a laser diode to operate on two longitudinal modes simultaneously using hole burning effects discussed in chapter 3. Ezbiri and Tatam[7.9] used a laser diode undergoing hole burning effects to generate two interferometric outputs at quadrature, achieved by tuning of the injection current and temperature. The wavelength separation of the two modes however could not be tuned, therefore the length of the sensor cavity has to be tuned to whatever the separation of the two modes of the diode decrees. In this case wavelength separation was ~ 3 nm and the cavity length was 19 μm. However, in a sensing system when an extrinsic miniature F-P cavity is being interrogated, it would be possible however to tune the wavelength separation of two longitudinal modes of a dual FBG external cavity laser[7.10] . Thus, when the sensor is embedded, hard to reach or requires recalibration, quadrature can be obtained by tuning the source.

7.8 Experimental results of FGEL interrogation of miniature F-P sensor

The dual FBG used in the experiment was as described in chapter 6 and in shown in Fig. 7.4

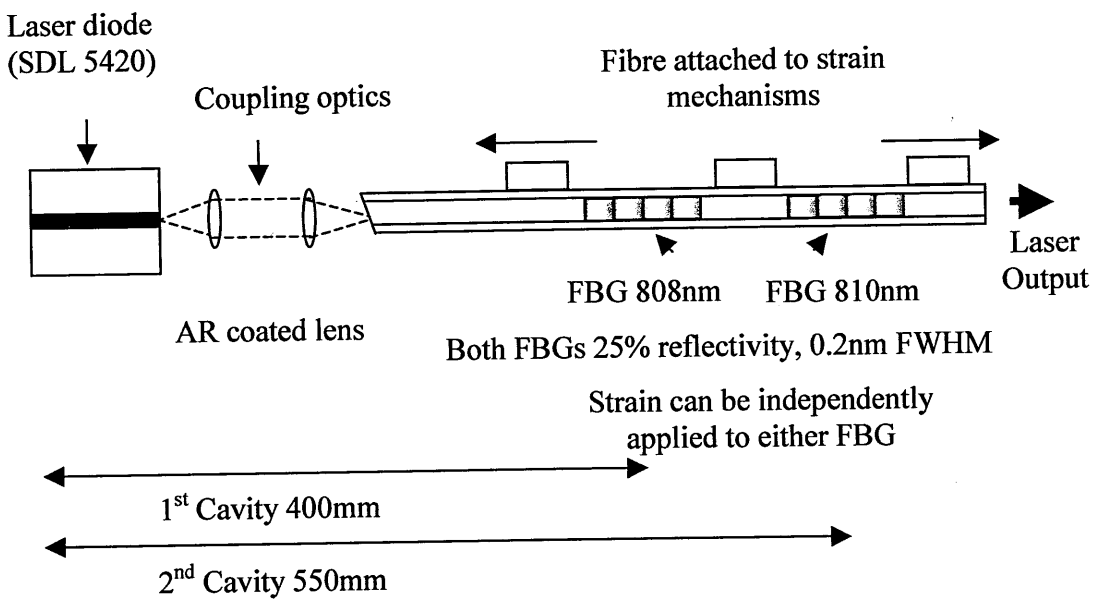

Fig 7.4 Dual FBG external cavity laser used for interrogation of F-P sensor cavity

The F-P cavity sensor was formed between the Fresnel reflection at the end of the SM addressing fibre and a mirror that was attached to a piezo-electric transducer (PZT) which was then modulated, by application of an AC voltage, to simulate a vibrating surface as shown in Fig. 7.5. The PZT was a Physik Instrumente P28620, which has a responsivity of 100 nm/V

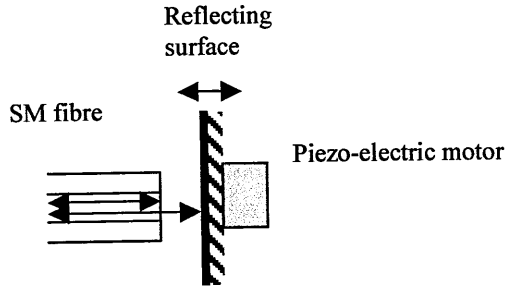

7.5 Extrinsic miniature F-P sensing cavity formed between the cleaved far end of a fibre SM fibre and reflecting surface attached to piezo-electric transducer.

The system is shown in Fig. 7.6. The laser was spliced onto a fibre pigtail from a 90/10 coupler. The coupler was used to minimise potentially destabilising reflections back into the laser cavity.

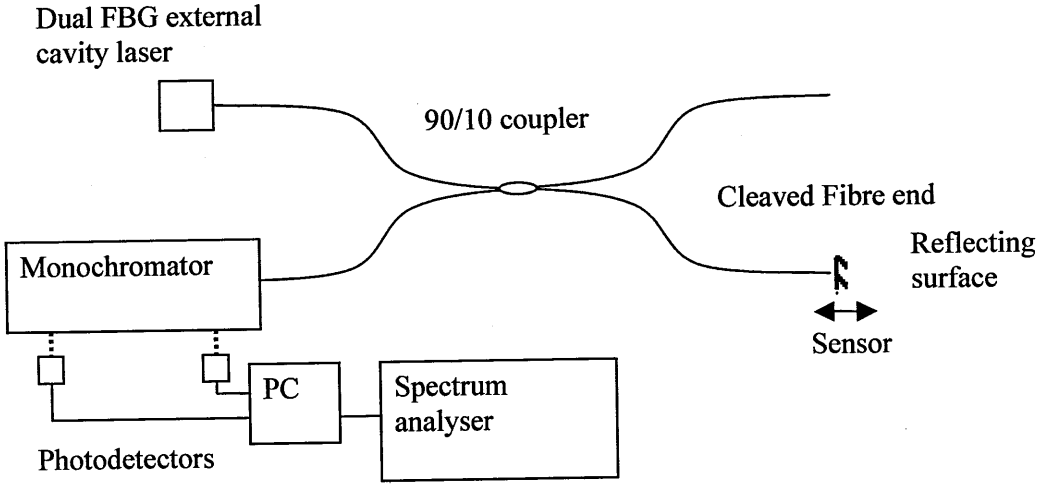

Fig. 7.6 Vibration sensing system using dual wavelength interrogation of a miniature Fabry-Perot cavity

The monochromator used was a Bentham with a 0.05 nm resolution; it was used to de-multiplex the two interference fringes of the two wavelengths. A reflecting prism was then used to direct the beams in opposite directions, for coupling into a PIN photodiode for each wavelength. High speed RS BPX photodiodes were used, which have a response time of 0.5 ns. The analogue outputs of the photodiodes where sampled by a National Instruments DAQ card, a specifically written LABVIEW program using real time triggering to ensure sampling occurred at an equal temporal spacing. The PC performed the required signal processing according to Eq. 7.5, to obtain the phase of the two interference fringes. The resulting phase signal was then converted to an analogue signal by a DAC and routed to a HP 35660A spectrum which performed a Fourier transform and displayed the signal on spectral graph.

The Labview software kept a rolling average of the interferometric outputs of the system to obtain the phase of each signal. The averaging array contained 5000 points so gave an average over 2.5 seconds at the highest sampling frequency of 2 kHz. If the average power of the illuminating wavelength is not obtained accurately this can lead too an error in the phase of the system. This can also be done by using another demultiplexing monochromator on the fourth arm of the interferometer, providing a reference for the interferometer.

7.8 Experimental results

Fig. 7.7 shows the interferometric outputs at both wavelengths when the cavity was at quadrature and a linear ramp in voltage was applied to the PZT to produce a linear displacement in the reflecting surface. The separation of the laser wavelengths was tuned by applying strain to the FBGs, to ensure quadrature. The F-P cavity size could be determined using an optical spectrum analyser. In this case quadrature was achieved at a wavelength separation of 3.5 nm, denoting a cavity size of 16 μm.

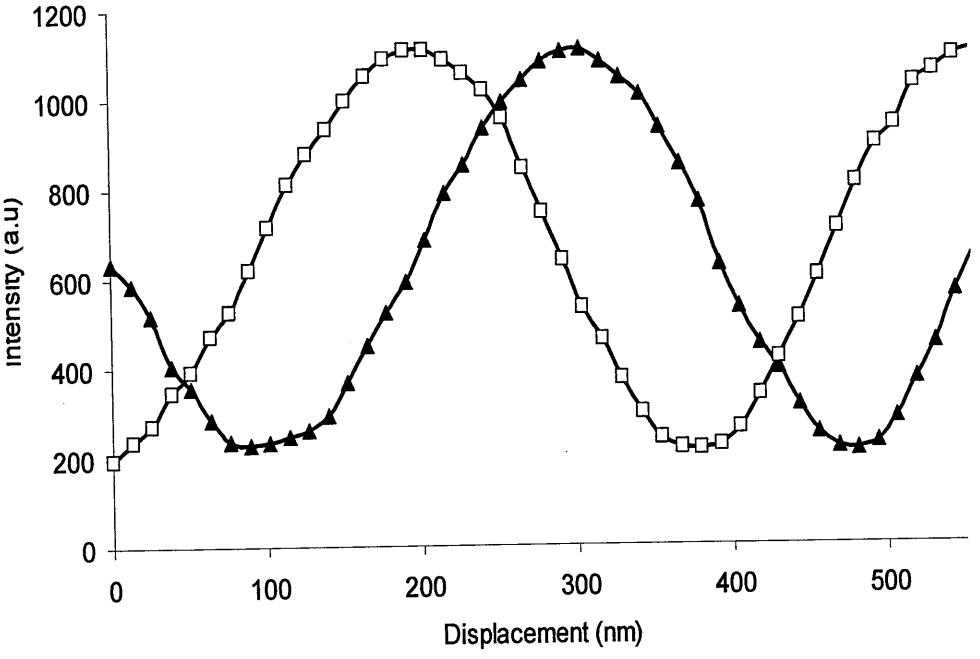

Fig. 7.7 Interference fringes of the two interrogating wavelengths as the reflecting surface is displaced

Fig 7.8 shows four traces, the first two traces A) & B) are the two photodetector outputs taken directly from a Tektronix oscilloscope. Trace C) is the sinusoidal signal applied to the PZT. Trace D) is the final output from the DAC after being processed by the computer software. A fraction of a millisecond delay could be seen in trace D) relative to A) due to the computer processing the signal, inducing a time delay. The computed phase was also not an exact replica of the voltage applied to the PZT, the phase change on the troughs of the signal being slower than the peaks. This is thought to be hysteresis in the PZT.

Fig 7.9 Illustrates the computed phase of the system displayed on HP 35660A electronic spectrum analyzer when a 500 Hz vibration was applied to a 16 μm cavity, which required a ~3.5 nm mode separation of the laser modes. An SNR of >30dB was achieved, although this is a result of PZT and photodiode performance. Fig 7.10 shows the electronic spectrum of the computed phase when a 250 Hz sinusoidal voltage was

applied to a 34 μm cavity (which required a ~1.5 nm mode separation). The sampling time of the PC was limited to around 2 kHz thus Nyquist limiting the vibration sensing to a maximum of 1 kHz.

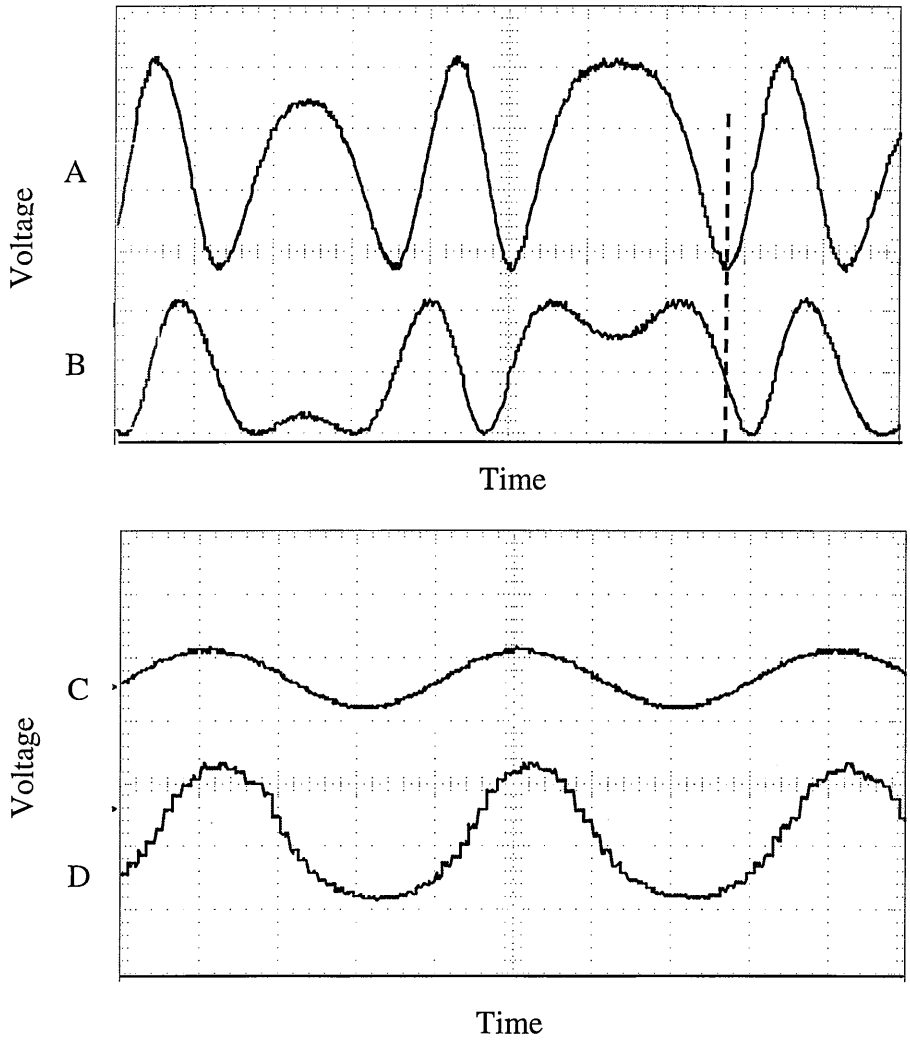

Fig 7.8 A) & B) Photodetector outputs for the two wavelengths. The dashed line highlights the quadrature condition of the two signals. C) Signal applied to the piezoelectric transducer. D) D/A output showing computed phase change. The y axis scale is 1 V/division, the x axis division is 2.5 ms/division

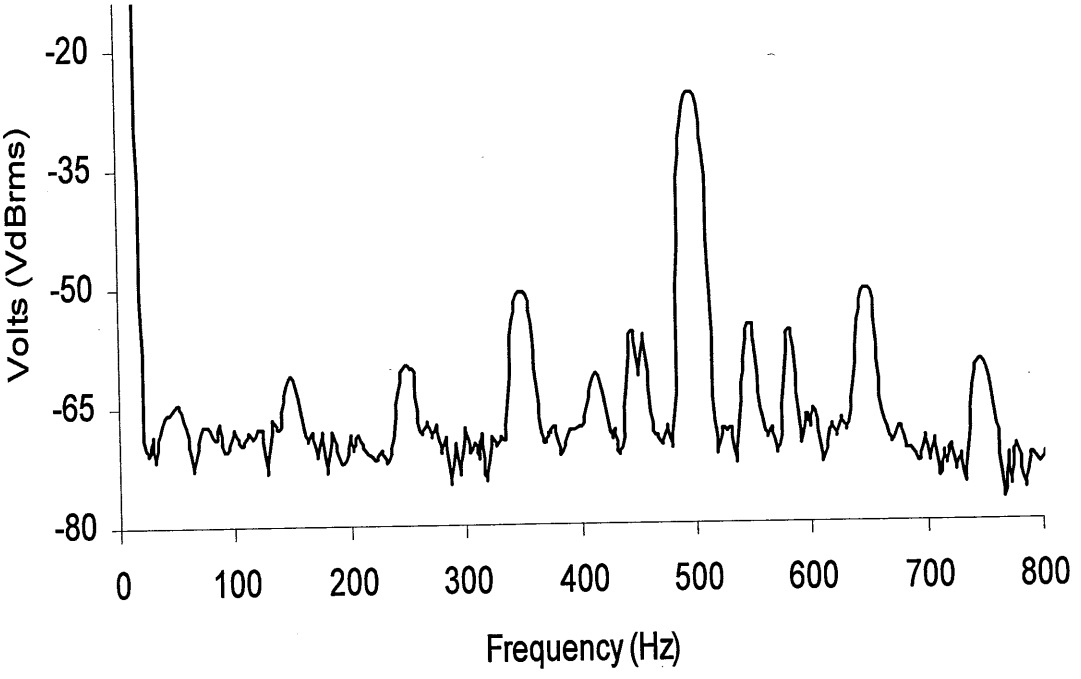

Fig. 7.9 Electronic spectrum obtained when a 500 Hz vibration applied to a 16 μm cavity (~3.5 nm mode separation)

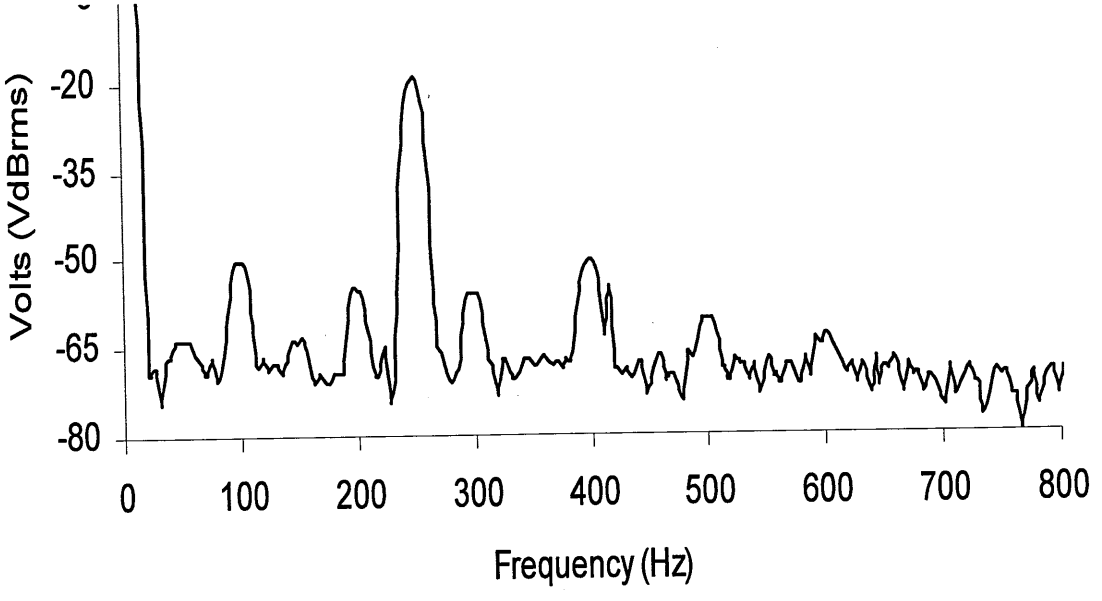

Fig. 7.10 Spectrum when a 250Hz vibration was applied to a 34μm cavity (~1.5nm mode separation)

7.9 Summary

Often there is a need for very localised and hence very small optical sensors. Miniature Fabry-Perot cavities are candidates for these applications and dual wavelength interrogation has been identified as a suitable signal processing technique as maintaining quadrature of these sensors can be done easily. However it is problematic selecting a suitable dual wavelength source, due to instabilities between separate lasers. Two longitudinal modes of a laser have an increased stability but tuning the separation between these modes is not possible, meaning a particular laser will only be able to correctly interrogate one length of sensor cavity, and in a sensing environment it may not always be possible to finely control the cavity size of the sensor. The unique properties of the dual FBG external cavity laser presented in chapter 6 allow the tuning of mode separation. Therefore the laser can be adapted to tune the modes to match the particular cavity requirements. This has been demonstrated by using a dual FBG laser to interrogate two different sized cavities, 16 μm and 34 μm, at different frequency vibrations, 500 Hz and 250 Hz. Chapter 6 also demonstrated the possibility of the external cavity entertaining 3 or more FBGs, this would allow the error factors to be improved over an increased range[7.11].

References

(7.1) B. Culshaw and J. Dakin, (ed) 'Optical Fibre sensors: components and subsystems', Atrech House, London, 1997.

(7.2) E. Hecht, 'Optics 3rd edition' Addison-Wesley, Harlow, England, 1998.

(7.3) T. Yoshino and Y. Ohno, 'Fibre Fabry-Perot interferometers', Proc. 3rd Int. Conf on integrated optics and optical fiber communications, San Francisco, CA, USA, 1981, pp. 128

(7.4) S.J. Petuchowski, T.G. Giallorenzi and S.K. Sheem, 'A sensitive fibre optic Fabry-Perot Interferometer" IEEE J. of Quantum Electronics, 1981, Vol. 17, pp. 2168-2170.

(7.5) T. Yoshino, K. Kurosawa, K. Itoh and T. Ose, 'Fibre-optic Fabry-Perot interferometer and its sensor applications', IEEE J. of Quantum Electronics, 1982, Vol. 18. pp. 1624-1633.

(7.6) C.E. Lee, J.J. Alcoz, Y. Yeh, W.N. Gilber, R.A. Atkins and H.F. Taylor, 'Optical fiber Fabry-Perot sensors for smart structures', Smart Material Structures, 1992, pp. 123-127.

(7.7) M. de Vries, M. Nasta, V. Bhatia, T. Tran, J. Greene, R.O. Claus and S. Masri, 'Performance of embedded short gauge length optical fibre sensors in a fatigue loaded reinforced concrete specimum', Smart Materials Structure, 1995, pp.107-113.

(7.8) A.D. Kersey, D.A. Jackson and M. Corke, 'A simple fibre Fabry-Perot sensor', Optics communications, 1983, Vol. 2, pp. 71-74.

(7.9) D. Hogg, B. Mason, T. Valis and R.M. Measures, 'Development of a fibre Fabry-Perot FFP strain gauge sytem', SPIE conf. on Active materials and Adaptive structures, 1992, pp. 667-672.

(7.10) Y.J.Rao and D.A. Jackson, 'A Prototype fibre optic based Fizeau medical pressure and temperature sensor using coherence reading', Measurement Science and technology, 1994, Vol. 5, pp. 741-746.

(7.11) S.A. Al-Chalabi, B. Culshaw and D.E.N. Davies, 'Partially coherent sources in interferometric sensors' Proc. 1st Int conf. on optical fibre sensors, London, IEE, 1983, 132-133.

(7.12) D.A. Jackson, R. Priest, A. Dandridge and A.B. Tvetven, 'Elimination of drift in a single mode optical fibre interferometer using a piezoelectrically stretched coiled fiber', Applied Optics, 1980, Vol. 19, pp 2926-2929.

(7.13) S.K. Sheem, T.G. Giallorenzi and K. Koo, 'Optical techniques to solve the signal fading problem in fiber interferometers', Applied Optics, 1982, Vol. 21. pp. 689-693.

(7.14) F.J. Eberhardt and F.A. Andrews,'Laser heterodynesystem for measurement and analysis of vibration', J. of Acoustic Soc. of Am., 1970, Vol. 48, pp. 603.

(7.15) A. Ezbiri, 'Passive signal processing techniques for miniature fibre Fabry-Perot interefometric sensors', PhD Thesis, Cranfield University, 1996.

(7.16) A. Ezbiri and R.P. Tatam, 'Passive signal processing for a miniature Fabry-Perot interferometric sensor with a multimode laser diode source', Optics Letts., 1995, Vol. 20, pp1818-1821.

(7.17) S. P. Reilly, S W James and R P Tatam, 'Tuneable and switchable dual wavelength lasers using optical fibre Bragg grating external cavities', Electronics Letts., 2002, Vol. 38, pp. 1033-1034.

(7.18) A. Ezbiri and R.P. Tatam, 'Five wavelength interrogation technique for miniature fibre optic Fabry-Perot sensors', Optics comms., 1997, Vol. 133, pp. 62-66.

8: Conclusions

Two designs of fibre Bragg grating external cavity lasers have been presented and experimentally tested in previous chapters of this thesis. In this chapter the main results are reiterated and directions of further research suggested. The ability of fibre Bragg grating external cavity lasers to reduce threshold, mode hopping and linewidth was previously known[8.1] In chapter 4 these properties are quantified with known parameters of the external cavity and a significant improvement was observed. The linewidth was reduced from 2.5 MHz to <500 kHz, at a controlled temperature over the full injection current range 10 mode hops occurred, however at the same stable temperature with an FBG external cavity mode hops were negligible.

A Hi-Bi FGEL laser configuration was presented based on the use of FBGs fabricated in Hi-Bi fibre, exploiting the difference in the wavelength of the Bragg reflections of light populating the orthogonally polarised eigenaxes of the fibre. Feedback from a FBG written in Hi-Bi fibre then results in the laser operating on two longitudinal modes that are separated in both wavelength and polarisation. The wavelength separation of the orthogonally polarised Bragg reflections can be calculated using the Bragg and birefringence equations. Although birefringence has been used before in a laser cavity[8.2] this is the first time it has been applied to an external cavity laser diode. Switchability was achieved by the use of a half wave plate and 3 regions of operation were identified – one corresponding to each of the axes of the fibre and a third in which both modes lased the modes were separated by 0.3 nm. Transverse strain on Hi-Bi fibre has previously been used for multi-axis sensors, in chapter 5 it is experimentally demonstrated as a method of tuning the dual wavelength separation and a tuning range of 0.15 nm was demonstrated.

A second design featuring dual FBGs was also demonstrated, two modes corresponding to each FBG lased simultaneously. One FBG could be tuned over a range of over 3 nm which allowed generation of a beat frequency from 130 GHz to 2.28 THz equivalent to a synthetic wavelength of 2.3 mm to 0.131 mm. A three FBG laser was also demonstrated which allowed three modes to lase simultaneous.

The dual wavelength laser was then used to interrogate a miniature Fabry-Perot cavity. Dual wavelength interrogation of a miniature cavity sensor has been demonstrated previously but the use of the dual FBG laser allowed the separation of the wavelengths to be tuned which meant the wavelengths could be tuned to fit a wide range of cavities sizes. This has practical applications as it is often not easy to adjust the size of the cavity when embedded in its application. The range over which the wavelengths can be tuned theoretically allows interrogation, at quadrature, of cavities of size 273.3 μm to 27.3 μm.

8.1 Further work

The following section will suggest some specific areas in which further research could be undertook to lead on from the work presented in chapters 5, 6 and 7.

8.1.1 Liquid crystal waveplate switching

The Hi-Bi laser presented in chapter 2 featured a half-wave plate being rotated to switch between wavelengths corresponding to each eigenmode. However, it is possible to do this electronically either with a servo or non-mechanically with a liquid crystal. Liquid crystals are an organic compound that can flow and yet maintain their characteristic molecular orientations. The application of a voltage across the crystal can alter the orientation of the birefringence so therefore it becomes an electronically controllable waveplate[8.3]. The long axis of the liquid crystal molecules is the slow index with no voltage present the molecules lie parallel to the direction of propagation of the electro- magnetic wave, causing maximum retardance. When voltage is applied across the liquid layer the molecules tip parallel to the applied electric field. The response time of the liquid crystal waveplate is around 20 ms when retardance increases, which is the relaxation time of the molecules. The response to when retardance decreases though is 5 ms as the electric field is applied. The inclusion of a liquid crystal waveplate in the external cavity would allow rapid switching between all three states of operation and all electrical control of the laser.

8.1.2 Multiple FBGs

The use of more than two FBGs in an external cavity was demonstrated in chapter 6 when 3 FBGs were fabricated adjacent to each other in a fibre used for an external cavity. All three modes corresponding to the FBG's were seen to lase simultaneously. This suggests that the number of FBGs allowed is limited by the spectral width of luminescence band of the laser and the spatial length of the fibre which FBGs can fit sequentially on and still allow single mode operation. Single mode operation has been demonstrated here in a cavity of 650 mm and results have been published of single mode operation in a cavity of 2 m[8.5] . As each FBG is approximately 5-10 mm spectral limitations are likely to be more limiting. As the FWHM of the luminescence band being around 10 nm if each FBG needs a spacing of 0.3 nm as suggested by results in chapter 6 then up to 30 FBG could be used. However to sustain this amount of modes a huge population inversion would be required from the injection current and spectral hole burning is likely to be a factor.

An application of an increasing number of controllable FBG modes is for the interrogation of the miniature cavities demonstrated in chapter 7. In section 7.5 errors inherent in the interrogation of these sensors were highlighted. A study undertaken in ref 8.4 demonstrated the benefits of interrogation by more than two wavelengths and analysed up to five interrogating wavelengths. The problem of miscalibration is further helped by the nature of the multiple FBG external cavity laser which allows separate tuning of each wavelength.

8.1.3 Theoretical Investigations

Although there has been some theoretical work on FBG external cavity lasers[8.6] most of these publications focus on the laser response to injection current modulation and a definitive picture of the parameters needed to ensure single mode operation is yet to be defined. A qualitative approach can be used by analysing the results contained within this thesis along with the publications on FBG external cavity lasers, through details of parameters such as FBG bandwidth, cavity length and FBG reflectivity, which are closely related to coupling efficiency between laser and fibre. Length of the

laser cavity is a key issue, stabilised dual mode operation was demonstrated in this thesis in a cavity of 650 mm while single mode operation in a cavity of length 2 m has been reported[8.5] . This disproves the theory Fabry-Perot mode separation exists within an FBG external cavity. Using experience gained experimentally during the attempted construction of the FGEL lasers, it is possible to prioritise FBG bandwidth, followed by reflectivity and coupling efficiency and then cavity length. The hardest issue to resolve during the experimental work within this thesis was the bandwidth of FBG due to difficulties in both manufacturing narrow bandwidth FBG's but also in measuring their spectral reflectivity as most optical spectrum analysers have a maximum resolution of 0.1 nm. However, it was observed that no FBG with a FWHM over 0.2 nm was able to effectively induce single mode behaviour in an FGEL, whereas single mode behaviour at the Bragg wavelength could still be observed at least a cavity length of 650 mm and coupling efficiency ~15%.

References

(8.1) F.N. Timofeev, P. Bayvel, L Reekie, J. Tucknott, J.E Midwinter and D.N Payne, 'Spectral characteristic of a reduced cavity single-mode semiconductor fibre grating laser for applications in DWDM systems' in proc. 21st European conf. Optic. Commun. (ECOC 95) pp.477-480.

(8.2) Hernandez-Cordero, V.A. Kozlov, A.L.G. Carter and T.F. Morse, 'Fiber Laser Polarization tuning using a Bragg grating in a Hi-Bi Fiber', IEEE Photonics Technology Lett., 1998, Vol. 10, pp.941-943.

(8.3) Meadowlark company information catalogue, www.meadowlark.com

(8.4) A. Ezbiri, 'Passive signal processing techniques for miniature fibre Fabry-Perot interferometric sensors' Ph.D. Thesis, Cranfield university, 1996.

(8.5) E. Brinkmeyer, W. Brennecke, M. Zurn and R. Ulrich, 'Fibre Bragg reflector for mode selection and line narrowing of injection lasers', Electronics Lett., 1986, Vol. 22, pp.134-135,

(8.6) M. Premaratne, A.J. Lowery, Z. Ahmed and D. Novak, 'Modeling noise and modulation performance of fiber grating external cavity lasers', IEEE J. of selected topics in Quantum Electronics, 1997, Vol. 3, pp.290-303.

Appendix A

Beat frequencies: The addition of Waves of different frequency

Rarely is light strictly monochromatic, therefore it is far more realistic to refer to light as quasi-monochromatic that is composed of a narrow range of frequencies. Two waves that have equal amplitudes and zero initial phase angles.

$$E_1 = E_{01}\cos(k_1 x - \varpi_1 t)$$

$$E_2 = E_{01}\cos(k_2 x - \varpi_2 t)$$

Where E_{01} is the amplitude of the signal, k is the wave number defined as $k \equiv 2\pi/\lambda$, that is the number of waves per unit length (ie per metre). ϖ is the angular temporal frequency, defined as $\varpi \equiv 2\pi/\tau = 2\pi\nu$. τ is the temporal period, the amount of time it takes one complete wave to pass a stationary point and x is distance. Upon superimposition the net wave is

$$E = E_{01}\left[\cos(k_1 x - \varpi_1 t) + \cos(k_2 x - \varpi_2 t)\right]$$

This can be reformulated as

$$E = 2E_{01}\cos\frac{1}{2}\left[(k_1 + k_2)x - (\varpi_1 + \varpi_2)t\right] * \cos\frac{1}{2}\left[(k_1 - k_2)x - (\varpi_1 - \varpi_2)t\right]$$

Using the identity

$$\cos\alpha + \cos\beta = 2\cos\tfrac{1}{2}(\alpha + \beta)\cos\tfrac{1}{2}(\alpha - \beta)$$

$\bar{\varpi}$ is the average angular frequency is thus defined as $\bar{\varpi} \equiv \frac{1}{2}(\varpi_1 + \varpi_2)$, ϖ_m is the modulation frequency and is defined as $\varpi_m \equiv \frac{1}{2}(\varpi_1 - \varpi_2)$. $\bar{k}$ and k_m are the average propagation number and modulation propagation number. They are define as:

$$\bar{k} \equiv \tfrac{1}{2}(k_1 + k_2)$$

$$k_m \equiv \tfrac{1}{2}(k_1 - k_2)$$

$$\therefore\ E = 2E_{01}\cos(k_m x - \varpi_m t)\cos(\bar{k}x - \bar{\varpi}t)$$

The total disturbance may be thought of as a travelling wave of frequency $\bar{\varpi}$, and time varying modulated amplitude $E_{0t}(x,t)$

$$E(x,t) = E_0(x,t)\cos(\bar{k}x - \bar{\varpi}t)$$

$$E_0(x,t) = 2E_{01}\cos(k_m x - \varpi_m t)$$

For cases of different wavelength mixing here, generally $\varpi_1 \approx \varpi_2$, this will result in $\bar{\varpi} >> \varpi_m$ and $E_0(x,t)$ will change relatively slowly. However, E(x,t) will vary rapidly the irradiance is proportional to:

$$E_0^2(x,t) = 4E_{01}^2\cos^2(k_m x - \varpi_m t)$$

Or

$$E_0^2(x,t) = 2E_{01}^2[1 + \cos(2k_m x - 2\varpi_m t)]$$

$E_0^2(x,t)$ oscillates at about a value of $2E_{01}^2$ with a frequency of $2\varpi_m$ which is the beat frequency. Therefore E_0 varies at the modulation frequency and E_0^2 varies at twice this frequency.

Publications List

1 S.P. Reilly, S.W. James and R.P. Tatam, 'Dual wavelength fibre Bragg grating external cavity semiconductor laser sources for sensor applications' 2002 15th Optical fiber sensors conference technical digest, OFS 2002, 6-10th May 2002, Hilton Portland, Portland, OR, USA, pp. 281-284. ISBN: 0-7803-7289-1

2 S.P. Reilly, S.W. James and R.P. Tatam, 'Tunable and switchable dual wavelength lasers using optical fibre Bragg grating external cavities', Electronics letters, 29th August 2002, Vol.38, No. 18, pp. 1033-1034

3 S.P. Reilly, S.W. James and R.P. Tatam, 'Dual wavelength fibre Bragg grating external cavity lasers', Institute of Physics, Photon02 2-5th September, Cardiff international arena, Abstract book, ISBN:0-75030916-4, pp. 13-14.

4 S. Reilly, 'Conference report: 15th Conference on Optical Fibre sensors, OFS 2002, Portland, Oregon, USA', www.raeng.org.uk